A description of sources detected by *INTEGRAL* during the first 4 years of observations

A. Bodaghee[1,2], T.J.-L. Courvoisier[1,2], J. Rodriguez[3], V. Beckmann[4], N. Produit[1,2], D. Hannikainen[5], E. Kuulkers[6], D.R. Willis[1], and G. Wendt[1]

[1] *INTEGRAL* Science Data Centre, Chemin d'Ecogia 16, CH–1290 Versoix, Switzerland
[2] Observatoire Astronomique de l'Université de Genève, Chemin des Maillettes 51, CH–1290 Sauverny, Switzerland
[3] CEA-Saclay/DSM/DAPNIA/SAp, F-91191 Gif-sur-Yvette, France
[4] NASA Goddard Space Flight Center, Astrophysics Science Division, Greenbelt, MD 20771, USA
[5] Observatory, P.O. Box 14, FI-00014 University of Helsinki, Finland
[6] ISOC, ESA/ESAC, Urb. Villafranca del Castillo, P.O. Box 50727, 28080 Madrid, Spain

ABSTRACT

Context. In its first 4 years of observing the sky above 20 keV, *INTEGRAL*-ISGRI has detected 500 sources, around half of which are new or unknown at these energies. Follow-up observations at other wavelengths revealed that some of these sources feature unusually large column densities, long pulsations, and other interesting characteristics.

Aims. We investigate where new and previously-known sources detected by ISGRI fit in the parameter space of high-energy objects, and we use the parameters to test correlations expected from theoretical predictions. For example, the influence of the local absorbing matter on periodic modulations is studied for Galactic High-Mass X-ray Binaries (HMXBs) with OB supergiant and Be companions. We examine the spatial distribution of different types of sources in the Milky Way using various projections of the Galactic plane, in order to highlight signatures of stellar evolution and to speculate on the origin of the group of sources whose classifications are still uncertain.

Methods. Parameters that are available in the literature, such as positions, photoelectric absorption (N_H), spin and orbital periods, and distances or redshifts, were collected for all sources detected by ISGRI. These values and their references are provided online.

Results. ISGRI has detected similar numbers of X-ray Binaries and Active Galactic Nuclei (AGN). The former group contains new members of the class of HMXBs with supergiant stellar companions. Usually, this type of object presents strong intrinsic absorption which leads to a peak emission in an energy range that ISGRI is ideally suited to detect. Thanks to these additional systems, we are able to show that HMXBs are generally segregated in plots of intrinsic N_H versus the orbital period of the system and versus the spin period of the pulsar, based on whether the companion is a Be or an OB supergiant star. We also find a tentative but expected anti-correlation between N_H and the orbital period, and a possible and unexpected correlation between the N_H and the spin period. While only a handful of new Low-Mass X-ray Binaries (LMXBs) have been discovered, there are many sources that remain unclassified and they appear to follow a spatial distribution typical of Galactic sources (especially LMXBs) rather than extragalactic sources.

Key words. Gamma-rays: observations, catalogues – X-rays: binaries

1. Introduction

In just over 4 years, *INTEGRAL*-IBIS/ISGRI (Lebrun et al. 2003; Ubertini et al. 2003) has detected ∼ 300 previously-known sources in the hard X to soft γ-ray band (20–100 keV), and discovered ∼ 200 sources that were previously unknown at these energies. We will hereafter refer to the latter sources as IGRs [1] (for *INTEGRAL* Gamma-Ray sources). Generally, these sources were detected by creating long-exposure mosaic images captured by ISGRI (e.g., Bird et al. 2007). The *INTEGRAL* core programme (Winkler et al. 2003) is beginning to fill in underexposed regions of the sky.

Most of the sources that ISGRI has detected are Low and High-Mass X-ray Binaries (LMXBs and HMXBs, respectively), or Active Galactic Nuclei (AGN). Both LMXBs and HMXBs feature a compact object such as a neutron star (NS) or a black hole (BH) accreting material from a companion star: a faint old

dwarf in LMXBs ($M \lesssim 1\ M_\odot$), a bright young giant in HMXBs ($M \gtrsim 10\ M_\odot$), or sometimes an intermediate-mass companion. Accretion typically occurs via Roche-lobe overflow in LMXBs or through the wind in HMXBs. An accretion disk can be found in both types of systems and is an important component of the optical/UV and X-ray emission from AGN and LMXBs.

Subclasses exist within the 3 most common groups. In the case of HMXBs, the spectral type of the stellar companion determines the sub-classification beyond the NS or BH nature of the compact object. A majority of HMXBs host main-sequence (MS) Be stars that have not filled their Roche lobe (Waters & van Kerkwijk 1989). These systems are usually transient with flares produced whenever the sometimes wide and eccentric orbit brings the compact object close to its companion. Persistent HMXBs are typically accompanied by an evolved supergiant (SG) O or B star whose wind steadily feeds the compact object. Their variability stems from inhomogeneities in the wind. Similarly, LMXBs can be classified based on the type of compact object (NS or BH) it has. Neutron star LMXBs can be divided further into Z or Atoll sources depending on the tracks

---

[1] an updated list of IGRs can be found at http://isdc.unige.ch/~rodrigue/html/igrsources.html

they follow in a color-color diagram. The 2 primary groups of AGN are Seyfert 1 and 2, with the latter being more absorbed and showing narrow emission lines only.

Our understanding of the different populations of *INTEGRAL* sources is limited by the large number of sources about which very little is known. Roughly half of all IGRs remain unclassified. The nature of these sources is difficult to elucidate given that many are faint or transient. Furthermore, the images, spectrum, and timing analysis gathered from a single energy range are usually insufficient to classify an object. Information from other wavelengths such as soft X-rays, infrared or radio are necessary to help identify the nature of a source. For example, radio emission can be the signature of a jet or pulsar, while the optical spectral type can help distinguish between LMXBs and HMXBs, and the redshift can place it at extragalactic distances. Follow-up observations with soft X-ray telescopes (i.e. *Chandra*, *RXTE*, *Suzaku*, *Swift* and *XMM-Newton*) can provide fine timing analyses which enable short-period modulations to be found, and they can describe the shape of the continuum below ISGRI's ~20 keV lower limit, in an energy range where potential photoelectric absorption (N_H) and iron fluorescence lines are detectable. Precise X-ray coordinates from *Chandra*, *Swift* or *XMM-Newton* can be used to search for counterparts in dedicated radio, optical, and IR observations or in catalogues. However, many sources are clustered in the Galactic center and along the plane, which, because of the density of stars and the amount of obscuring dust, can hinder the identification of the optical/IR counterpart.

Perhaps the most interesting result from follow-up observations is that a number of IGRs present column densities that are much higher than would be expected along the line of sight. These large absorptions are therefore intrinsic and could be the reason these sources eluded discovery with previous (softer) X-ray missions. The first new source discovered by *INTEGRAL* is IGR J16318−4848 (Courvoisier et al. 2003) which is one of the most absorbed Galactic sources known with $N_H \sim 2 \cdot 10^{24}$ cm^{-2} or roughly 2 orders of magnitude more than the intervening Galactic material (Dickey & Lockman 1990). Since this discovery, other sources joined the growing class of heavily-obscured X-ray sources described by Walter et al. (2004) and Kuulkers (2005).

A certain number of these absorbed sources consist of X-ray pulsars: e.g. IGR J16320−4751 (Rodriguez et al. 2006), IGR J16393−4643 (Bodaghee et al. 2006), and IGR J17252−3616 (Zurita Heras et al. 2006). Their persistent emission, their long pulse periods (~ 1 ks), and their large column densities suggest that these systems are likely to be SG HMXBs, with the NS deeply embedded in the wind of its massive stellar companion (Walter et al. 2006). These kinds of systems are still a minority compared to Be HMXBs, but *INTEGRAL* is expanding their ranks.

Supergiant Fast X-ray Transients (SFXT: see Sguera et al. (2005) for a review) are another type of object whose numbers are increasing thanks to *INTEGRAL*. These objects are HMXBs whose X-ray emission is characterised by short strong outbursts (a peak flux of up to a Crab or more during a few seconds to a few hundred seconds), sometimes with recurrence timescales that can reach several hundred days. Despite the intensity of their outbursts, SFXTs are usually not detected in deep mosaic images because the accumulation of exposure time attenuates their significance. Therefore, the search for SFXTs involves scanning archival light curve data and short-exposure mosaic images for rapid bursts from known transients or at new locations.

ISGRI has also detected other types of Galactic objects such as Cataclysmic Variables (CVs), Supernova Remnants (SNRs), Pulsar Wind Nebulae (PWN), Anomalous X-ray Pulsars (AXPs), etc., which are referred to henceforth as Miscellaneous.

The most extensive catalogues of sources detected by ISGRI are the catalogues of Bird et al. (2006) and Bird et al. (2007). These catalogues represent fairly large and homogeneous samples that can be used to study the general characteristics of populations of high-energy sources (e.g. Lebrun et al. 2004; Dean et al. 2005; Lutovinov et al. 2005; Beckmann et al. 2006b).

This research presents the parameters of all sources detected by ISGRI and reported between its launch on Oct. 17, 2002, until Dec. 1, 2006. Absorption values, pulse and orbital periods, and distances or redshifts were collected from the literature and were used to study the populations of high-energy sources, to test various correlations expected from theoretical predictions, and to investigate where the new and previously-known sources detected by ISGRI fit in the parameter space of high-energy objects.

2. Data & Analysis

We selected all sources from Version 27 of the *INTEGRAL* General Reference Catalogue (Ebisawa et al. 2003) which were detected by ISGRI (i.e. those with "ISGRI_FLAG==1"). These flags were set to the value of 1 as soon as confirmation of a detection by ISGRI is announced in an article, conference proceeding, Astronomer's Telegram or IAU circular. Therefore, the completeness of the sample is difficult to evaluate given that by definition, the present sample contains all sources that were detected above 20 keV while within the ISGRI FOV at some point during the last ~4 years, without considering the detection significance, nor the amount of exposure time that was required to make the detection.

The exposure map that can be seen in Fig. 1 was created by accumulating all public pointings in revolutions 30–484 (UTC: 11/1/2003–1/10/2006). Due to the core programme observation strategy, the Galactic centre (GC) is heavily exposed ($t_{exp} > 10$ Ms) whereas some regions have less than 10 ks of exposure time dedicated to them. The exposure is uneven along the Galactic plane as well, with exposure biases in the directions of the spiral arms. The sensitivity limit of a source in the most exposed regions is as low as ~ 1 mCrab for a transient object detected at the 6σ level (Bird et al. 2006). In fact, some sources were detected only because the instrument serendipitously caught a flaring event. Using the fact that the Log(N)–Log(S) relation for extragalatic sources follows a power law with a slope of −3/2 (Forman et al. 1978), we can estimate a sensitivity limit of ≲ 5 mCrab (= $3.78 \cdot 10^{-11}$ ergs cm^{-2} s^{-1} in 20–40 keV) for our sample based on where the distribution of AGN from Bird et al. (2006) deviates from the expected slope.

A number of IGRs have soft X-ray counterparts that were sometimes detected by earlier missions. For example, IGR J16393−4643 was known as AX J1639.0−4642 by *ASCA*, and IGR J17252−3616 as EXO 1722−360 by *EXOSAT*, and many IGRs have ROSAT counterparts (Stephen et al. 2006). Since ISGRI was the first to detect them above 20 keV, it is legitimate to group them together as a population of new soft γ-ray sources. They can then be compared to sources detected by ISGRI that were previously known to emit above 20 keV (e.g., Crab, Vela X-1, etc.). Note that the so-called previously-known sources actually include a few objects that were discovered after the launch of *INTEGRAL* (e.g. by *HETE*, *RXTE* or *Swift*).

Table 2. The number of sources from each of the major classes detected by ISGRI are listed for new (≡ IGRs) and previously-known sources. Miscellaneous (Misc.) sources are Galactic objects that are not X-ray binaries (e.g. CVs, SNRs, AXPs, etc.) and Uncl. refers to the group of sources that have yet to be classified.

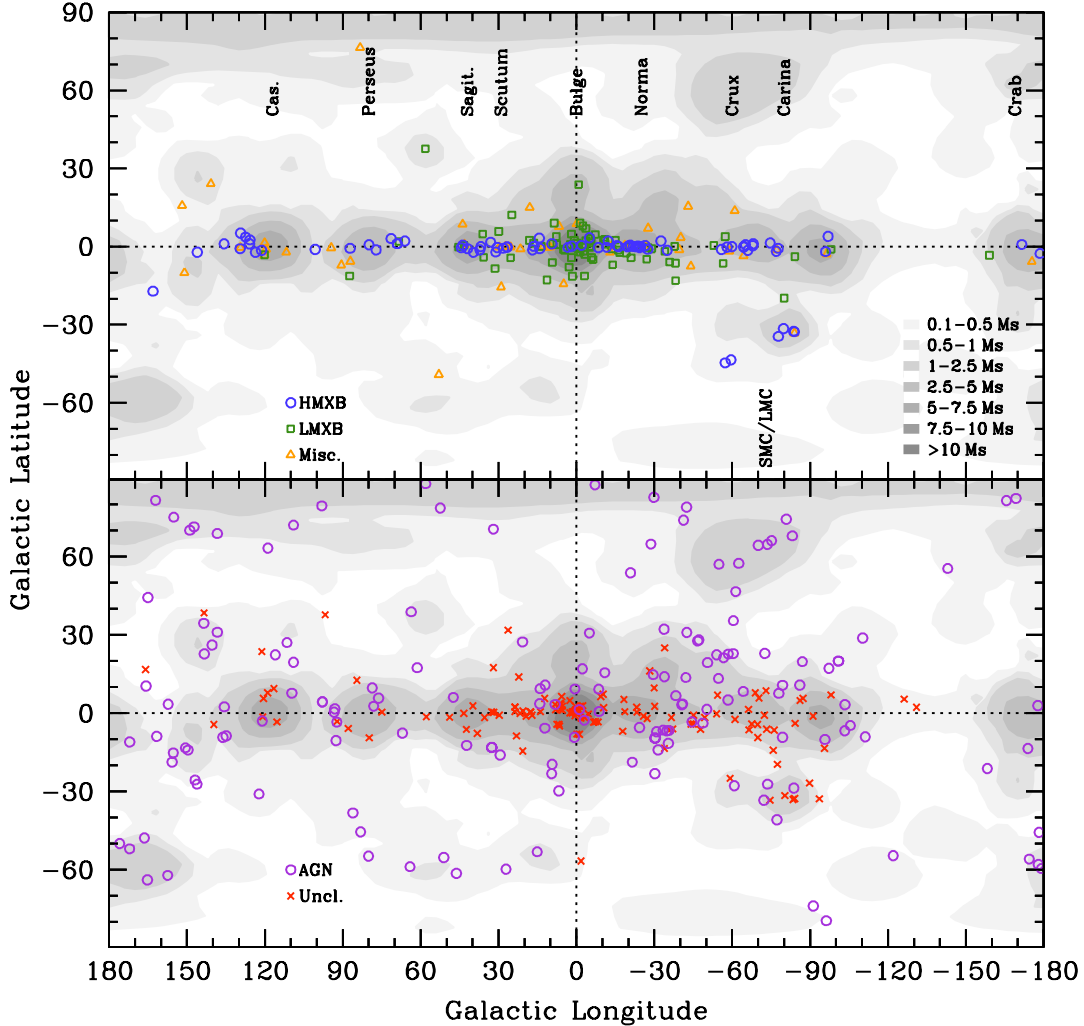|	HMXBs	LMXBs	AGN	Misc.	Uncl.	Total
IGRs	32 (15%)	6 (3%)	50 (23%)	15 (7%)	111 (52%)	214
previously-known	46 (16%)	76 (27%)	113 (40%)	32 (11%)	18 (6%)	285
Total	78 (16%)	82 (16%)	163 (33%)	47 (9%)	129 (26%)	499

Fig. 1. Spatial distribution in Galactic coordinates of sources detected so far by ISGRI. The figure at the top presents the distributions of HMXBs (stars), LMXBs (squares) and miscellaneous sources (triangles). The figure at the bottom displays extragalactic sources (circles) and unclassified sources (crosses). The directions to the spiral arm tangents and other areas of interest are indicated, as are the cumulative exposure times at each location (from public data in revs. 30–484). The number of sources in each class is listed in Table 2.

The name or position of each source in our sample was queried to the SIMBAD and ADS servers for references that could provide any of the following parameters: position and error radius, classification, column density (N_H), spin period, orbital period, and distance (or redshift). Besides a rough X-ray position, very little is known about some sources, while other sources were so thoroughly studied that choices had to

be made between sometimes conflicting values (notably N_H and distance). The index of parameters that we have constructed (see Table 1 [2]) represents what we know about sources detected by

---

[2] Table 1 is only available in electronic form at the CDS via anonymous ftp to cdsarc.u-strasbg.fr (130.79.125.5) or via http://cdsweb.u-strasbg.fr/Abstract.html
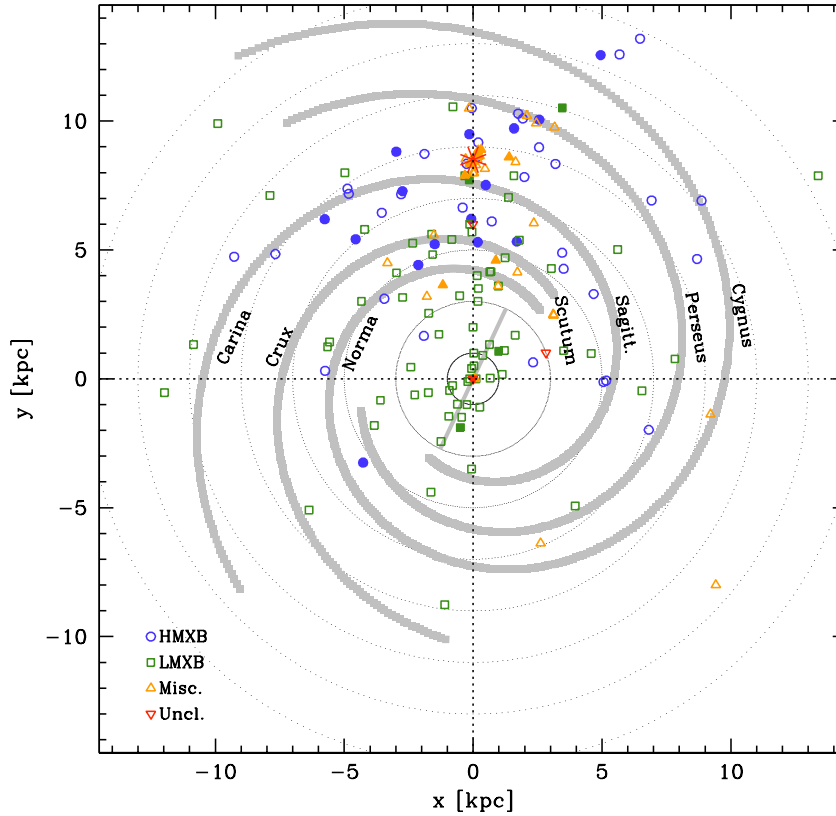
Fig. 2. Galactic distribution of HMXBs (49, circles), LMXBs (74, squares), miscellaneous sources (37, triangles), and unclassified sources (3, inverted triangles). Filled symbols represent IGR sources. Also plotted is the 4-arm Galactic spiral model from Russeil (2003) with the Sun located at 8.5 kpc from the centre. The concentric circles indicate radii of 1, 3, 5,..., kpc from the centre.

ISGRI to date (until December 1, 2006). The structure of Table 1 is as follows:

– *Name*:
  Most sources have more than 1 name owing to detections by various instruments operating at different energies. As in Ebisawa et al. (2003), we selected names that are commonly used in high-energy astrophysics and that are accepted as an identifier in SIMBAD. This eases comparisons with other catalogs.

– *Position*:
  Source positions are from the X-rays unless a more accurate position at other wavelengths is known for a confirmed counterpart. Right Ascension and Declination in J2000 coordinates are given in "hh mm ss.s" and "deg arcmin arcsec" formats, respectively. The uncertainty (in arcmin) of the position from the reference is given as an individual entry, and it is reflected in the representation of the source positions. Galactic coordinates are also provided.

– *Absorption*:
  Column densities (in 10^{22} cm^{-2}) were gathered from the literature whenever a model fit to the X-ray spectrum required an absorption component. Extracting a single $N_{\rm H}$ for a source and comparing this value to those of other sources is not a straightforward exercise since intrinsic column densities are not static. A measurement made during flaring or quiescent periods, or at different orbital epochs, will heavily influence the $N_{\rm H}$. The geometry of the system, the energy

range of the satellite that gathered the data, and the model used to describe the resulting spectrum also affect the $N_{\rm H}$ value. Therefore, the uncertainties are often large or only upper limits are provided. Whenever possible, we selected the $N_{\rm H}$ value of the model that best fits a recent X-ray spectrum taken with a telescope that covers the soft X-ray domain well.

– *Modulations*:
  Spin periods (in seconds) and/or orbital periods (in days) have been reported for a large number of Galactic objects detected by ISGRI. Some systems are known to spin down, so we selected the most recent value from *RXTE* whenever possible, even though this level of precision is not needed for the purpose of our study. The spin period can refer to the spin of the NS in X-ray binaries, or to the spin of the White Dwarf in CVs. The catalogs of Liu et al. (2000) and Liu et al. (2001), and the systematic analysis of *RXTE* data by Wen et al. (2006) are among the main references of spin and orbital periods in this work.

– *Distances*:
  The distances to extragalactic objects are given as a measure of the redshift (denoted by brackets). Objects in the Milky Way and Magellanic Clouds have distances in units of kpc. Opinions sometimes differ as to the distances of some Galactic sources. We favored distance measurements that were recent, precise and that were the least model-dependent. Even so, the distance uncertainties quoted in the literature can be large. The distance measurements are from,
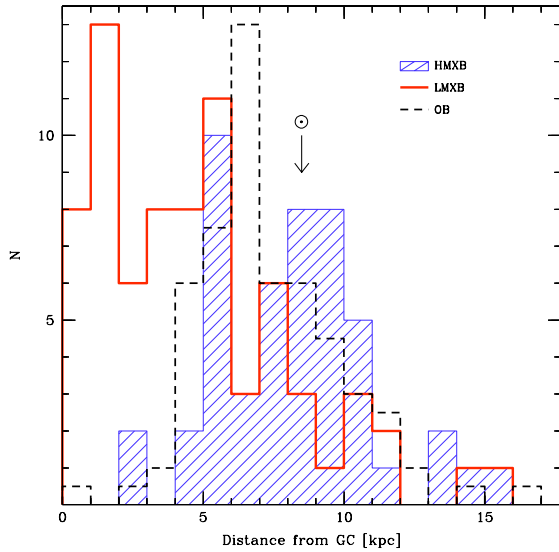
Fig. 3. Distribution of galactocentric distances of HMXBs (49, shaded histogram) and LMXBs (74, thick histogram). The dashed histogram represents OB star-forming complexes from Russeil (2003) (divided by 2).

among others, White & van Paradijs (1996), Grimm et al. (2002), Jonker & Nelemans (2004), Bassani et al. (2006), Beckmann et al. (2006a), or from references in Liu et al. (2000) and Liu et al. (2001). Note that the distances in Grimm et al. (2002) sometimes represent an average over several competing distance estimates.

– *Type*:
Source classifications are based on the concensus opinion in the literature. Peculiar behaviour, such as quasi-periodic oscillations, transience, and Z-track or Atoll shapes, are also noted since they can help us distinguish between systems within the same class. If the source classification has not yet been confirmed, it is simply called "unclassified." The transient identification of a source is given by any of the following: 1) the label was assigned by its discoverers or by other authors (e.g. "Discovery of a new *transient* IGR J..."); 2) the source has not been detected by anyone else since its discovery announcement, e.g. it is not listed in the all-data, all-sky catalogs of Bird et al. (2006) and Bird et al. (2007)); 3) the source is detected only in mosaic images of a single or a few consecutive revolutions according to Bird et al. (2007), but not in their all-data mosaic images.

– *References*:
All parameters are referenced so that the reader can assess the methods that were used to determine the quoted values and uncertainties.

3. Results

3.1. Spatial Distribution

Table 2 lists the major source populations detected by ISGRI that are either new (≡ IGRs) or that were previously known. ISGRI has discovered many new HMXBs and AGN, but their proportions relative to the other classes are similar to what was known before the launch of *INTEGRAL*. Only a few LMXBs have been discovered by ISGRI. This is because LMXBs are generally less
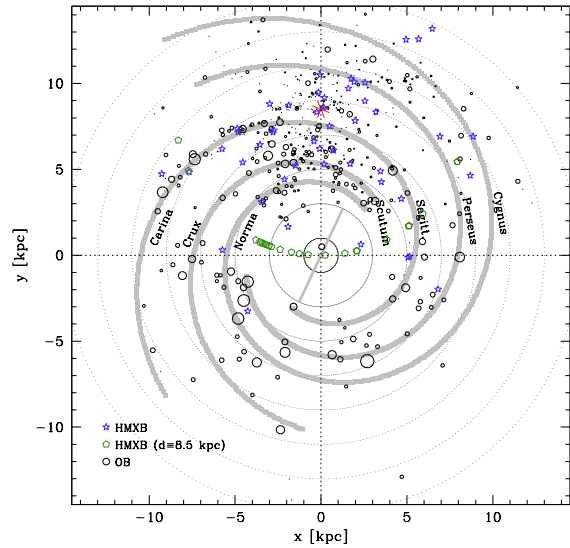
Fig. 4. Galactic distribution of HMXBs whose distance are known (49, star symbols) and the locations of star-forming complexes from Russeil (2003) (464, circles). The symbol size of the latter is proportional to the activity of the complex. HMXBs whose distances are unknown have been placed at 8.5 kpc (23, pentagons).
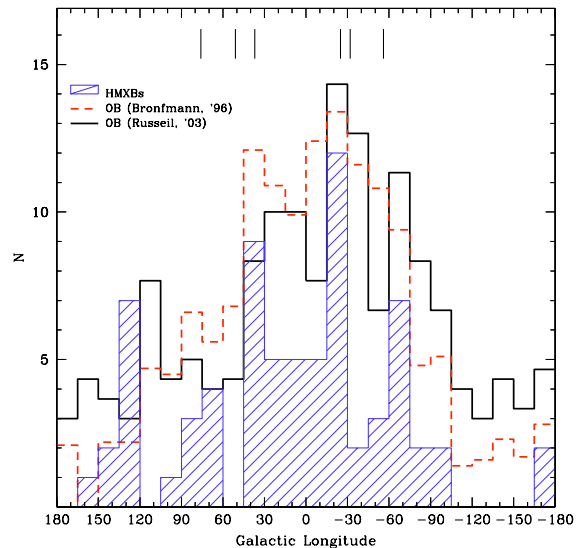
Fig. 5. Histograms of Galactic longitudes integrated over the latitude for HMXBs with $|b| < 6°$ (shaded histogram) and star-forming regions from Russeil (2003) (thick histogram, divided by 3) and from Bronfman et al. (1996) (dashed histogram, divided by 10). The vertical lines indicate the tangential directions of the 4-arm spiral model from Russeil (2003)

intrinsically obscured than HMXBs or AGN, and are therefore easier to detect with previous satellites. Around 50 sources have been detected that belong to the group of miscellaneous sources (i.e. CVs, SNRs, PWN, AXPs, etc.), while ∼ 130 IGRs await classification.

The spatial distributions, in Galactic coordinates, of the major classes of γ-ray sources detected by ISGRI are presented in
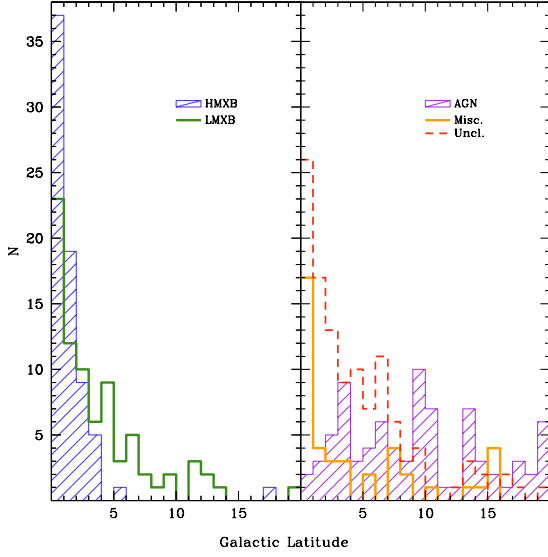
Fig. 6. Angular distribution (in degrees, for $|b| < 20°$) from the Galactic plane of sources that have been detected by ISGRI. Shaded histograms are HMXBs (left) and AGN (right), and the clear histograms represent LMXBs (left) and miscellaneous sources (right). The dashed histogram denotes unclassified sources. The distributions have been summed over the northern and southern Galactic hemispheres. The curves represent fits to the data from the model and parameters described in the text.

Fig. 1. Naturally, ISGRI detects sources in regions that are exposed. Given the heterogeneous exposure map of the sky gathered in the last 4 years of observations, detections are biased towards regions of the sky that have been exposed the longest (i.e. the Galactic plane and bulge).

However, Fig. 1 also demonstrates the effect that the evolution of each type of source has on its spatial distribution. Because their optical companions belong to an old stellar population, LMXBs are found predominantly in the Galactic bulge and/or they have had time to migrate off the plane of the Milky Way ($|b| \gtrsim 3$–$5°$). On the other hand, the stellar companions of HMXBs are young stars, so these systems must remain close to sites of recent stellar formation. Thus, the angular distribution of HMXBs reflects the spiral structure of the Galaxy, with an uneven distribution along the Galactic plane punctuated by peaks that are roughly consistent with the tangential directions to the inner spiral arms. Those HMXBs that have been detected at longitudes $|l| \gtrsim 90°$ correspond to systems located around spiral arms near the Sun. Evolutionary signatures like these were noticed in the past by *Ginga* (Koyama et al. 1990), *RXTE* (Grimm et al. 2002), and more recently with *INTEGRAL* (Dean et al. 2005; Lutovinov et al. 2005), although their samples were smaller than the one presented here.

Another way to demonstrate the role of stellar evolution in shaping the spatial distributions of LMXBs and HMXBs is to plot the positions of sources whose distances are known on a spiral arm model of the Milky Way. Russeil (2003) developed the Galactic spiral arm model that we used. Their model is based on the locations of star-forming complexes that include groups of OB stars, molecular clouds, H II regions, and diffuse ionised gas. The locations of these complexes are derived from a variety of tracers such as Hα, CO, the radio continuum and absorption lines.
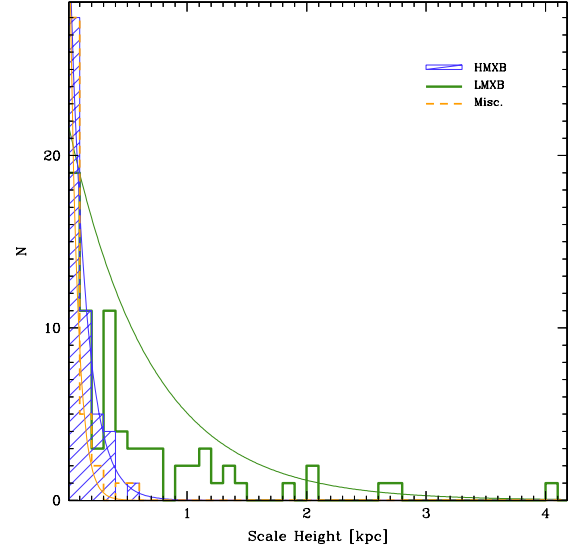
Fig. 7. Vertical scale height (in kpc) from the Galactic plane of HMXBs, LMXBs and miscellaneous sources whose distances are known. The distributions have been summed over the northern and southern Galactic hemispheres. Sources from the Magellanic Clouds are excluded. The curves represent the exponential model described in the text fit to the data (see Table 3 for parameters).

Table 3. Parameters from the model described in the text fit to the distributions of scale heights from the Galactic plane for HMXBs, LMXBs and miscellaneous sources whose distances are known. Objects from the Magellanic Clouds are excluded.

	k	α	h_0 [pc]
HMXBs	36 ± 3	7.5 ± 1.7	134^{+39}_{-25}
LMXBs	22 ± 3	1.5 ± 0.5	680^{+320}_{-160}
Misc.	41 ± 3	15 ± 4	66^{+23}_{-14}

While the uncertainties on distances can be large, Fig. 2 shows that HMXBs tend to occupy the outer disk and arms where young stars are formed, whereas LMXBs are clustered near the bulge where old globular clusters reside. A histogram of galactocentric radii (Fig. 3) shows LMXBs peaked at the center and decreasing gradually, while HMXBs roughly follow the distributions from H II/CO surveys (Russeil 2003) which are underabundant in the central few kpc and peak at the spiral arms. According to a Kolmogorov-Smirnov (KS) test, the probability is less than 0.01% that the galactocentric distributions of LMXBs and HMXBs are statistically compatible.

The distribution of LMXBs in the central Galaxy suggests an association with the Galactic bar (Fig. 2). Low-mass X-ray binaries whose distances are known and that have been detected by ISGRI are not prevalent on either side of the bar. Only 1 LMXB with a distance measurement has been detected in the Galactic center region bound by $0 < x < 3$ kpc and $-3 < y < 0$ kpc, indicating that the bar might be responsible for preventing an identification and distance measurement to be made for the faint counterparts to LMXBs situated behind it. As viewed from the Sun, the orientation of the bar leads to an apparent asymmetry of LMXBs in the central 3 kpc of the Galaxy ($|l| \lesssim 20°$): in this direction, ISGRI has detected 50%

more LMXBs at negative longitudes than at positive longitudes. Maps of Galactic absorption are expected to be symmetrical in this region (Dickey & Lockman 1990).

In Fig. 4, we present the Galactic distribution of star-forming complexes Russeil (2003) with the symbol size proportional to the excitation parameter in that region ($\equiv$ amount of ionising photons as determined from the radio continuum flux). High-mass X-ray binaries whose distances are known are symbolised by stars, while those with unknown distances were assigned a distance of 8.5 kpc and are represented by pentagons. The 4-arm spiral model of Russeil (2003) is also drawn. Figure 5 presents histograms of Galactic longitudes (integrated over the latitude) of HMXBs (shaded histogram, with $|b| < 6°$, in order to exclude sources in the Magellanic Clouds). Also shown are angular distributions of star-forming complexes from Russeil (2003) (divided by 3, thick histogram), and of ultra-compact H II regions detected by *IRAS* (Bronfman et al. 1996) (divided by 10, dashed histogram).

In general, the distribution of HMXBs along the plane of the Milky Way coincides with the expected radial distribution of young massive star-forming regions. A KS test yields a probability of 22% that the distributions of HMXBs and *IRAS* sources (shaded and dashed histograms, respectively, in Fig. 5) are statistically compatible. Excluding HMXBs that lie outside the survey region covered by Bronfman et al. (1996) ($|b| < 2°$ for $|l| < 60°$, and $|b| < 4°$ elsewhere) increases the probability of statistical compatibility to 34%. Peaks at Galactic longitudes $l \sim \pm30°$ are observed in both data sets corresponding to the direction of the inner spiral arm tangents (Norma and Scutum/Sagittarius arms). Bronfman et al. (1996) remark that the peaks in their distribution are also consistent with another active formation site of young, massive stars: a molecular ring situated at a radius of ~3 kpc from the Galactic center.

At first glance, the distributions of star-forming complexes of Russeil (2003) and HMXBs are also compatible (thick histogram in Fig. 5). The KS test returns a probability of only 3% which is misleading given the large number of objects in Russeil (2003) that are not very active. When selecting complexes with an excitation parameter > 10 pc cm^{-2}, which still represents 70% of the sample, the statistical compatibility improves to 41%.

Lutovinov et al. (2005) and Dean et al. (2005) found that the distribution of HMXBs was offset with respect to the directions of the spiral arm tangents. Lutovinov et al. (2005) note that ~ 10 Myr must elapse before one of the stars in a binary system collapses into a NS or BH, and that Galactic rotation will induce changes in the apparent positions of the arms relative to the Sun. This implies a delay between the epoch of star formation and the time when the number of HMXBs reaches its maximum. The observed displacement could simply stem from uncertainties in the distances to the HMXBs. Another problem is that the exact location of the arms depends on which Galactic model is used. Changes in the Sun-GC distance or in the pitch angles of the arms affects the radial scaling and shifts the tangential directions.

The propagation of density waves is believed to promote star formation in the spiral arms (Lin et al. 1969). Depending on the distance to the GC, the spiral arm pattern has angular velocities in the range of $\Omega \sim 20$–60 Gyr^{-1} (Bissantz et al. 2003). Hence, in the last ~ 10 Myr (corresponding roughly to the epoque when the inner spiral arms and the current density maxima of HMXBs overlapped), the inner arms of the Galaxy have rotated around the GC by $\sim 40°$. Individual stars (such as the Sun) or groups of stars have negligible movement in this scenario. Instead, star-forming sites that are now active (e.g. from

Russeil (2003)) should be about $\sim 40°$ away from those regions that were active some 10 Myr ago and that produced the current crop of HMXBs. Therefore, in order to reproduce the distribution of active star-forming sites as they were some 10 Myr ago, we introduced differential Galactic rotation to "unwind" the distribution of current star-forming complexes from Russeil (2003). Kolmogorov-Smirnov tests suggest that the effects of Galactic rotation are negligible, even when only the most active sites are considered.

The distribution of angular distances from the Galactic plane (in degrees, for $|b| < 20°$) of sources detected by ISGRI is shown in Fig. 6. The distributions were summed over the northern and southern Galactic hemispheres. Shaded histograms are HMXBs (left) and AGN (right), and the thick histograms represent LMXBs (left) and miscellaneous sources (right). The distribution of unclassified sources is given by the dashed histogram. Not surprisingly, the spread of the latitude distributions is larger in LMXBs than it is in HMXBs owing to the relative youth of the optical primaries in the latter. Also expected is the distribution of AGN which is more or less flat and which roughly follows the exposure map. However, the Galactic plane ($|b| \lesssim 3°$) is noticeably deficient in AGN detections despite the fact that the exposure map is biased here. This highlights the difficulty in detecting AGN at high energies and at low latitudes; these objects tend to be intrinsically absorbed, they are further obscured by the Galactic plane, and their counterparts have to be identified within a crowded field. Sazonov et al. (2007) noted that the exclusion of sources in the Galactic plane region ($|b| < 5°$) from an all-sky survey resulted in only a marginal reduction in the number of identified AGN, whereas the number of unclassified sources dropped significantly.

It is useful to examine the unclassified sources as they help to define the limits of our study. Almost all of the sources that are unclassified have position accuracies that are no better than a few arcminutes. This precludes establishing an optical counterpart for many unclassified sources located in crowded regions such as the Galactic plane. The transient nature of many unclassified sources implies a lack of immediate follow-up observations that would permit a classification. Because of their transience, many unclassified sources appear fainter than average in long-exposure mosaic images. Masetti et al. (2006) suggest that up to half of all unclassified sources could be AGN situated behind the Galactic plane, whereas Dean et al. (2005), working on a smaller sample, favor a Galactic origin for the unclassified sources of Bird et al. (2004) based on the slope of the Log(N)–Log(S) relation and other factors.

Unclassified sources have a distribution of Galactic latitudes that peaks in the central 3° from the Galactic plane and decreases gradually, suggesting a population of sources that are Galactic rather than extragalactic in origin (see Fig. 6). Many of the unclassified sources also happen to be transient, whereas AGN can vary but tend to emit persistently. Furthermore, the angular distribution of unclassified sources is very similar to the distribution of LMXBs with a KS-test probability of nearly 40% of statistical compatibility between unclassifieds and LMXBs, compared with 13% for miscellaneous sources, and less than 0.01% for either AGN or HMXBs.

While there are extragalactic sources among them, the population of unclassified sources is therefore likely to be composed primarily of Galactic sources such as LMXBs and miscellaneous sources. We are unable to elaborate on the proportions of the different classes, but it is clear from Fig. 6, and from the results of KS tests, that the unclassified sources are most similar to the LMXBs and miscellaneous sources in their distribution off
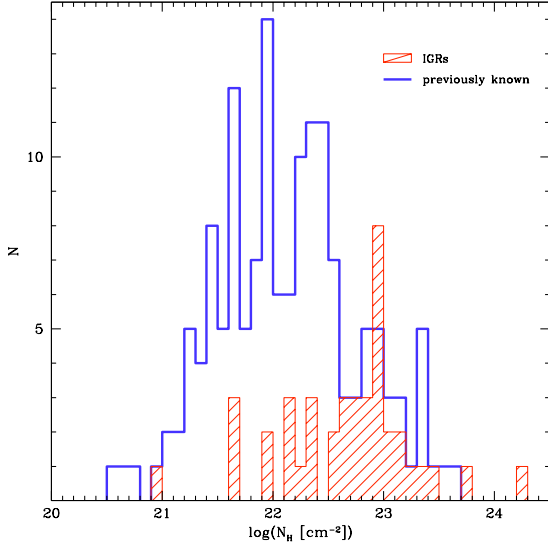
Fig. 8. The distribution of reported column densities (N_H) for Galactic sources (including sources in the Magellanic Clouds) detected by ISGRI that were previously known (152, clear histogram) and for IGRs (41, shaded histogram).

the Galactic plane. The reasons they have avoided classification (and detection by previous missions) are: the companion stars to LMXBs are usually faint in the optical/IR spectrum; they are located near the Galactic plane where absorption and source confusion prevent an identification; and, for many of these sources, their transient emission complicates efforts to perform follow-up observations. Recent improvements in Target of Opportunity campaigns aimed at new IGRs have uncovered as many new LMXBs in the last year than during the first 3 years of observations combined.

Figure 7 presents the distributions of scale heights (in kpc) for HMXBs (shaded histogram) and LMXBs (clear histogram) whose distances are known. Sources from the Magellanic Clouds are excluded. Following the procedure in Dean et al. (2005), we set the number of sources as a function of the distance in kpc above the Galactic plane (h) according to $N = k \cdot e^{-\alpha \cdot h}$ where $\alpha \equiv 1/h_0$ describes the steepness of the exponential. The parameters that best fit this model are listed in Table 3. The value that we derive for the characteristic scale height (h_0) of HMXBs is ~ 130 pc which is compatible with the value found by Grimm et al. (2002) with *RXTE* data, but slightly less than the value from Dean et al. (2005) ($\gtrsim 200$ pc). The characteristic scale height that we derive for LMXBs (~ 600 pc) is larger than the scale heights found by Grimm et al. (2002) and Dean et al. (2005) which were closer to ~ 400 pc. This is probably due to the greater coverage of the sky and larger sample size of our study. Miscellaneous sources have a distribution that is more similar to HMXBs than it is to LMXBs.

3.2. Absorption

The column densities along the light of sight of some sources in our sample are higher than the value expected from radio maps (Dickey & Lockman 1990) which implies absorbing material intrinsic to the source. On average, Galactic IGRs are more absorbed than the sources seen before *INTEGRAL* (by a factor of ~4) with IGRs representing a sizable contingent of objects that

have $N_H \sim 10^{23}$ cm^{-2} (see Fig. 8). The average column density of sources that were previously known is $N_H = 1.2 \cdot 10^{22}$ cm^{-2} ($\sigma \sim 0.7$) whereas IGRs have an average $N_H = 4.8 \cdot 10^{22}$ cm^{-2} ($\sigma \sim 0.6$). A KS test yields a probability of less than 0.01% that the two distributions are statistically compatible.

The classified Galactic IGRs are mostly HMXBs (Table 2) which usually exhibit high column densities, either intrinsically due to the geometry of the system or extrinsically due to their location along the dusty Galactic plane. Note, however, that the highest value of Galactic N_H is $\sim 3 \cdot 10^{22}$ cm^{-2} so objects with very large N_H can not be explained by interstellar absorption alone. Also keep in mind that the absorption from Dickey & Lockman (1990) tends to be underestimated given that local small-scale inhomogeneities and the contribution from molecular hydrogen are ignored. The main reason that more absorbed sources are being found is that by operating above 20 keV, ISGRI is immune to the absorption that prevented their discovery with earlier soft X-ray telescopes. A large absorption is also a common feature of extragalactic IGRs. However, our data show that as a group, they are not more absorbed than pre-*INTEGRAL* AGN, in agreement with the conclusions of Beckmann et al. (2006a) and Sazonov et al. (2007).

Figure 9 presents an all-sky map of sources detected by ISGRI with symbol sizes proportional to reported column densities (N_H). Contours of expected line-of-sight absorption (Dickey & Lockman 1990) are provided for levels of 10^{21}, $5 \cdot 10^{21}$ and 10^{22} cm^{-2}. One of the benefits of such a map is that potential clustering or asymmetries in the local distribution of matter can be studied. The lower portion of Fig. 9 shows that the Norma Arm region hosts many of the most heavily-absorbed Galactic sources ($N_H \geq 10^{23}$ cm^{-2}) continuing a previously noted trend (e.g., Kuulkers 2005; Lutovinov et al. 2005; Walter et al. 2006). This region also happens to be the most active formation site of young supergiant stars (Bronfman et al. 1996). These stars are the precursors to the absorbed HMXBs that ISGRI is discovering in the Norma Arm. The Galactic Bulge and the Scutum/Sagittarius Arms are also represented by obscured sources but to a lesser extent than in the Norma Arm.

For sources whose distance are known, we did not find any clear dependence of the intrinsic N_H on the distance to the source, nor did we find a dependence of N_H with the luminosity as derived from the soft-band fluxes (20–40 keV) listed in Bird et al. (2007).

3.3. Modulations

The strong magnetic fields in some NS X-ray binaries can produce non-spherically symmetric patterns of emission. If the magnetic and rotation axes are misaligned, this results in pulsations in the X-ray light curve.

Most IGRs for which a pulsation has been measured have spin periods (P_s) in the range of 100–1000 s, or around 10 times longer than the average pulse period of pre-*INTEGRAL* sources (Fig. 10). There are notable IGRs that represent extreme cases: IGR J00291+5934 has a pulse period of only 1.7 ms making it the fastest accretion-powered pulsar ever observed (Galloway et al. 2005), whereas IGR J16358−4726 has a spin period as long as 6000 s (Lutovinov et al. 2005; Patel et al. 2006). One of the reasons that IGRs have longer pulse periods than average is because many of them are SG HMXBs which are wind-fed systems with strong magnetic fields that tend to have the longest pulse periods (e.g. Corbet 1984). Another reason is that *INTEGRAL* and *XMM-Newton* feature long orbital periods around the Earth. This means that the source can be observed
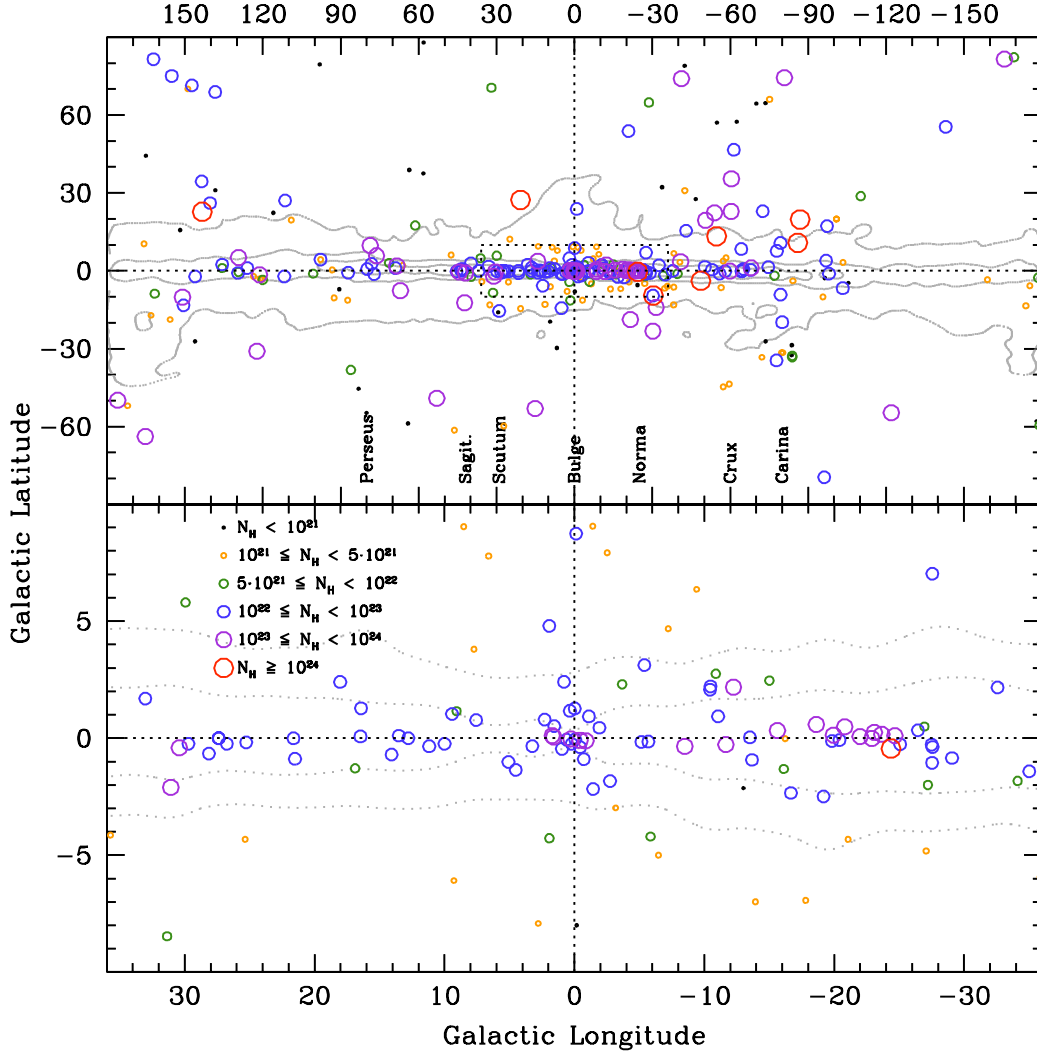
Fig. 9. Spatial distribution, in Galactic coordinates, of all sources detected by ISGRI for which N_H has been reported. The symbol size is proportional to the published column density. The figure at the top shows the whole sky and includes extragalactic sources, while the figure at the bottom focuses on the Bulge region (boxed region in the figure at the top) and excludes extragalactic sources. Contours denote Galactic absorption levels of 10^{21}, $5 \cdot 10^{21}$, and 10^{22} cm^{-2} (Dickey & Lockman 1990).

for long periods of time without interruptions, so that pulsations on the order of a few hundreds of seconds or more can be detected. Meanwhile, the previously-known sources in Fig. 10 include millisecond pulsars and other LMXBs, radio pulsars, CVs, etc., which are underrepresented among IGRs. To illustrate this, we performed a KS test which returned a very low probability (0.0007%) of statistical compatibility between the distributions of 18 IGRs (shaded histogram) and 92 previously-known pulsars of all types (clear histogram) as they are presented in Fig. 10. The KS-test probability improved by an order of magnitude when IGRs were compared to 49 previously-known HMXBs, and it improved by 3 orders of magnitude when IGRs were compared to 14 previously-known SG HMXBs. So *INTEGRAL* is not just finding new pulsars that are HMXBs, but these HMXBs are predominantly long-period systems with SG companions.

The distribution of orbital periods (P_o) of IGRs exhibits a similar bimodal shape to that seen in the distribution of orbital periods known before *INTEGRAL* (Fig. 11). The probability of statistical compatibility is nearly 80% according to a KS test.

The bimodal distribution represents 2 underlying populations: LMXBs (and miscellaneous sources) which tend to have short orbital periods, and HMXBs which tend to have longer orbital periods (Fig. 12).

In a Corbet P_s–P_o diagram (Corbet 1984), members of each subclass of HMXBs segregate into different regions of the plot owing to the complex feedback processes between the modulation periods and the dominant accretion mechanism. Figure 13 shows that the majority of IGRs are located among other known SG HMXBs. The figure also shows that Be HMXBs have longer orbital periods than SG HMXBs, in general. While this fact was already known (e.g. Stella et al. 1986), the discrepancy remains even though *INTEGRAL* has nearly doubled the number of such systems.

3.4. Modulations vs. Absorption

Accretion affects the spin period of a NS. If the velocity at the corotation radius (the radius at which the magnetic field regu-
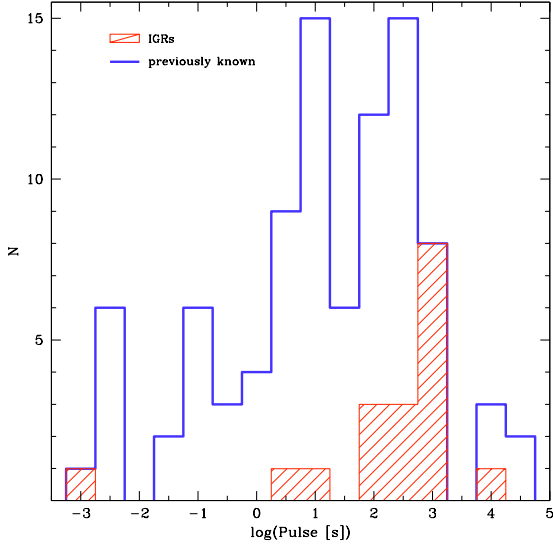
Fig. 10. Spin periods reported for sources detected by ISGRI that were previously known (92, clear histogram) and for IGRs (18, shaded histogram).
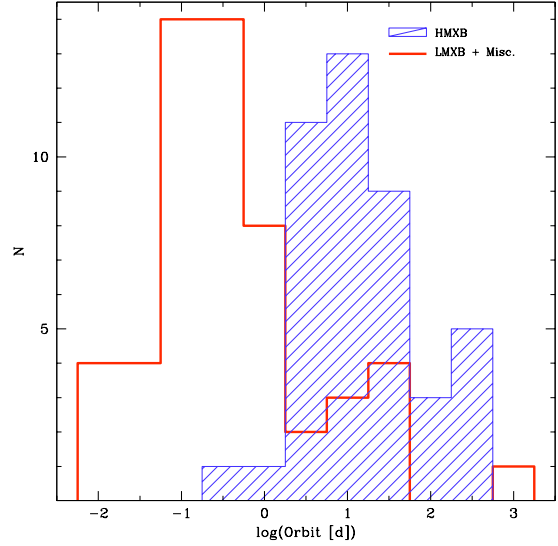
Fig. 12. Distribution of orbital periods of HMXBs (43, shaded histogram) compared with LMXBs and Miscellaneous sources (54, clear histogram).
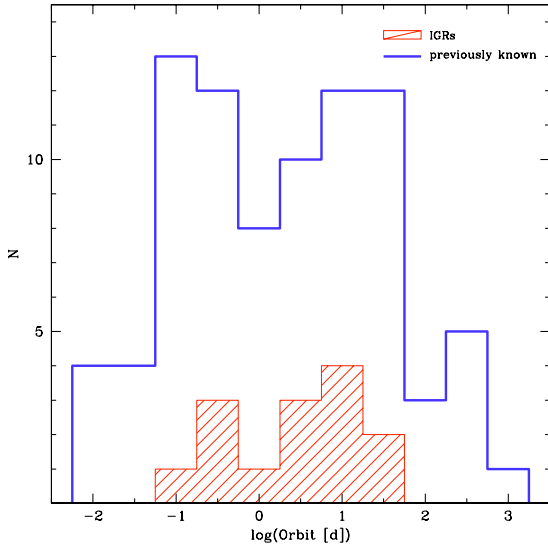
Fig. 11. Published orbital periods of sources detected by ISGRI. The clear histogram represents sources that were previously known (84) while the shaded histogram represents IGRs (14).
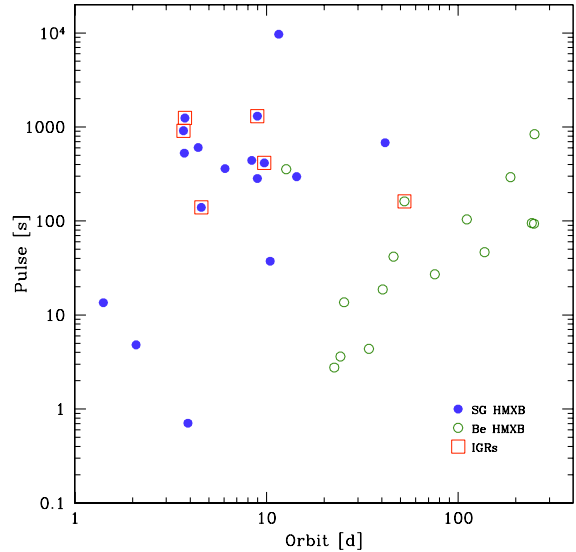
Fig. 13. Corbet diagram of spin vs. orbital period of HMXBs detected by ISGRI whose companions are OB supergiants (17, filled circles) or Be stars (15, empty circles). IGRs are boxed.

lates the motion of matter) exceeds the Keplerian velocity, then material will be spun away taking angular momentum with it and the NS will slow down due to the "propellor mechanism" (Illarionov & Sunyaev 1975). For corotation velocities smaller than the Keplerian velocity, the material is able to accrete onto the NS magnetosphere which will either spin up or spin down the NS depending on whether the angular momentum of the accreted material has the same or an opposite direction as the NS spin (Waters & van Kerkwijk 1989). So the spin rate of the pulsar in a HMXB is regulated by, among other things, the angular momentum of the wind of the stellar companion.

Assuming spherically-symmetric accretion from a radiation-driven wind of a SG star, the density of the wind as a function

of radius is $\rho(r) \propto r^{-2}$. On the other hand, the structure of the winds of Be stars is believed to consist of dense slow equatorial outflows and thin fast polar winds (Lamers & Waters 1987). The density drops much faster with the radius ($\rho(r) \propto r^{-3}$) (Waters et al. 1988). Therefore, the winds of Be stars present stronger density and velocity gradients inside the capture radius of the NS, in both radial and azimuthal directions, which suggests that wind-fed accretion is more efficient at delivering angular momentum to the NS in Be HMXBs than it is in SG HMXBs (Waters & van Kerkwijk 1989).

Given the density structures described above, and assuming a steady accretion rate of material whose angular momentum has the same direction as the spin of the NS, the

spin period of the NS will reach an equilibrium value $P_{\rm eq} \propto \rho^{-3/7}$. However, the present-day spin periods of NS in SG systems are much longer than predicted and are actually closer to $P_{\rm eq}$ of the stellar winds while the star was still on the MS (Waters & van Kerkwijk 1989). The equilibrium spin period in Be systems is constantly adjusting to the changing conditions in the winds (Waters & van Kerkwijk 1989). As with the SG systems, pulsars in Be systems are not currently spinning at $P_{\rm eq}$ but reflect the values of an earlier evolutionary stage (King 1991). So even though the transport of positive angular momentum through the wind is so inefficient that it can not spin up the pulsar to its expected equilibrium spin period, this does not influence how well the pulsar can be spun down by the "propellor mechanism" (Waters & van Kerkwijk 1989).

With a few exceptions, HMXBs from the Milky Way that have been detected by ISGRI are segregated into distinct regions of a $P_{\rm s}$–$N_{\rm H}$ diagram (Fig. 14) stemming from the higher average $N_{\rm H}$ and longer average $P_{\rm s}$ of SG HMXBs compared to Be HMXBs. The SG HMXBs set apart from the others ($P_{\rm s} < 50$ s) are Cen X-3 which is a Roche-lobe overflow system, and OAO 1657−415 which might be transitioning from a wind-fed to a disk-fed system (Audley et al. 2006). The $N_{\rm H}$ values of sources in Fig. 14 have been normalised by the line-of-sight values ($N_{\rm H}^{\rm G}$) from Dickey & Lockman (1990). This normalisation does not affect our conclusions but it helps to reduce the scatter in the vertical direction, particularly for nearby sources such as X Per.

There could be a weak positive correlation between the $N_{\rm H}$ and spin period for HMXBs as a group. There are no highly-absorbed sources ($N_{\rm H} > 10^{23}$ cm^{-2}) with spin periods shorter than a few tens of seconds, and there are no pulsars with $P_{\rm s} > 100$ s that are poorly absorbed ($N_{\rm H} < 10^{22}$ cm^{-2}). A least-squares fit to the data yields $P_{\rm s} \propto N_{\rm H}^{5/7}$. If we consider the $N_{\rm H}$ to be a reliable estimate of the density of matter around the compact object, then the slope that we find contradicts the slope expected from the equilibrium values ($\sim -3/7$). However, as noted above, the pulsars in Fig. 14 are spinning at periods that are longer than their equilibrium values would suggest.

Since Be HMXBs tend to have longer orbital periods than SG HMXBs (see Fig. 13), a distinction is also seen among the distributions of the $N_{\rm H}$ values and orbital periods of HMXBs with Be or SG companions (Fig. 15). There also appears to be an anti-correlation of $N_{\rm H}$ and orbital period: a least-squares fit to the data returns $P_{\rm o} \propto N_{\rm H}^{-3/7}$. In both types of systems, a shorter orbital period implies a compact object that is embedded deeper or spends more time in the dense regions of its stellar companion's wind resulting in more absorption. Therefore, Be HMXBs continue the trend set by SG HMXBs into long-orbital periodicity and low-$N_{\rm H}$ regions of the plot.

Spearman rank tests to the $P_{\rm s}$–$N_{\rm H}$ and $P_{\rm o}$–$N_{\rm H}$ distributions return weak positive and negative correlations with coefficients of 0.37 and −0.33, respectively, suggesting that the null hypothesis of mutual independence between $N_{\rm H}$ and $P_{\rm s}$ or $P_{\rm o}$ can be rejected. From Monte Carlo simulations, we determined that the probability of finding a Spearman rank coefficient $\gtrsim 0.33$ is around 5%. Admittedly, the scatter in the data is large as can be seen in Figs. 14–15. Because there are large uncertainties in the $N_{\rm H}$ and practically no uncertainty in the spin and orbital periods, the slope from a least-squares fit will tend to overestimate the real slope. Futhermore, the conclusions that we derive for how divergent species of objects react to changes in the local absorbing matter are based on a simplification of the underlying physics. The inclinations of the systems and their eccentricities, for example, are ignored. Even if we can not fit a slope of −3/7
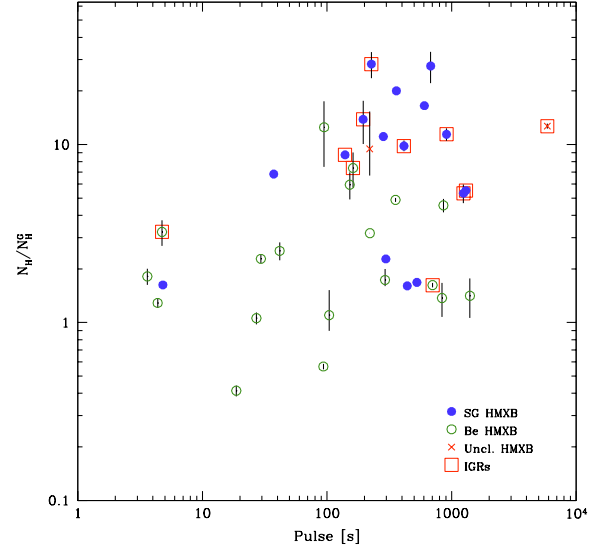
Fig. 14. Spin period as a function of reported $N_{\rm H}$ value (normalised by the expected Galactic value from (Dickey & Lockman 1990)) for HMXBs detected by ISGRI whose companions are OB supergiants (16, filled circles), Be stars (19, empty circles), or unclassified (2, crosses). IGRs are boxed and Magellanic Cloud sources are excluded.
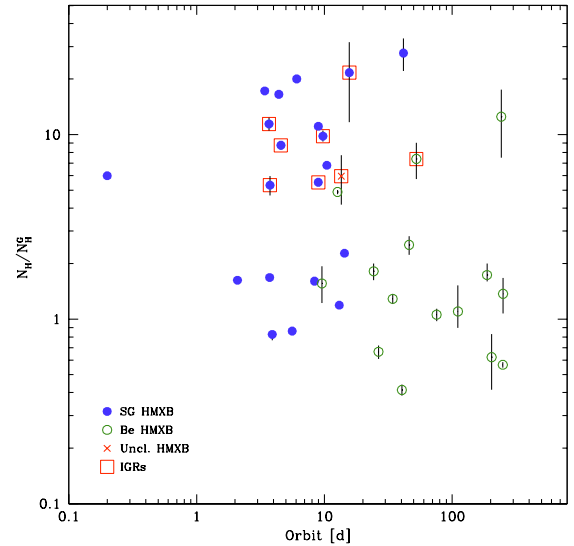
Fig. 15. Orbital period versus reported $N_{\rm H}$ value (normalised by the expected Galactic value from (Dickey & Lockman 1990)) for HMXBs detected by ISGRI whose companions are OB supergiants (20, filled circles), Be stars (15, empty circles) or unclassified (1, cross). IGRs are boxed and Magellanic Cloud sources are excluded.

to the data in Fig. 14, the correlations that we find in Figs. 14–15 might simply be due to the segregation of the 2 populations into distinct regions of the plots, rather than being due to physical processes.

Nevertheless, as more sources are added to these diagrams, the potential trends that have emerged could help constrain models describing the influence of local absorbing matter on the
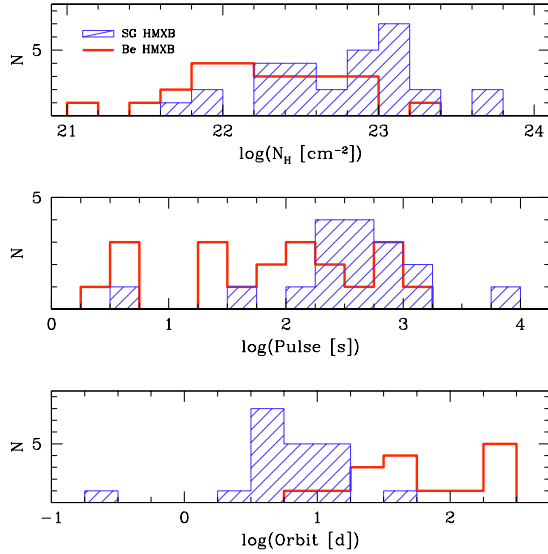
Fig. 16. Distribution of reported N_H (top), pulse periods (middle), and orbital periods (bottom) among HMXBs detected by ISGRI whose companions are OB supergiants (shaded histograms) or Be stars (clear histograms). Magellanic Cloud sources are excluded.

modulations. Another advantage of these plots is that the probable designation of an unidentified source is much more likely to be correct than when only a single parameter is used. This is illustrated in Fig. 16 where distributions of the 3 parameters in question (N_H, P_s and P_o) are presented for SG and Be HMXBs. Other than in the orbital periods, and in the extremities of the N_H and P_s distributions, there is little that differentiates the 2 groups. A HMXB selected from an average bin in either N_H or P_s has a roughly equal probability of hosting a SG or Be star. However, a random HMXB in the N_H–P_s plot will tend to be located among other members of its group.

Therefore, these diagrams could serve as new tools to help distinguish between SG and Be HMXBs when only N_H and either the spin or orbital periods are known. For example, IGR J19140+0951 has an orbital period of around 13 days and $N_H \sim 10^{23}$ cm^{-2}. It is positioned among other SG HMXBs so its companion is probably an OB supergiant (boxed cross in Fig. 15). This designation has already been suggested based on other criteria such as the source's persistent emission (Rodriguez et al. 2005). Recent IR observations of the source indicate a spectral type of B0.5-Ia which confirms the supergiant nature of the companion (D. Hannikainen, private communication). Similarly, AX J1749.2−2725 which is currently an unclassified HMXB could have a SG companion based on its position in Fig. 14 ($N_H > 10^{23}$ cm^{-2} and pulse period over 100 s). The other unclassified HMXB in Fig. 14 is IGR J16358−4726, whose NS has an unusually long spin period suggesting a magnetar nature for the source (Patel et al. 2006). This object is clearly in the SG HMXB camp based on its position in the plot.

4. Summary & Conclusions

We have compiled a catalogue of all ~500 sources that were detected by ISGRI during its first 4 years of observations. This includes published parameters such as positions, column densities, spin and orbital periods, and distances or redshifts. The primary aims of this catalogue were to gather in a single place the most important parameters of high-energy sources detected by ISGRI and to use this large sample to test against various theoretical predictions, to search for possible trends in the data, and to determine where new sources fit in the parameter space established by previously-known high-energy sources.

Clustered towards the spiral arm tangents and at low Galactic latitudes, HMXBs follow the distributions of tracers of star-forming regions. In contrast, most LMXBs are found in the Galactic bulge or have had time to migrate to high latitudes, typical of an older stellar population. The discrepancy is seen again in galactocentric profiles where the number of LMXBs gradually decreases from its maximum in the central kpcs, while HMXBs avoid the central kpcs and are overrepresented at the peaks of H II/CO distributions.

Over 200 new sources have been discovered by ISGRI but many of them remain unclassified. Although some may be AGN behind the plane, unclassified sources have a spatial distribution that resembles a Galactic population (notably LMXBs and CVs) rather than an extragalactic one. If the unclassified sources are composed primarily of LMXBs, as their spatial distributions and the transient emission of most them seem to suggest, then the reason they remain unclassified is because the faint optical/IR counterparts of such sources are difficult to identify in the crowded and obscure Galactic plane.

Since it operates above 20 keV and is unhindered by absorption, ISGRI is discovering many new HMXBs and AGN that are intrinsically absorbed ($N_H \sim 10^{22}$–10^{24} cm^{-2}). On average, Galactic IGRs are more absorbed (by a factor of ~4) than sources that were previously known.

Spin periods for most IGR pulsars are between a few hundred to a few thousand seconds or somewhat longer than the average spin periods of sources known before *INTEGRAL*. The distribution of orbital periods for IGRs closely resembles the bimodal distribution set by previously-known sources. The peaks correspond to 2 underlying populations: LMXBs and miscellaneous sources such as CVs and SNRs which tend to have short orbital periods, and HMXBs which have longer orbital periods, in general. Almost all IGRs for which both spin and orbital periods have been measured are located in the region of wind-fed accretion in the Corbet diagram. This is a testament to the number of new SG HMXBs that *INTEGRAL* has discovered.

Thanks to the larger sample size of these new SG HMXBs, we were able to test for dependences of the spin and orbital periods of HMXBs on the amount of absorbing matter local to the source. While scatter is an issue, there is a clear segregation of HMXBs in both plots which could be used to help assign Be or SG sompanions to sources that are still unclassified. There could be trends in both the P_s–N_H and P_o–N_H diagrams. The possible correlation of $P_s \propto N_H^{5/7}$ appears to contradict the expected slope (−3/7, e.g. (Corbet 1984)) which confirms that current spin periods are longer than the predicted equilibrium values, and that the spin-up of the pulsar via the wind is not as effective as the spin-down via the "propellor mechanism." The potential anti-correlation in the P_o–N_H plot means that the average column density varies inversely with the distance between the objects as one would expect. However, intrinsic absorption values can change and the potential trends we see, rather than being due to physical processes that make the parameters inter-dependent, could simply be the result of 2 populations of sources occupying different parameter spaces, i.e. SG HMXBs are generally more absorbed, they spin slower, and they have shorter orbits than Be HMXBs. Nevertheless, given N_H and either P_s or P_o for a HMXB, improves the chances of correctly predicting the type

of counterpart it has, compared with relying on only a single parameter. Of course, confirmation of the spectral type of the donor star in a HMXB still requires an optical/IR observation.

This work takes advantage of multi-wavelength observations in order to understand the nature of IGRs, and to help clarify the mechanisms that govern each type of source. Among the challenges facing more detailed population studies is the limited sample size of each subclass. This can only be alleviated by using large-FOV instruments such as *INTEGRAL* to search for new sources, and by regularly observing each new source in other wavelengths so that the accumulation of evidence rules out all but a single type of object. Many of the new sources which have been classified are absorbed HMXBs with supergiant companions. The increasing number of these systems discovered by *INTEGRAL* could alter our view of the Galactic population of hard X-ray sources and the evolutionary scenarios of their massive stellar companions.

References

Audley, M. D., Nagase, F., Mitsuda, K., Angelini, L., & Kelley, R. L. 2006, MNRAS, 367, 1147

Bassani, L., Molina, M., Malizia, A., et al. 2006, ApJ, 636, L65

Beckmann, V., Gehrels, N., Shrader, C. R., & Soldi, S. 2006a, ApJ, 638, 642

Beckmann, V., Soldi, S., Shrader, C. R., Gehrels, N., & Produit, N. 2006b, ApJ, 652, 126

Bird, A. J., Barlow, E. J., Bassani, L., et al. 2006, ApJ, 636, 765

Bird, A. J., Barlow, E. J., Bassani, L., et al. 2004, ApJ, 607, L33

Bird, A. J., Malizia, A., Bazzano, A., et al. 2007, ApJ in press, astro-ph/0611493

Bissantz, N., Englmaier, P., & Gerhard, O. 2003, MNRAS, 340, 949

Bodaghee, A., Walter, R., Zurita Heras, J. A., et al. 2006, A&A, 447, 1027

Bronfman, L., Nyman, L.-A., & May, J. 1996, A&AS, 115, 81

Corbet, R. H. D. 1984, A&A, 141, 91

Courvoisier, T. J.-L., Walter, R., Rodriguez, J., Bouchet, L., & Lutovinov, A. A. 2003, IAU Circ., 8063, 3

Dean, A. J., Bazzano, A., Hill, A. B., et al. 2005, A&A, 443, 485

Dickey, J. M. & Lockman, F. J. 1990, ARA&A, 28, 215

Ebisawa, K., Bourban, G., Bodaghee, A., Mowlavi, N., & Courvoisier, T. J.-L. 2003, A&A, 411, L59

Forman, W., Jones, C., Cominsky, L., et al. 1978, ApJS, 38, 357

Galloway, D. K., Markwardt, C. B., Morgan, E. H., Chakrabarty, D., & Strohmayer, T. E. 2005, ApJ, 622, L45

Grimm, H.-J., Gilfanov, M., & Sunyaev, R. 2002, A&A, 391, 923

Illarionov, A. F. & Sunyaev, R. A. 1975, A&A, 39, 185

Jonker, P. G. & Nelemans, G. 2004, MNRAS, 354, 355

King, A. R. 1991, MNRAS, 250, 3P

Koyama, K., Kawada, M., Kunieda, H., Tawara, Y., & Takeuchi, Y. 1990, Nature, 343, 148

Kuulkers, E. 2005, in AIP Conf. Proc. 797: Interacting Binaries: Accretion, Evolution, and Outcomes, ed. L. Burderi, L. A. Antonelli, F. D'Antona, T. di Salvo, G. L. Israel, L. Piersanti, A. Tornambè, & O. Straniero, 402–409

Lamers, H. J. G. L. M. & Waters, L. B. F. M. 1987, A&A, 182, 80

Lebrun, F., Leray, J. P., Lavocat, P., et al. 2003, A&A, 411, L141

Lebrun, F., Terrier, R., Bazzano, A., et al. 2004, Nature, 428, 293

Lin, C. C., Yuan, C., & Shu, F. H. 1969, ApJ, 155, 721

Liu, Q. Z., van Paradijs, J., & van den Heuvel, E. P. J. 2000, A&AS, 147, 25

Liu, Q. Z., van Paradijs, J., & van den Heuvel, E. P. J. 2001, A&A, 368, 1021

Lutovinov, A., Revnivtsev, M., Gilfanov, M., et al. 2005, A&A, 444, 821

Masetti, N., Morelli, L., Palazzi, E., et al. 2006, A&A, 459, 21

Patel, S. K., Zurita, J., Del Santo, M., et al. 2006, ApJ in press, astro-ph/0610768

Rodriguez, J., Bodaghee, A., Kaaret, P., et al. 2006, MNRAS, 366, 274

Rodriguez, J., Cabanac, C., Hannikainen, D. C., et al. 2005, A&A, 432, 235

Russeil, D. 2003, A&A, 397, 133

Sazonov, S., Revnivtsev, M., Krivonos, R., Churazov, E., & Sunyaev, R. 2007, A&A, 462, 57

Sguera, V., Barlow, E. J., Bird, A. J., et al. 2005, A&A, 444, 221

Stella, L., White, N. E., & Rosner, R. 1986, ApJ, 308, 669

Stephen, J. B., Bassani, L., Malizia, A., et al. 2006, A&A, 445, 869

Ubertini, P., Lebrun, F., Di Cocco, G., et al. 2003, A&A, 411, L131

Walter, R., Courvoisier, T. J.-L., Foschini, L., et al. 2004, in The INTEGRAL Universe. Proceedings of the Fifth INTEGRAL Workshop. 16-20 February 2004, Munich, Germany. Editor: B. Battrick, Scientific Editors: V. Schoenfelder, G. Lichti, & C. Winkler. ESA SP-552, Noordwijk: ESA Publication Division, ISBN 92-9092-863-8, 2004, p. 417-422., 417–422

Walter, R., Zurita Heras, J., Bassani, L., et al. 2006, A&A, 453, 133

Waters, L. B. F. M., van den Heuvel, E. P. J., Taylor, A. R., Habets, G. M. H. J., & Persi, P. 1988, A&A, 198, 200

Waters, L. B. F. M. & van Kerkwijk, M. H. 1989, A&A, 223, 196

Wen, L., Levine, A. M., Corbet, R. H. D., & Bradt, H. V. 2006, ApJS, 163, 372

White, N. E. & van Paradijs, J. 1996, ApJ, 473, L25+

Winkler, C., Courvoisier, T. J.-L., Di Cocco, G., et al. 2003, A&A, 411, L1

Zurita Heras, J. A., de Cesare, G., Walter, R., et al. 2006, A&A, 448, 261

Table 1. The parameters of sources detected by ISGRI.

Name	R.A. (J2000)	Dec.	Error (min)	l	b (deg)	N_H (10^{22} cm^{-2})	Spin (s)	Orbit (d)	Distance (kpc or [z])	Type	Ref.
IGR J00040+7020	00 04 01	+70 20 10	3.8	118.930	7.834	–	–	–	–	Unclassified (AGN?)	1
IGR J00234+6141	00 22 54	+61 42 22	4.8	119.557	−0.978	–	570	–	0.3	CV (IP)	1,2,3
IGR J00245+6251	00 24 28	+62 50 35	2.3	119.860	0.132	–	–	–	–	GRB	1
4U 0022+63	00 25 17	+64 09 32	3.6	120.086	1.432	–	–	–	2.83(79)	SNR	1,4
IGR J00254+6822	00 25 26	+68 22 50	2.3	120.529	5.630	–	–	–	–	Unclassified (Sey-2?)	5
V709 Cas	00 28 48.87	+59 17 21.8	0.017	120.042	−3.455	0.8±0.4	312.746(3)	0.2225(2)	0.230(20)	CV (DQ Her)	6,7,8,9
IGR J00291+5934	00 29 03.08	+59 34 19.2	0.01	120.096	−3.176	$0.43^{+0.07}_{-0.05}$	0.0016698(1)	0.1023622(4)	$5.1^{+0.3}_{-0.4}$	LMXB (P, T)	10,11,12,13,14
IGR J00335+6126	00 33 35	+61 26 52	3.3	120.800	−1.350	–	–	–	–	Unclassified	5
1ES 0033+59.5	00 35 52.63	+59 50 04.6	0.017	120.976	−2.978	0.36±0.08	–	–	0.086	BL Lac	15,16
IGR J00370+6122	00 37 09.63	+61 21 36.5	0.002	121.221	−1.464	13±6	–	15.670(4)	3	HMXB (SG)	17,18,19,20
Mrk 348	00 48 47.14	+31 57 25.1	0.017	122.276	−30.911	~30	–	–	0.0154	Sey-2	21,22,23
RX J0053.8−7226	00 53 55.0	−72 26 47	0.167	302.669	−44.681	0.23±0.11	46.63(4)	137.4(4)	65	HMXB (Be, P, T, in SMC)	24,25,26,27
gam Cas	00 56 42.53	+60 43 00.3	0.002	123.577	−2.148	0.3±0.1	–	203.59(29)	0.19	HMXB (Be)	17,28,29,30
SMC X−1	01 17 05.09	−73 26 36.0	0.002	300.415	−43.559	0.255±0.009	0.7071801(44)	3.8921(4)	65	HMXB (SG, P, E)	19,31,32
3A 0114+650	01 18 02.70	+65 17 29.8	0.002	125.710	2.563	–	9700	11.588(3)	7.0(3.2)	HMXB (P)	17,33,34,35
H 0115+634	01 18 31.9	+63 44 24	0.017	125.924	1.026	1.74±0.18	3.614690(2)	24.31535(5)	8(1)	HMXB (Be, P, T)	24,36,37,38
NGC 526	01 23 54.2	−35 03 55	0.017	263.758	−79.459	1.6±0.2	–	–	0.0192	Sey-1.5	39,40,41
IGR J01363+6610	01 36 05	+66 09 58	3.7	127.427	3.685	–	–	–	2	HMXB (Be, T)	1,42
ESO 297−18	01 38 37.18	−40 00 40.7	0.017	268.727	−73.829	–	–	–	0.0252	Sey-2	43,44
4U 0142+614	01 46 22.41	+61 45 03.2	0.017	129.384	−0.431	0.96±0.02	8.6882(2)	–	2.7	AXP	30,45,46
RX J0146.9+6121	01 47 00.17	+61 21 23.7	0.034	129.541	−0.800	1.2±0.3	1404.2	–	2.5	HMXB (Be, P, T?)	24,47,48
IGR J01528−0326	01 53 01	−03 26 28	4	157.442	−62.114	–	–	–	0.01691	Sey-2	1,49
IGR J01583+6713	01 58 18.2	+67 13 26	0.058	129.352	5.189	~10	–	–	6.4	HMXB (Be, T)	3,50,51
NGC 788	02 01 06.45	−06 48 55.9	0.017	165.254	−63.805	21±0.5	–	–	0.0136	Sey-2	16,22,52
IGR J02097+5222	02 09 46	+52 22 48	3	134.876	−8.666	–	–	–	0.0492	Sey-1	44,53
SWIFT J0216.3+5128	02 16 33	+51 25 52	5	136.183	−9.238	–	–	–	–	Sey-2	1
Mrk 1040	02 28 14.59	+31 18 39.4	0.017	146.115	−27.166	~0.067	–	–	[0.016338(314)]	Sey-1.5	54,55,56
IGR J02343+3229	02 34.3	+32 29	2	146.869	−25.563	–	–	–	0.01574	Sey-2	49
NGC 985	02 34 37.77	−08 47 15.4	0.017	180.836	−59.490	$0.6^{+0.5}_{-0.2}$	–	–	[0.04274(5)]	Sey-1	57,58,59
GT 0236+610	02 40 31.67	+61 13 45.6	0.017	135.675	1.086	0.60±0.05	–	26.52(4)	2.5	HMXB (Be, muQSO)	17,30,60,61
NGC 1052	02 41 04.80	−08 15 20.8	0.017	182.019	−57.925	$0.041^{+0.16}_{-0.020}$	–	–	[0.004930(87)]	Sey-2	56,62,63
RBS 345	02 42 16	+05 31 48	5.5	166.437	−47.759	–	–	–	0.069	Sey-1	1,64
NGC 1068	02 42 40.83	−00 00 48.4	0.017	172.104	−51.934	~0.1	–	–	[0.003786(33)]	Sey-2	54,56,65
QSO B0241+62	02 44 57.70	+62 28 06.5	0.017	135.636	2.430	1.5±0.3	–	–	[0.04456(51)]	Sey-1	16,56,66
IGR J02501+5440	02 50 11	+54 40 41	3	139.619	−4.300	–	–	–	–	Unclassified (AGN?)	5
MCG−02−08−014	02 52 23.3	−08 30 38	0.017	185.556	−55.885	–	–	–	[0.016758(13)]	Sey-2	56,67
NGC 1142	02 55 12.32	−00 11 01.7	0.017	175.876	−49.889	~45	–	–	[0.028847(47)]	Sey-2	22,54,68
QSO B0309+411	03 13 01.962	+41 20 01.18	0.017	149.577	−14.098	–	–	–	0.136	Sey-1	62,69
IGR J03184−0014	03 18 24	−00 13 44	4	181.762	−45.644	–	–	–	–	QSO	1

Table 1. continued.

Name	R.A. (J2000)	Dec.	Error	l (deg)	b	N_H (10^{22} cm^{-2})	Spin (s)	Orbit (d)	Distance (kpc or [z])	Type	Ref.
NGC 1275	03 19 48.16	+41 30 42.1	0.017	150.576	−13.261	1.5±0.7	–	–	0.017559	Sey-2	16,62
1H 0323+342	03 24 41.161	+34 10 45.86	0.017	155.727	−18.757	~0.1	–	–	0.062	Sey-1	22,70,71
GK Per	03 31 11.82	+43 54 16.8	0.017	150.955	−10.104	17.54±0.29	351.34	2.00	0.420	CV (IP)	6,9,72
IGR J03334+3718	03 33 18.8	+37 18 11	0.017	155.275	−15.202	–	–	–	0.05471	Sey-1	73
NGC 1365	03 33 36.5	−36 08 17	0.017	237.952	−54.598	44±8	–	–	0.005559	Sey-1.8	40,56,74
EXO 0331+530	03 34 59.9	+53 10 23	0.017	146.052	−2.194	1.10±0.07	4.3751(2)	34.25(10)	7.5(1.5)	HMXB (Be, P, QPO, T)	24,75,76,77,78
IGR J03532−6829	03 53 14	−68 28 59	3.6	282.738	−40.784	–	–	–	0.087	BL Lac	1,3
X Per	03 55 23.08	+31 02 45.0	0.002	163.081	−17.136	0.129±0.028	837.8(1)	250.3(6)	0.700(300)	HMXB (Be, P)	17,19,79,80,81
3C 111	04 18 21.28	+38 01 35.8	0.017	161.676	−8.820	~0.9	–	–	0.0485	Sey-1	16,82
UGC 3142	04 43 46.89	+28 58 19.0	0.017	172.089	−10.996	–	–	–	[0.02183(19)]	Sey-1	54,56
LEDA 168563	04 52 04.7	+49 32 45	0.017	157.252	3.419	–	–	–	0.029	Sey-1	56,83
ESO 33−2	04 55 59.6	−75 32 26	0.017	287.767	−33.285	~0.1	–	–	[0.01843(46)]	Sey-2	22,56,84
IGR J05007−7047	05 00 46.08	−70 44 36.0	0.01	282.167	−34.525	1.0±0.2	–	–	50	HMXB (in LMC)	85,86
IGR J05053−7343	05 05 19	−73 42 58	3.6	285.463	−33.309	–	–	–	–	Unclassified (T)	1
4U 0517+17	05 10 45.5	+16 29 55	0.017	186.114	−13.499	~0.1	–	–	0.017879	Sey-1.5	22,87,88
Ark 120	05 16 11.48	−00 09 00.6	0.017	201.695	−21.132	–	–	–	0.033687	Sey-1	54,74
SGR 0526−66	05 26 00.89	−66 04 36.3	0.01	276.087	−33.246	0.54±0.02	8.0470(2)	–	–	SGR (P)	89
IGR J05270−6631	05 27 01	−66 30 40	4.4	276.585	−33.088	–	–	–	–	Unclassified	1
EXO 053109−6609.2	05 31 13.3	−66 07 05	0.067	276.058	−32.718	$0.69^{+0.07}_{-0.13}$	13.66817(1)	25.4	50	HMXB (Be, P, T, in LMC)	90,91
IGR J05319−6601	05 31.9	−66 02	3.5	275.949	−32.659	–	–	–	–	Unclassified (T)	92
LMC X−4	05 32 49.79	−66 22 13.8	0.017	276.335	−32.529	~0.055	13.503(1)	1.40841(2)	55	HMXB (SG, P)	93,94,95
Crab	05 34 31.97	+22 00 52.1	0.017	184.558	−5.784	0.260±0.001	0.0335(1)	–	2	SNR (PWN)	96,97,98,99
IGR J05346−5759	05 34.6	−58 00	3.5	266.390	−32.811	–	–	–	–	Unclassified (T, CV?)	92
1A 0535+262	05 38 54.57	+26 18 56.8	0.017	181.445	−2.644	$0.65^{+0.25}_{-0.12}$	104	111.0(4)	$2^{+0.4}_{-0.7}$	HMXB (Be, P, T)	17,24,100,101
LMC X−1	05 39 38.7	−69 44 36	0.05	280.203	−31.516	0.46±0.02	–	3.9081(15)	55	HMXB (SG, BHC)	24,102,103,104
PSR B0540−69.3	05 40 07.72	−69 20 05.1	0.017	279.721	−31.520	0.43±0.02	0.0504988(1)	–	55	Unclassified (P, in LMC)	31,105,106
BY Cam	05 42 48.90	+60 51 31.8	0.017	151.833	15.690	~0.001	11960.2(2)	0.139759(3)	0.190	CV (AM Her)	6,9,107,108
MCG+08−11−011	05 54 53.63	+46 26 21.8	0.017	165.731	10.407	$0.183^{+0.006}_{-0.003}$	–	–	0.020484	Sey-1.5	16,54,109
IRAS 05589+2828	06 02 09.7	+28 28 17	0.017	182.238	2.892	–	–	–	0.0330	Sey-1	22,110
SWIFT J0601.9−8636	06 05 39.1	−86 37 52	0.082	299.201	−27.747	–	–	–	[0.006(1)]	AGN (Sey-2?)	111,112
IGR J06074+2205	06 07.4	+22 05	2	188.392	0.798	–	–	–	1	HMXB (Be)	3,113
PKS 0611−663	06 11 43.20	−66 24 30.0	0.017	276.241	−28.639	0.048±0.011	–	–	–	AGN	114,115
Mrk 3	06 15 36.31	+71 02 14.9	0.017	143.296	22.719	127^{+24}_{-22}	–	–	[0.01344(31)]	Sey-2	54,56,116
H 0614+091	06 17 07.3	+09 08 13	0.017	200.877	−3.364	0.37±0.02	0.0030(2)	–	$2.2^{+0.8}_{-0.7}$	LMXB (P, QPO, B, A)	117,118,119,120
IGR J06239−6052	06 23 55	−60 53 53	4.9	270.195	−26.761	–	–	–	–	Unclassified (T, AGN?)	1
IGR J06253+7334	06 25 22	+73 36 07	5.2	140.832	24.137	–	1187.3(1)	0.1965(2)	0.5	CV (IP)	1,9,121
IGR J06292+4858	06 29 12	+48 58 26	5	165.939	16.703	–	–	–	–	Unclassified	1
PKS 0637−752	06 35 46.51	−75 16 16.8	0.002	286.368	−27.158	0.035±0.005	–	–	0.651	Sey-1	62,122
Mrk 6	06 52 12.32	+74 25 36.8	0.017	140.328	26.107	$1.94^{+0.09}_{-0.14}$	–	–	[0.01868(83)]	Sey-1.5	54,56,123

Table 1. continued.

Name	R.A. (J2000)	Dec.	Error	l (deg)	b	N_H (10^{22} cm^{-2})	Spin (s)	Orbit (d)	Distance (kpc or [z])	Type	Ref.
LEDA 96373	07 26 26.3	−35 54 21	0.017	248.767	−9.076	–	–	–	[0.029624(544)]	Sey-2	56
IGR J07295−1329	07 29 30	−13 09 29	5.4	228.966	2.262	–	–	–	–	Unclassified	1
IGR J07437−5137	07 43 41	−51 37 01	5	264.477	−13.447	–	–	–	–	Unclassified	1
EXO 0748−676	07 48 33.8	−67 45 09	0.017	279.978	−19.811	8^{+5}_{-3}	–	0.1593375(6)	$8.0^{+1.1}_{-1.2}$	LMXB (B, D, T)	19,117,124,125
IGR J07506−1547	07 50 35	−15 47 17	1.7	233.770	5.423	–	–	–	–	Unclassified (T)	126
IGR J07565−4139	07 56 19.62	−41 37 42.1	0.01	256.656	−6.723	1.1±0.2	–	–	[0.021(1)]	Sey-2	85,86
IGR J07597−3842	07 59 41.819	−38 43 56.03	0.002	254.495	−4.679	~0.05	–	–	[0.040(1)]	Sey-1.2	86,127
ESO 209−12	08 01 57.6	−49 46 42	0.017	264.253	−10.026	~0.1	–	–	[0.03959(58)]	Sey-1.5	22,56
IGR J08023−6954	08 02.3	−69 55	3	282.616	−19.589	–	–	–	–	Unclassified (T)	128
PG 0804+761	08 10 58.66	+76 02 42.5	0.017	138.279	31.033	0.023±0.011	–	–	0.100	Sey-1	122,129
Vela Pulsar	08 35 20.66	−45 10 35.2	0.017	263.552	−2.787	0.033±0.003	0.0893	–	$0.294^{+0.076}_{-0.050}$	SNR (PWN)	62,130,131
Ginga 0836−429	08 37 23.6	−42 54 02	0.167	261.954	−1.124	2.2±0.3	–	–	10.0	LMXB (B, T)	30,117,132
Fairall 1146	08 38 30.7	−35 59 35	0.017	256.585	3.230	~0.1	–	–	[0.0318(3)]	Sey-1.5	22,56
IGR J08408−4503	08 40 47.97	−45 03 29.8	0.09	264.041	−1.950	–	–	–	3	HMXB (SG, SFXT)	133
QSO B0836+710	08 41 24.37	+70 53 42.2	0.017	143.541	34.426	$1.1^{+1.6}_{-0.8}$	–	–	2.172	Blazar	21,62,134
Vela X−1	09 02 06.86	−40 33 16.9	0.017	263.058	3.930	$5.6^{+0.3}_{-0.2}$	283.2(1)	8.965(4)	1.9(2)	HMXB (SG, P, E)	17,19,135,136,137
IGR J09025−6814	09 02 27	−68 14 06	5.1	284.169	−14.178	–	–	–	–	Unclassified (T)	1
IGR J09026−4812	09 02 40	−48 12 58	2.3	268.866	−1.072	–	–	–	–	Unclassified	126
IGR J09103−3741	09 10 18	−37 40 30	5.2	261.972	7.035	–	–	–	–	Unclassified (T)	1
SWIFT J0917.2−6221	09 16 09.41	−62 19 29.5	0.017	280.612	−9.195	~1	–	–	[0.05715(21)]	Sey-1	56,138,139
EXMS B0918−549E	09 20 05	−55 08 35	0.9	275.771	−3.837	–	–	–	–	Unclassified (T)	126
H 0918−549	09 20 26.95	−55 12 24.7	0.01	275.853	−3.845	0.24±0.03	–	–	$5.0^{+0.8}_{-0.7}$	LMXB (B, QPO)	125,140
Mrk 110	09 25 12.87	+52 17 10.5	0.017	165.011	44.364	0.019±0.001	–	–	[0.035398(510)]	Sey-1 (NL)	55,56,57
IGR J09253+6929	09 25 17	+69 29 17	4.7	143.423	38.392	–	–	–	–	Unclassified	1
IGR J09446−2636	09 44.6	−26 36	3	259.106	19.968	~0.1	–	–	0.1425	Sey-1	22
1RXS J094436.5−263353	09 44 36.50	−26 33 53.0	0.017	259.081	19.995	~0.1	–	–	0.0492	Sey-1	22,141
4U 0937−12	09 45 42.05	−14 19 35.0	0.017	249.706	28.781	$0.85^{+0.05}_{-0.04}$	–	–	[0.007710(13)]	Sey-2	40,52,68
IGR J09469−4603	09 46 53	−46 02 46	4.8	272.736	5.726	–	–	–	–	Unclassified	1
MCG−05−23−016	09 47 40.2	−30 56 54	0.017	262.744	17.234	1.80±0.23	–	–	[0.00823(16)]	Sey-2	56,142,143
IGR J09485−4726	09 48 29	−47 25 37	4.9	273.838	4.843	–	–	–	–	Unclassified	1
IGR J09523−6231	09 52 17	−62 30 58	3.9	283.832	−6.490	–	–	–	–	Unclassified	1
IGR J10043−8702	10 04.3	−87 02	3.4	300.753	−24.899	–	–	–	–	Unclassified (T)	144
GRO J1008−57	10 09 46	−58 17 32	0.017	282.998	−1.822	0.86±0.03	93.57(9)	248.9(5)	5	HMXB (Be, P, T)	24,30,103,145
SWIFT J1009.3−4250	10 09 48.3	−42 48 44	0.083	273.979	10.792	~100	–	–	0.03355	Sey-2	146
IGR J10101−5654	10 10 11.866	−56 55 32.06	0.002	282.257	−0.672	–	–	–	–	HMXB (T)	86
IGR J10109−5746	10 11 02.95	−57 48 13.9	0.017	282.855	−1.325	–	–	–	–	Symbiotic Star	147
IGR J10147−6354	10 14 42	−63 53 31	5	286.695	−6.078	–	–	–	–	Unclassified	1
NGC 3227	10 23 30.62	+19 51 53.7	0.017	216.992	55.445	6.8±0.3	–	–	0.003827	Sey-1.5	54,65,148
IGR J10252−6829	10 25 00.49	−68 27 27.3	0.01	290.112	−9.311	–	–	–	–	Unclassified (T)	85

Table 1. continued.

Name	R.A.	Dec. (J2000)	Error	l (deg)	b (deg)	$N_{\rm H}$ (10^{22} cm^{-2})	Spin (s)	Orbit (d)	Distance (kpc or [z])	Type	Ref.
NGC 3281	10 31 52.06	−34 51 13.3	0.017	273.007	19.783	151^{+20}_{-19}	–	–	[0.011475(87)]	Sey-2	56,149,150
4U 1036−56	10 37 33.8	−56 47 58	0.017	285.350	1.431	4.6±0.4	860(2)	–	5.0	HMXB (Be, P, T)	30,141,151
SWIFT J1038.8−4942	10 38 45.0	−49 46 55	0.055	282.049	7.633	$1^{+2}_{-0.7}$	–	–	[0.060(1)]	Sey-1.5	112,139
IGR J10404−4625	10 40 23	−46 24 58	1.5	280.617	10.700	~1	–	–	[0.0240(6)]	Sey-2	56,126,152
IGR J10448−5945	10 44 47	−59 45 18	5.2	287.599	−0.708	–	–	–	–	Unclassified	1
IGR J10500−6410	10 50.1	−64 10	4	290.181	−4.341	–	–	–	–	Unclassified (T)	144
IGR J11085−5100	11 08 50.48	−51 02 32.8	0.01	286.954	8.619	–	–	–	–	Unclassified (T)	85
IGR J11098−6457	11 09 46	−64 56 46	5.5	292.432	−4.168	–	–	–	–	Unclassified	1
IGR J11114−6723	11 11 25	−67 23 31	1.7	293.521	−6.366	–	–	–	–	Unclassified (T)	126
IGR J11187−5438	11 18 42	−54 37 59	4	289.690	5.837	–	–	–	–	Unclassified	1
Cen X−3	11 21 15.78	−60 37 22.7	0.017	292.091	0.337	1.95±0.03	4.81423(1)	2.0871384(1)	10(1)	HMXB (SG, P, E)	93,153,154,155
IGR J11215−5952	11 21 46.9	−59 51 42	0.083	291.893	1.075	11±3	195(10)	–	6.2	HMXB (SG, P, SFXT)	152,156,157,158
IGR J11305−6256	11 31 06	−62 56 20	1.2	293.941	−1.478	–	–	–	3	HMXB (Be, T)	1,152
IGR J11321−5311	11 32.1	−53 11	2	291.087	7.854	–	–	–	–	Unclassified (T, BHC?)	159
IGR J11366−6002	11 36 38	−60 02 02	4.9	293.713	1.492	–	–	–	–	Unclassified (AGN?)	1
NGC 3783	11 39 01.78	−37 44 18.7	0.017	287.456	22.948	1.8±0.3	–	–	[0.00965(67)]	Sey-1	56,149,160
EXMS B1136−650	11 39 29	−65 24 18	3.2	295.533	−3.572	–	–	–	–	RS CVn Star (T)	1
IGR J11435−6109	11 44 00.4	−61 07 16	1.4	294.880	0.692	9±2	161.76(1)	52.46(6)	–	HMXB (Be, P, T)	161,162
1E 1145.1−6141	11 47 28.6	−61 57 14	0.017	295.490	−0.010	~3.3	296.573(2)	14.365(2)	8.5(1.5)	HMXB (SG, P)	24,163
H 1145−619	11 48 00.02	−62 12 24.9	0.017	295.611	−0.240	$2.6^{+0.4}_{-0.2}$	292.4	187.5	3.1(5)	HMXB (Be, P, T)	17,24,164,165
IGR J12026−5349	12 02 47.63	−53 50 07.7	0.01	295.714	8.353	2.2±0.3	–	–	[0.028(1)]	Sey-2	85,86
NGC 4051	12 03 09.63	+44 31 53.2	0.017	148.883	70.085	0.3±0.1	–	–	0.002336	Sey-1.5	54,65,166
NGC 4138	12 09 29.87	+43 41 06.0	0.017	147.305	71.404	8±1	–	–	[0.00296(13)]	Sey-1.9	54,56,65
NGC 4151	12 10 32.73	+39 24 19.6	0.017	155.077	75.064	7.5±0.1	–	–	[0.003262(67)]	Sey-1.5	54,56,65
NGC 4180	12 13 02.97	+07 02 17.8	0.017	276.792	67.940	–	–	–	[0.00690(21)]	AGN	54,56
EXMS B1210−645	12 13 05.28	−64 53 49	4.9	298.877	−2.328	–	–	–	–	Unclassified (T)	1
Was 49	12 14 17.81	+29 31 43.4	0.017	194.392	81.485	~10	–	–	0.064	Sey-2	71,167,168
Mrk 766	12 18 26.63	+29 48 45.6	0.017	190.681	82.271	~0.8	–	–	[0.012662(364)]	Sey-1.5	54,56,166
NGC 4258	12 18 57.54	+47 18 14.3	0.101	138.320	68.842	8.7±0.3	–	–	[0.001541(90)]	Sey-1.9	54,56,65
4C 04.42	12 22 22.55	+04 13 15.8	0.017	284.819	66.066	~0.1	–	–	[0.965001(207)]	Blazar	55,56,62
Mrk 50	12 23 24.14	+02 40 44.8	0.017	286.393	64.647	~0.018	–	–	[0.023196(277)]	Sey-1	55,56,169
NGC 4388	12 25 46.93	+12 39 43.3	0.017	279.124	74.336	27±2	–	–	[0.008426(57)]	Sey-2	54,56,65
NGC 4395	12 25 48.93	+33 32 47.8	0.017	162.095	81.533	5.3±0.3	–	–	0.001064	Sey-1.8	54,65,166
GX 301−2	12 26 37.6	−62 46 14	0.05	300.098	−0.035	50±10	679.5(5)	41.59(6)	4.1	HMXB (P, F, T)	19,24,170,171
XSS J12270−4859	12 28 02	−48 53 35	4.3	298.974	13.799	–	–	–	–	CV (IP)	1
3C 273	12 29 06.69	+02 03 08.6	0.017	289.951	64.360	$0.090^{+0.003}_{-0.005}$	–	–	0.15834	QSO	17,134,166
IGR J12349−6434	12 34 54.7	−64 33 56	0.1	301.158	−1.751	–	–	–	–	Symbiotic Star	172
NGC 4507	12 35 36.55	−39 54 33.3	0.017	299.639	22.861	29±2	–	–	[0.01177(14)]	Sey-2	16,56,149
SWIFT J1238.9−2720	12 38 54.5	−27 18 28	0.06	299.514	35.481	10^{+22}_{-7}	–	–	[0.025208(117)]	Sey-2	39,139

Table 1. continued.

Name	R.A.	Dec. (J2000)	Error	l (deg)	b (deg)	N_H (10^{22} cm^{-2})	Spin (s)	Orbit (d)	Distance (kpc or [z])	Type	Ref.
IGR J12391−1612	12 39 06.29	−16 10 47.1	0.01	298.621	46.589	1.9±0.3	–	–	0.0367	Sey-2	85
NGC 4593	12 39 39.43	−05 20 39.3	0.017	297.483	57.403	0.023±0.003	–	–	0.009	Sey-1	16,173,174
IGR J12415−5750	12 41 25.8	−57 50 03	0.017	301.595	5.012	~0.11	–	–	[0.0242(3)]	Sey-2	56,127,175
1H 1249−637	12 42 50.266	−63 03 31.05	0.017	301.958	−0.203	1.38±0.30	–	–	0.300(50)	HMXB (Be)	17,176,177
PKS 1241−399	12 44 29.34	−40 12 46.4	0.017	301.495	22.639	–	–	–	0.191	QSO	178
3A 1246−588	12 49 39.61	−59 05 13.3	0.005	302.703	3.784	0.29±0.09	–	–	5	LMXB (T)	179,180
ESO 323−32	12 53 20.35	−41 38 13.8	0.017	303.313	21.233	–	–	–	[0.015941(147)]	Sey-1	56,181
3C 279	12 56 11.17	−05 47 21.5	0.017	305.104	57.062	~0.02	–	–	0.53620	Blazar	16,62,166
1H 1254−690	12 57 37.2	−69 17 21	0.017	303.482	−6.424	0.31±0.01	–	0.163890(3)	13(3)	LMXB (B, D)	103,117,182,183
Coma Cluster	12 59 48.7	+27 58 50	0.017	58.079	87.958	0.0094±0.0009	–	–	0.0231	Cluster of Galaxies	166,184,185
IGR J13000+2529	13 00.0	+25 29	3	352.806	87.473	–	–	–	–	AGN	16
IGR J13020−6359	13 01 58.8	−63 58 10	0.05	304.088	−1.121	2.48±0.07	704.2(1.1)	–	5.5(1.5)	HMXB (Be, P)	186
Mrk 783	13 02 58.841	+16 24 27.46	0.017	317.527	78.951	0.046±0.014	–	–	0.067	Sey-1.5	55,57,71
IGR J13038+5348	13 03 59.39	+53 47 30.2	0.017	118.814	63.236	–	–	–	0.02988	Sey-1	73,187
NGC 4945	13 05 26.1	−49 28 15	0.017	305.268	13.337	425±25	–	–	[0.001908(60)]	Sey-2	56,188
IGR J13057+2036	13 05 42.56	+20 34 51.7	0.017	330.166	82.686	–	–	–	–	AGN	189
ESO 323−77	13 06 26.6	−40 24 50	0.017	306.020	22.368	55±33	–	–	[0.014904(73)]	Sey-1.2	16,56,84
IGR J13091+1137	13 09 05.60	+11 38 02.9	0.01	318.764	73.961	90±10	–	–	[0.02520(9)]	Sey-2	56,85
IGR J13109−5552	13 10 44	−55 51 47	3.4	305.657	6.907	–	–	–	–	Unclassified (AGN?)	1
NGC 5033	13 13 27.59	+36 35 36.9	0.017	98.057	79.448	~0.03	–	–	0.002919	Sey-1.9	54,65,166
IGR J13149+4422	13 15 15.73	+44 24 27	0.017	108.998	72.071	–	–	–	0.036698	Sey-2	190,191
IGR J13186−6257	13 18 36	−62 56 46	3.8	306.015	−0.237	–	–	–	–	Unclassified	1
Cen A	13 25 27.62	−43 01 08.8	0.017	309.516	19.417	10.0±0.6	–	–	0.00183	Sey-2	62,166,192
4U 1323−62	13 26 36.1	−62 08 10	0.017	307.028	0.456	2.42±0.14	–	0.1222(2)	15(5)	LMXB (B, D)	117,193,194
ESO 383−18	13 33 26.30	−34 00 58.7	0.017	312.787	28.050	–	–	–	0.0124	Sey-2	22,195
1RXS J133447.5+371100	13 34 47.808	+37 10 56.69	0.002	83.323	76.407	–	–	18.692	–	RS CVn	17,196
MCG−06−30−015	13 35 53.8	−34 17 44	0.017	313.292	27.680	0.03±0.01	–	–	[0.00789(16)]	Sey-1.2	56,197,198
NGC 5252	13 38 16.00	+04 32 32.5	0.017	331.299	64.803	$0.68^{+0.16}_{-0.07}$	–	–	[0.022219(884)]	Sey-2	40,54,56
Mrk 268	13 41 11.14	+30 22 41.2	0.017	52.467	78.630	–	–	–	[0.040408(804)]	Sey-2	56,167
4U 1344−60	13 47 32	−60 36 36	1	309.764	1.515	2.64±0.07	–	–	[0.012(1)]	Sey-1.5	1,166,199
IC 4329A	13 49 19.29	−30 18 34.4	0.017	317.496	30.920	0.42±0.02	–	–	[0.01602(15)]	Sey-1.2	16,56,149
IGR J14003−6326	14 00 37	−63 26 49	3.9	310.572	−1.606	–	–	–	–	Unclassified	1
V834 Cen	14 09 07.46	−45 17 17.1	0.017	316.979	15.454	1.03±0.39	–	0.07042	0.080	CV (DQ Her)	6,9,200
Circinus Galaxy	14 13 08.90	−65 20 27.0	0.017	311.324	−3.809	430^{+40}_{-70}	–	–	[0.00142(8)]	Sey-2	56,201,202
NGC 5506	14 13 14.87	−03 12 27.0	0.017	339.150	53.810	$3.42^{+0.24}_{-0.14}$	–	–	[0.00607(13)]	Sey-2	56,57,203
IGR J14175−4641	14 17 03.662	−46 41 41.19	0.002	317.862	13.680	–	–	–	[0.076(1)]	Sey-2	86
NGC 5548	14 17 59.65	+25 08 13.4	0.017	31.962	70.495	0.5±0.1	–	–	0.01676	Sey-1.5	54,204,205
RHS 39	14 19 22.2	−26 38 41	0.017	326.227	32.219	~0.05	–	–	[0.02224(17)]	Sey-1	16,56,64
IGR J14298−6715	14 29 21	−67 15 36	4.3	312.203	−6.168	–	–	–	–	Unclassified	1

Table 1. continued.

Name	R.A.	Dec. (J2000)	Error	l (deg)	b	$N_{\rm H}$ (10^{22} cm^{-2})	Spin (s)	Orbit (d)	Distance (kpc or [z])	Type	Ref.
IGR J14319−3315	14 31 57	−33 14 42	4.8	326.018	25.081	–	–	–	–	Unclassified	1
IGR J14331−6112	14 33 26	−61 12 14	3.7	314.901	−0.725	–	–	–	–	Unclassified	1
IGR J14471−6414	14 46 21	−64 17 38	4.6	314.998	−4.148	–	–	–	–	Unclassified	1
IGR J14471−6319	14 47 14.881	−63 17 19.24	0.002	315.521	−3.283	–	–	–	[0.038(1)]	Sey-2	86
IGR J14492−5535	14 49 13	−55 34 44	1.5	319.097	3.552	$10.1^{+6.3}_{-4.3}$	–	–	–	AGN	126,127
IGR J14515−5542	14 51 33.131	−55 40 38.40	0.002	319.350	3.318	~0.1	–	–	[0.018(1)]	Sey-2	22,86
IGR J14532−6356	14 53 14.88	−63 55 37	5.3	315.837	−4.151	–	–	–	–	Unclassified (T)	1
IGR J14536−5522	14 53 41.055	−55 21 38.74	0.002	319.763	3.465	–	–	–	0.190	CV (AM Her)	86
IGR J14552−5133	14 55 17.8	−51 34 17	0.017	321.716	6.726	~0.1	–	–	[0.016(1)]	Sey-1 (NL)	22,86
IGR J14579−4308	14 57 43.1	−43 07 48	0.017	326.120	13.984	–	–	–	[0.016261(150)]	Sey-2	84,206
IGR J15094−6649	15 09 26.013	−66 49 23.29	0.002	315.925	−7.499	–	–	–	0.140	CV (IP)	86
PSR B1509−58	15 13 54.6	−59 08 15	0.017	320.318	−1.162	0.82±0.03	0.1507477(1)	–	5.2(1.4)	SNR (PWN)	141,207,208,209
ESO 328−36	15 14 47.0	−40 21 31	0.017	330.405	14.745	–	–	–	0.0237	Sey-1	44,84
IGR J15161−3827	15 16 09	−38 26 53	5.3	331.711	16.206	–	–	–	–	Unclassified (AGN?)	1
Cir X−1	15 20 40.9	−57 10 01	0.017	322.118	0.037	1.6±0.1	–	16.55(1)	$9.2^{+1.3}_{-1.4}$	LMXB (B, A, T)	19,117,125,210
IGR J15283−4443	15 28.4	−44 44	3	330.056	9.715	–	–	–	–	Unclassified (T)	144
IGR J15359−5750	15 35 52	−57 49 55	1.3	323.431	−1.660	–	–	–	–	Unclassified	126
H 1538−522	15 42 23.3	−52 23 10	0.017	327.419	2.164	1.63±0.04	526.854(13)	3.7284(3)	6.4(1.0)	HMXB (SG, P, E)	19,24,211,212,213
XTE J1543−568	15 44 02	−56 42 43	4.2	324.985	−1.421	1.3±0.1	27.12156(59)	75.56(25)	10.0	HMXB (Be, P, T)	1,30,214
4U 1543−624	15 47 54.69	−62 34 05.4	0.01	321.757	−6.336	$0.31^{+0.02}_{-0.06}$	–	0.01264(7)	7	LMXB (NS?)	140,215,216
IGR J15479−4529	15 48 14.5	−45 28 45	0.15	332.439	7.022	9.5±0.8	693.01(6)	0.411(1)	0.69(15)	CV (IP)	217,218,219
NGC 5995	15 48 24.95	−13 45 28.0	0.017	354.960	30.719	–	–	–	[0.025091(357)]	Sey-2	56,220
XTE J1550−564	15 50 58.7	−56 28 36	0.034	325.882	−1.827	$0.88^{+0.12}_{-0.09}$	–	1.5420(10)	5.3(2.3)	LMXB (BHC, T)	125,221,222,223
IGR J15529−5029	15 52 56	−50 29 24	3.9	329.886	2.634	–	–	–	–	Unclassified	1
IGR J15539−6142	15 53 21	−61 40 16	3.9	322.822	−6.041	–	–	–	–	Unclassified (AGN?)	1
1H 1556−605	16 01 02.3	−60 44 18	0.017	324.139	−5.932	$0.30^{+0.01}_{-0.02}$	–	0.3807(3)	4.0	LMXB	30,117,215,224
IGR J16024−6107	16 02 26	−61 07 26	4.7	324.011	−6.333	–	–	–	–	Unclassified (AGN?)	1
IGR J16056−6110	16 05 35	−61 10 16	5	324.264	−6.622	–	–	–	–	AGN	1
IGR J16119−6036	16 11 51.4	−60 37 55	0.017	325.196	−6.744	~0.1	–	–	[0.015818(257)]	Sey-1	22,56,225
H 1608−522	16 12 43.0	−52 25 23	0.017	330.926	−0.850	1.28±0.06	–	0.5370(15)	3.3(5)	LMXB (B, T, A)	117,125,226,227
IGR J16167−4957	16 16 37.74	−49 58 44.5	0.01	333.056	0.496	$0.5^{+0.3}_{-0.2}$	–	–	0.170	CV (IP)	86,228
PSR J1617−5055	16 17 29.3	−50 55 13.2	0.017	332.499	−0.275	$1.6^{+2.4}_{-1.0}$	0.0693618(1)	–	3.3	Radio P	229,230,231,232
2E 1613.5−5053	16 17 36.3	−51 02 25	0.004	332.429	−0.374	$3.1^{+4.3}_{-2.1}$	21492^{+1692}_{-1584}	–	$0.7^{+3.8}_{-0.8}$	LMXB (P)	230,233,234
IGR J16185−5928	16 18 36.441	−59 27 17.36	0.002	326.630	−6.485	–	–	–	[0.035(1)]	Sey-1 (NL)	86
IGR J16194−2810	16 19 26	−28 09 36	1.5	349.076	15.539	–	–	–	–	AGN	126
IGR J16195−4945	16 19 32.20	−49 44 30.7	0.01	333.557	0.339	7^{+5}_{-3}	–	–	–	HMXB (SG, SFXT?)	228
Sco X−1	16 19 55.07	−15 38 24.8	0.002	359.094	23.784	2.37±0.5	–	0.78893(10)	2.8(3)	LMXB (QPO, Z)	125,235,236,237
IGR J16207−5129	16 20 46.26	−51 30 06.0	0.01	332.459	−1.050	$3.7^{+1.4}_{-1.2}$	–	–	4.6	HMXB (SG)	86,228

Table 1. continued.

Name	R.A.	Dec. (J2000)	Error	l (deg)	b	N_H (10^{22} cm^{-2})	Spin (s)	Orbit (d)	Distance (kpc or [z])	Type	Ref.
IGR J16248−4603	16 24 50	−46 02 35	4.7	336.804	2.322	–	–	–	–	Unclassified (T)	1
SWIFT J1626.6−5156	16 26 36.2	−51 56 33	0.058	332.780	−2.003	0.94±0.10	15.37682(5)	–	–	Unclassified (P, T, Be-HMXB?, LMXB?)	238,239
H 1624−490	16 28 02.83	−49 11 54.6	0.01	334.915	−0.263	$7.4^{+0.4}_{-0.2}$	–	0.86990(2)	15	LMXB (D)	19,240,241,242
IGR J16283−4838	16 28 10.7	−48 38 55	0.083	335.327	0.102	17^{+5}_{-4}	–	–	–	HMXB (T, NS?)	243,244
IGR J16287−5021	16 28 42	−50 20 38	4.4	334.161	−1.132	–	–	–	–	Unclassified	1
IGR J16316−4028	16 31.6	−40 28	3	341.700	5.281	–	–	–	–	Unclassified (T)	245
IGR J16318−4848	16 31 48.6	−48 49 00	0.067	335.617	−0.448	193±11	–	–	3.6(2.6)	HMXB	246,247,248
IGR J16320−4751	16 32 01.9	−47 52 27	0.05	336.330	0.169	$11.8^{+0.5}_{-0.4}$	1303.8(9)	8.96(1)	–	HMXB (SG, P)	249,250
4U 1626−67	16 32 16.8	−67 27 43	0.017	321.788	−13.092	0.11±0.02	7.66794(4)	0.028846(2)	9.0	LMXB (P)	30,117,251,252,253
IGR J16328−4726	16 32 46	−47 26 13	4.5	336.734	0.377	–	–	–	–	Unclassified (T)	1
4U 1630−47	16 34 00.4	−47 23 39	0.017	336.908	0.252	$11.03^{+0.28}_{-0.21}$	–	–	4.0	LMXB (BHC, D, T)	30,117,254
IGR J16351−5806	16 35 13.7	−58 04 48	0.017	329.128	−7.096	–	–	–	[0.009113(284)]	Sey-2	56
IGR J16358−4726	16 35 53.8	−47 25 41.1	0.01	337.099	−0.007	27.9±0.9	5871.3(3.5)	–	–	HMXB (P, T, LMXB?)	255,256
IGR J16377−6423	16 38 16.1	−64 20 50	0.017	324.604	−11.511	–	–	–	0.051	Cluster of Galaxies	257,258
IGR J16385−2057	16 38 30	−20 56 38	4.1	357.709	17.011	–	–	–	–	AGN	1
IGR J16393−4643	16 39 05.4	−46 42 12	0.067	338.002	0.075	25±2	911.3(1)	3.6875(6)	–	HMXB (SG, P)	259,260
H 1636−536	16 40 55.5	−53 45 05	0.017	332.915	−4.818	0.42±0.03	0.0017(1)	0.158048(2)	6.0(5)	LMXB (B, P, QPO, A)	103,117,261,262,263
IGR J16418−4532	16 41 51.0	−45 32 25	0.067	339.189	0.489	10.0±1.2	1246(100)	3.753(4)	–	HMXB (SG, P, E, SFXT?)	247,264
IGR J16426+6536	16 42 37	+65 35 38	4.5	96.716	37.678	–	–	–	–	Unclassified (T)	1
GX 340+0	16 45 47.7	−45 36 40	0.017	339.588	−0.079	3.9±0.4	–	–	11.0	LMXB (QPO, Z)	30,117,261
IGR J16460+0849	16 45 57	+08 49 05	5.2	26.297	31.853	–	–	–	–	Unclassified	1
IGR J16465−4507	16 46 35.5	−45 07 04	0.067	340.054	0.135	60±10	227(5)	–	12.5	HMXB (SG, P, T)	247,265
IGR J16479−4514	16 48 06.6	−45 12 08	0.067	340.163	−0.124	7.7±1.7	–	–	–	HMXB (SFXT?)	247
IGR J16482−3036	16 48 10	−30 35 35	1.1	351.432	9.231	$0.13^{+0.05}_{-0.13}$	–	–	[0.0313(6)]	Sey-1	126,127,152
IGR J16493−4348	16 49 26.92	−43 49 08.96	0.01	341.375	0.583	~10	–	–	–	Unclassified (HMXB?, LMXB?)	266,267
PSR J1649−4349	16 49 32	−43 50 08	0.62	341.372	0.561	–	0.8707116(1)	–	5.6	Radio P	268,269
IGR J16500−3307	16 50 01	−33 06 58	1.2	349.709	7.330	–	–	–	–	Unclassified	126
ESO 138−1	16 51 20.0	−59 14 02	0.017	329.609	−9.439	~150	–	–	0.009	Sey-2	16,56
NGC 6221	16 52 46.6	−59 12 59	0.017	329.740	−9.573	1.1±0.1	–	–	[0.00475(20)]	Sey-2	16,56
NGC 6240	16 52 58.97	+02 24 01.7	0.017	20.729	27.290	137±2	–	–	[0.024323(210)]	Sey-2	54,56,270
Mrk 501	16 53 52.22	+39 45 36.6	0.017	63.600	38.859	0.013±0.001	–	–	[0.033640(83)]	Blazar	56,62,271
GRO J1655−40	16 54 00.14	−39 50 44.9	0.002	344.982	2.456	$0.58^{+0.02}_{-0.01}$	–	2.621(7)	3.2(2)	LMXB (BHC, QPO, D, T)	103,117,125,272
IGR J16558−5203	16 56 05.618	−52 03 40.87	0.002	335.688	−5.492	~0.011	–	–	[0.054(1)]	Sey-1.2	86,127
SWIFT J1656.3−3302	16 56 16.56	−33 02 09.3	0.062	350.599	6.358	$0.390^{+0.17}_{-0.017}$	–	–	–	Unclassified (AGN?)	273
Her X−1	16 57 49.83	+35 20 32.6	0.017	58.149	37.523	$0.00019^{+0.00013}_{-0.00011}$	1.2377291(2)	1.70015(9)	6.6(4)	LMXB (P, E)	19,274,275,276,277
AX J1700.2−4220	17 00 18	−42 20.4	0.96	343.771	−0.027	$0.16^{+1.06}_{-0.16}$	–	–	–	HMXB (Be?)	278
OAO 1657−415	17 00 48.90	−41 39 21.6	0.008	344.369	0.319	12.0±0.4	37.348186(1)	10.44809(30)	7.1(1.3)	HMXB (SG, P, E)	279,280,281,282,283
IGR J17008−6425	17 00 49	−64 25 30	4.5	326.085	−13.473	–	–	–	–	Unclassified	1

Table 1. continued.

Name	R.A.	Dec. (J2000)	Error	l (deg)	b	$N_{\rm H}$ (10^{22} cm^{-2})	Spin (s)	Orbit (d)	Distance (kpc or [z])	Type	Ref.
XTE J1701−462	17 00 58.46	−46 11 08.6	0.002	340.813	−2.488	2.7±0.1	–	–	–	LMXB (QPO, T, Z)	284,285
GX 339−4	17 02 49.5	−48 47 23	0.017	338.939	−4.327	0.39±0.01	–	1.7563(3)	10^{+5}_{-4}	LMXB (BHC, QPO, T)	103,117,286,287
4U 1700−377	17 03 56.77	−37 50 38.9	0.017	347.754	2.173	12.7±0.3	–	3.4116(1)	1.9	HMXB (SG)	17,288,289,290
GX 349+2	17 05 44.5	−36 25 23	0.017	349.104	2.748	$0.673^{+0.048}_{-0.013}$	–	0.910(17)	9.2	LMXB (QPO, Z)	30,291,292,293
H 1702−429	17 06 15.31	−43 02 08.7	0.01	343.887	−1.318	~0.9	–	–	6.2(9)	LMXB (B, QPO, A)	125,240,294
H 1705−250	17 08 14.6	−25 05 29	0.034	358.587	9.057	~0.3	–	0.5213(13)	8.6(2)	LMXB (BHC, QPO, T)	117,125,295,296
IGR J17088−4008	17 08 49.0	−40 09 10	0.017	346.481	0.028	1.48±0.04	11.0017(4)	–	5	AXP	141,297
4U 1705−32	17 08 54.27	−32 19 57.1	0.01	352.780	4.672	0.40±0.10	–	–	13(2)	LMXB (B)	298
H 1705−440	17 08 54.47	−44 06 07.4	0.008	343.321	−2.342	1.42±0.06	–	–	8.4(1.2)	LMXB (B, A)	125,299
IGR J17091−3624	17 09 07	−36 24 25	0.5	349.524	2.214	~5	–	–	0.8	LMXB (BHC, muQSO, T)	1,300,301
XTE J1709−267	17 09 30.4	−26 39 19.9	0.01	357.473	7.912	0.44±0.02	–	–	10	LMXB (B, T)	30,302
IGR J17098−3628	17 09 45.9	−36 27 57	0.083	349.554	2.075	~1	–	–	–	BHC (T)	303
XTE J1710−281	17 10 12.3	−28 07 54	0.017	356.357	6.922	–	–	0.137	17.3(2.5)	LMXB (B, T)	117,125,304
4U 1708−40	17 12 23.83	−40 50 34.0	0.01	346.329	−0.929	3.3±0.5	–	–	–	LMXB (B)	305
Oph Cluster	17 12 26	−23 21 47	0.6	0.575	9.279	$0.20^{+0.09}_{-0.07}$	–	–	0.028	Cluster of Galaxies	126,306,307
SAX J1712.6−3739	17 12 34	−37 38.6	0.1	348.935	0.928	~1	–	–	6.9(1)	LMXB (B, T)	117,125,308
V2400 Oph	17 12 36.45	−24 14 44.6	0.017	359.867	8.739	4.3±1.7	927	0.1425	0.5	CV (DQ Her)	9,309,310,311,312
XTE J1716−389	17 15 46	−38 50 06	1.1	348.336	−0.279	10±5	–	–	–	HMXB (SG)	126,313
NGC 6300	17 16 59.2	−62 49 11	0.017	328.492	−14.051	29±2	–	–	[0.003706(50)]	Sey-2	16,56,84
IGR J17195−4100	17 19 35.88	−41 00 53.6	0.01	346.979	−2.137	$0.08^{+0.13}_{-0.08}$	–	–	0.110	CV (IP)	86,228
XTE J1720−318	17 19 54	−31 44 56	0.5	354.615	3.117	1.24±0.02	–	–	10	LMXB (BHC, T)	126,314,315
IGR J17200−3116	17 20 05.913	−31 16 59.65	0.002	355.022	3.347	–	–	–	–	HMXB (T)	86
IGR J17204−3554	17 20 25	−35 54 00	0.8	351.267	0.658	12±1	–	–	–	AGN	126,316
IGR J17252−3616	17 25 11.4	−36 16 59	0.067	351.497	−0.354	$15.3^{+1.1}_{-1.0}$	414.8(5)	9.741(4)	–	HMXB (SG, P, E)	317,318
IGR J17254−3257	17 25 25.5	−32 57 18	0.233	354.280	1.472	–	–	–	–	LMXB (B)	217
IGR J17269−4737	17 26 49.30	−47 38 25.5	0.002	342.203	−6.923	0.47±0.01	–	–	–	Unclassified (T, BHC?)	319,320
4U 1722−30	17 27 33.2	−30 48 07	0.017	356.320	2.298	0.78±0.05	–	–	$9.5^{+2.5}_{-2.0}$	LMXB (B, A)	117,321
IGR J17285−2922	17 28 41	−29 22 55	1.2	357.639	2.881	–	–	–	–	Unclassified (T, BHC?)	126
IGR J17303−0601	17 30 21.5	−05 59 34	0.116	17.929	15.013	–	127.99991(5)	0.6426(1)	–	CV (IP)	217,322
IGR J17314−2854	17 31 25	−28 53 42	3.2	358.375	2.650	–	–	–	–	Unclassified (T)	1
3A 1728−169	17 31 44.2	−16 57 42	0.017	8.513	9.038	0.19±0.01	–	0.174727(3)	4.4	LMXB (A)	30,103,117,323
GX 354−0	17 31 57.4	−33 50 05	0.017	354.302	−0.150	2.66±0.07	0.0028(1)	–	5.3(8)	LMXB (P, B, QPO, A)	117,125,324,325
V2487 Oph	17 31 59.8	−19 13 56	0.017	6.604	7.775	~0.4	–	–	–	CV (N)	309,326
GX 1+4	17 32 02.16	−24 44 44.0	0.017	1.937	4.795	2.30±0.04	138.170(1)	1160.8(12.4)	4.5	LMXB (P)	30,327,328,329
QSO B1730−130	17 33 02.71	−13 04 49.5	0.017	12.032	10.811	–	–	–	[0.90200(23)]	QSO	56,62
IGR J17331−2406	17 33 13	−24 09 22	1.8	2.580	4.888	–	–	–	–	Unclassified (T)	1
4U 1730−335	17 33 24.1	−33 23 16	0.017	354.841	−0.158	1.5±0.3	–	–	$8.8^{+3.3}_{-2.4}$	LMXB (B, T)	117,321
IGR J17348−2045	17 34 48	−20 45 00	4.3	5.666	6.407	–	–	–	–	Unclassified (T)	1
IGR J17354−3255	17 35 21	−32 56 13	2.2	355.441	−0.256	–	–	–	–	Unclassified	1

Table 1. continued.

Name	R.A. (J2000)	Dec.	Error	l (deg)	b	$N_{\rm H}$ (10^{22} cm^{-2})	Spin (s)	Orbit (d)	Distance (kpc or [z])	Type	Ref.
IGR J17364−2711	17 36.5	−27 12	2	0.409	2.626	–	–	–	–	Unclassified (T)	330
GRS 1734−292	17 37 28.35	−29 08 02.5	0.002	358.891	1.407	$1.05^{+0.58}_{-0.64}$	–	–	[0.0214(5)]	Sey-1	331,332
IGR J17379−3747	17 37 54	−37 46 59	5.3	351.630	−3.298	–	–	–	–	Unclassified (T)	1
SLX 1735−269	17 38 17.12	−26 59 38.6	0.01	0.796	2.400	1.70±0.05	–	–	8.5	LMXB (B)	30,305
4U 1735−444	17 38 58.3	−44 27 00	0.017	346.054	−6.994	0.34±0.02	–	0.1939(2)	9.4(1.4)	LMXB (B, A)	117,125,242,333
IGR J17391−3021	17 39 11.58	−30 20 37.6	0.002	358.068	0.445	3.2±0.3	–	–	$2.3^{+0.6}_{-0.5}$	HMXB (SG, SFXT)	334,335,336
AX J1739.3−2923	17 39 19	−29 23.9	0.96	358.882	0.926	$1.8^{+6.0}_{-0.1}$	–	–	–	Unclassified	335
XTE J1739−285	17 39 53.95	−28 29 46.8	0.002	359.714	1.298	–	–	–	12	LMXB (B, NS, T)	284,337
IGR J17404−3655	17 40 27	−36 54 47	3.5	352.638	−3.266	–	–	–	–	Unclassified	1
SLX 1737−282	17 40 39	−28 17 48	0.35	359.971	1.264	2.0±0.1	–	–	6.5(1.5)	LMXB (B, T)	268,335,338
IGR J17407−2808	17 40 41.2	−28 08 50	0.266	0.102	1.336	–	–	–	–	Unclassified (T, SFXT?)	339
IGR J17418−1212	17 41 51	−12 11 46	1.1	13.926	9.425	~0.1	–	–	[0.0372(1)]	Sey-1	22,126,340
IGR J17419−2802	17 41 56.0	−28 01 54.5	0.058	0.345	1.164	1.4±0.3	–	–	–	Unclassified (T)	341,342
IGR J17426−0258	17 42 35	−02 57 47	4.3	22.202	13.854	–	–	–	–	Unclassified (T)	1
XTE J1743−363	17 43 00.0	−36 20 41	0.017	353.392	−3.402	–	–	–	–	Unclassified (T)	343
1E 1740.7−2942	17 43 54.83	−29 44 42.6	0.002	359.116	−0.106	$11.8^{+2.3}_{-1.9}$	–	12.73(5)	8.5	LMXB (BHC, T)	344,345,346,347
IGR J17445−2747	17 44 32	−27 46 59	1.5	0.859	0.806	–	–	–	–	Unclassified (T)	126
IGR J17448−3232	17 44 55	−32 33 00	2.2	356.837	−1.755	–	–	–	–	Unclassified	1
KS 1741−293	17 44 56	−29 21 07	0.6	359.567	−0.089	20.3±1.7	–	–	–	LMXB (B, T)	117,335
IGR J17456−2901	17 45 40.04	−29 00 28.1	0.017	359.944	−0.046	$7.81^{+0.02}_{-0.04}$	–	–	8.5	BHC	348,349
1A 1742−294	17 46 05.5	−29 30 55	0.017	359.559	−0.389	6.6±0.1	–	–	$8.1^{+1.1}_{-1.2}$	LMXB (B, T)	125,278,339
IGR J17461−2853	17 46 06	−28 52 55	0.6	0.101	−0.061	–	–	–	–	Unclassified (Mol. Cloud?)	1
IGR J17461−2204	17 46 08	−22 03 32	3.7	5.939	3.475	–	–	–	–	Unclassified	1
IGR J17464−3213	17 46 16	−32 13 59	0.2	357.256	−1.834	~2.3	–	–	10.4(2.9)	LMXB (BHC, QPO, T, muQSO?)	1,350,351
1E 1743.1−2843	17 46 21.0	−28 43 44	0.025	0.260	−0.029	20.2±0.4	–	–	8	LMXB	352
1RXS J174607.8−213333	17 46.4	−21 33	0.2	6.408	3.685	–	–	–	–	Unclassified (T)	353
1A 1743−288	17 47 02.60	−28 52 58.9	0.002	0.207	−0.238	7.2±1.6	–	–	7.5(1.3)	LMXB (B, T)	354,355,356
IGR J17472+0701	17 47 11	+07 01 05	5.3	31.942	17.466	–	–	–	–	Unclassified	1
IGR J17475−2822	17 47 17	−28 26 42	0.7	0.609	−0.057	8±2	–	–	8.5	Mol. Cloud	126,357
IGR J17473−2721	17 47 18.06	−27 20 38.9	0.013	1.553	0.510	5.2±0.4	–	–	–	Unclassified (T)	358,359
SLX 1744−299	17 47 26	−30 01 14	0.17	359.278	−0.900	4.3±0.1	–	–	–	LMXB (B)	268,335
IGR J17476−2253	17 47 37	−22 53 13	1.8	5.407	2.754	–	–	–	–	Unclassified (AGN?, QSO?)	1
GX 3+1	17 47 56.0	−26 33 49	0.05	2.294	0.794	$1.59^{+0.07}_{-0.12}$	–	–	$5.0^{+0.8}_{-0.7}$	LMXB (B, QPO, A)	117,360
1A 1744−361	17 48 19.22	−36 07 16.6	0.017	354.140	−4.204	~0.79	0.002	0.0067(15)	9	LMXB (P, B, QPO, D, T)	361,362
IGR J17487−3124	17 48 41	−31 22 55	3	358.251	−1.833	–	–	–	–	Unclassified	1
H 1745−203	17 48 53.5	−20 22 02	1	7.724	3.795	0.47±0.07	–	–	$8.4^{+1.5}_{-1.3}$	LMXB (T)	117,321
IGR J17488−3253	17 48 55.129	−32 54 52.15	0.002	356.961	−2.664	$0.22^{+0.07}_{-0.05}$	–	–	[0.020(1)]	Sey-1	86,127
AX J1749.1−2733	17 49 09	−27 33.2	0.96	1.586	0.051	25^{+57}_{-21}	–	–	–	Unclassified (T, HMXB?, SFXT?)	335

Table 1. continued.

Name	R.A.	Dec. (J2000)	Error	l (deg)	b	$N_{\rm H}$ (10^{22} cm^{-2})	Spin (s)	Orbit (d)	Distance (kpc or [z])	Type	Ref.
AX J1749.2−2725	17 49 10.1	−27 25 16	1	1.701	0.116	$15.4^{+9.6}_{-4.5}$	220.38(20)	–	–	HMXB (P, T)	24,335,363
IGR J17497−2821	17 49 38.04	−28 21 17.4	0.017	0.953	−0.453	4.2±0.1	–	–	–	LMXB (BHC, T)	364
SLX 1746−331	17 49 50.6	−33 11 55	0.583	356.816	−2.976	∼0.4	–	–	–	LMXB (BHC, T)	117,305
1H 1746−370	17 50 12.7	−37 03 08	0.017	353.531	−5.005	$0.20^{+0.25}_{-0.06}$	–	0.215137(7)	$11.0^{+0.9}_{-0.8}$	LMXB (B, A)	103,117,321,365
IGR J17507−2647	17 50 42	−26 47 31	2.6	2.416	0.146	–	–	–	–	Unclassified	1
IGR J17507−2856	17 50 43	−28 56 28	2.2	0.572	−0.957	–	–	–	–	Unclassified (T)	1
GRS 1747−312	17 50 45.5	−31 17 32	0.017	358.555	−2.168	1.39±0.08	–	0.5149803(1)	$9.5^{+3.3}_{-2.5}$	LMXB (T)	117,321,365,366
IGR J17513−2011	17 51 13.623	−20 12 14.58	0.002	8.145	3.407	–	–	–	[0.047(1)]	Sey-1.9	86
1RXS J175113.3−201214	17 51 25	−20 12 07	0.77	8.169	3.370	–	–	–	–	Unclassified (T)	268
IGR J17515−1533	17 51 32	−15 32 38	4.8	12.214	5.704	–	–	–	–	Unclassified (T)	1
SWIFT J1753.5−0127	17 53 28.26	−01 27 06.1	0.008	24.898	12.186	0.20±0.04	–	–	–	LMXB (BHC, QPO, T)	367,368
IGR J17536−2339	17 53.6	−23 39	4	5.454	1.183	–	–	–	–	Unclassified (T, SFXT?)	369
IGR J17541−2252	17 54.1	−22 52	4	6.188	1.481	–	–	–	–	Unclassified (T, SFXT?)	369
IGR J17544−2619	17 54 25.28	−26 19 52.6	0.01	3.236	−0.336	1.8±0.3	–	–	3.2(1.0)	HMXB (SG, SFXT)	247,370,371
IGR J17586−2129	17 58 38	−21 19 37	3.3	8.047	1.346	–	–	–	–	Unclassified	1
IGR J17597−2201	17 59 45.7	−22 01 39	0.067	7.570	0.770	4.5±0.7	–	–	7.5(2.5)	LMXB (B, D)	247,372
GX 5−1	18 01 08.2	−25 04 45	0.05	5.077	−1.019	2.2±0.2	–	–	7.2	LMXB (Z)	30,117,261
GRS 1758−258	18 01 12.7	−25 44 26	0.017	4.511	−1.361	$1.81^{+0.08}_{-0.05}$	–	18.45(1)	8.5	LMXB (BHC)	30,117,346,373
GX 9+1	18 01 32.3	−20 31 44	0.05	9.077	1.154	0.8±0.1	–	–	4.4(1.3)	LMXB (A)	117,374
IGR J18027−2016	18 02 42.0	−20 17 18	0.067	9.420	1.036	9.1±0.5	139.61(4)	4.5696(9)	–	HMXB (SG, P)	247,375
IGR J18027−1455	18 02 47.375	−14 54 54.78	0.001	14.114	3.659	∼19	–	–	[0.034(1)]	Sey-1	166,376
IGR J18048−1455	18 04 38.96	−14 56 47.3	0.01	14.307	3.252	–	–	–	–	HMXB	73
XTE J1807−294	18 06 59.8	−29 24 30	0.017	1.935	−4.273	$0.56^{+0.02}_{-0.01}$	0.0052459(1)	0.0278292(3)	5.5(2.5)	LMXB (P, QPO, T)	377,378
SGR 1806−20	18 08 39.32	−20 24 39.5	0.008	9.996	−0.242	6.6±0.2	7.5604(8)	–	$15.1^{+1.8}_{-1.3}$	SGR (P)	379,380,381,382
PSR J1811−1926	18 11 29.22	−19 25 27.6	0.01	11.181	−0.348	$2.22^{+0.78}_{-0.57}$	0.0646732(1)	–	5	SNR (PWN)	383,384,385,386
IGR J18134−1636	18 13 24	−16 35 53	3.8	13.879	0.610	–	–	–	–	Unclassified	1
IGR J18135−1751	18 13 27	−17 50 56	1.1	12.787	0.001	$5.15^{+1.70}_{-1.24}$	–	–	4	SNR (PWN?)	126,387,388
GX 13+1	18 14 31.55	−17 09 26.7	0.017	13.517	0.106	3.2±0.2	–	24.065(18)	7(1)	LMXB (B, QPO, A)	93,389,390,391
4U 1812−12	18 15 06.18	−12 05 47.1	0.01	18.033	2.398	1.1±0.2	–	–	4.0(6)	LMXB (B)	125,305
IGR J18159−3353	18 15.9	−33 53	4	358.865	−8.054	–	–	–	–	Unclassified (T, SFXT?)	392
GX 17+2	18 16 01.4	−14 02 11	0.017	16.432	1.278	$2.00^{+0.05}_{-0.03}$	–	–	$14.0^{+2.0}_{-2.1}$	LMXB (B, QPO, Z)	117,125,393
IGR J18173−2509	18 17 19	−25 09 04	2.2	6.784	−4.261	–	–	–	–	Unclassified	1
XTE J1817−330	18 17 43.53	−33 01 07.5	0.004	359.817	−7.996	$0.092^{+0.005}_{-0.004}$	–	–	2.5(1.5)	BHC (QPO, T)	394,395,396
XTE J1818−245	18 18 24.8	−24 32 15	0.116	7.444	−4.192	–	–	–	–	BHC (T)	397
SAX J1818.6−1703	18 18 37.89	−17 02 47.9	0.01	14.080	−0.704	6.0±0.7	–	–	–	HMXB (SG, SFXT)	398
IGR J18193−2542	18 19 17	−25 42 11	1.5	6.503	−4.912	–	–	–	–	Unclassified (T)	126
AX J1820.5−1434	18 20 29.5	−14 34 24	0.5	16.472	0.070	9.8±1.7	152.26(4)	–	8.2(3.5)	HMXB (Be, P, T)	24,399
IGR J18214−1318	18 21 22	−13 18 29	0.9	17.688	0.479	–	–	–	–	Unclassified (T)	126

Table 1. continued.

Name	R.A.	Dec. (J2000)	Error	l (deg)	b	N_H (10^{22} cm^{-2})	Spin (s)	Orbit (d)	Distance (kpc or [z])	Type	Ref.
1RXS J182129.0−131641	18 21 29.0	−13 16 41	0.433	17.728	0.468	–	–	–	–	Unclassified (T)	400
H 1820−303	18 23 40.48	−30 21 40.1	0.001	2.788	−7.913	0.160±0.003	–	0.0079284(1)	7.6(4)	LMXB (B, A)	103,321,401
IGR J18244−5622	18 24 15	−56 21 47	5	338.441	−18.741	12±2	–	–	[0.017(1)]	Sey-2	1,86,402
IGR J18246−1425	18 24 39	−14 25 05	4.4	17.081	−0.746	–	–	–	–	Unclassified (T)	1
IGR J18249−3243	18 24 56.66	−32 42 59.8	0.002	0.782	−9.212	–	–	–	–	AGN	403
H 1822−000	18 25 22.02	−00 00 43.0	0.01	29.939	5.793	0.97±0.18	–	–	3.6	LMXB	30,404
IGR J18256−1035	18 25 37	−10 35 13	1.5	20.579	0.835	–	–	–	–	Unclassified	126
3A 1822−371	18 25 46.8	−37 06 19	0.017	356.850	−11.291	$0.123^{+0.016}_{-0.014}$	0.5931(1)	0.23	2.5(5)	LMXB (P, D)	117,405,406,407,408
IGR J18259−0706	18 25 56	−07 06 22	2	23.697	2.388	–	–	–	–	Unclassified (T, AGN?)	126
1RXS J182557.5−071021	18 25 57.5	−07 10 21	0.184	23.641	2.352	–	–	–	–	Unclassified (T)	141
RX J1826.2−1450	18 26 15.034	−14 50 53.59	0.002	16.882	−1.289	$0.72^{+0.03}_{-0.05}$	–	3.90603(17)	2.5(1)	HMXB (SG, muQSO)	409,410,411
Ginga 1826−24	18 29 28.2	−23 47 29	0.034	9.277	−6.085	$0.429^{+0.021}_{-0.019}$	–	0.088	7.5(5)	LMXB (BHC, B)	291,412,413,414
AX J1830.6−1002	18 30 39	−10 02.7	0.96	21.634	−0.009	$3.07^{+3.42}_{-2.60}$	–	–	–	Unclassified	278
IGR J18308−1232	18 30 47	−12 31 55	3.3	19.445	−1.189	–	–	–	–	Unclassified	1
IGR J18325−0756	18 32 28	−07 56 24	0.7	23.708	0.567	–	–	–	–	Unclassified (T)	126
SNR 021.5−00.9	18 33 35	−10 33 29	0.7	21.513	−0.886	2.1±0.1	0.0618657(1)	–	4.7(4)	SNR (PWN)	126,415,416
PKS 1830−211	18 33 39.89	−21 03 39.8	0.002	12.166	−5.712	$1.94^{+0.28}_{-0.25}$	–	–	2.507	Blazar	122,417,418
3C 382	18 35 03.390	+32 41 46.86	0.002	61.305	17.446	~0.88	–	–	[0.058137(577)]	Sey-1	56,70,419
XB 1832−330	18 35 44.0	−32 58 55	0.017	1.540	−11.368	0.85±0.15	–	0.0303(4)	9.6(4)	LMXB (B, T)	117,420,421
AX J1838.0−0655	18 38 02	−06 54 14	0.8	25.263	−0.181	6.7±1.3	–	–	–	SNR (PWN?)	126,422
ESO 103−35	18 38 20.3	−65 25 41	0.017	329.778	−23.175	$18.8^{+2.16}_{-1.12}$	–	–	[0.01325(18)]	Sey-2	56,84,332
Ser X−1	18 39 57.5	+05 02 09	0.017	36.118	4.842	0.50±0.03	–	–	11.1(1.6)	LMXB (B)	117,125,360
PSR J1840+13	18 40 09	+13 31 58	0.1	43.800	8.586	–	0.472331(1)	–	3.4	Radio P	423
IGR J18406−0539	18 40.6	−05 39	3	26.670	−0.173	–	–	–	1.1	HMXB (Be, muQSO?)	424
IGR J18410−0535	18 41 00.54	−05 35 46.8	0.01	26.764	−0.239	6.1±1.0	4.7394(8)	–	–	HMXB (Be, P, SFXT)	425,426
PSR B1841−04	18 41 19.34	−04 56 11.2	0.005	27.387	−0.007	$2.54^{+0.15}_{-0.13}$	11.766684(5)	–	$6.8^{+0.7}_{-0.8}$	AXP	427,428,429,430
AX J1841.3−0455	18 41 19.34	−04 56 11.2	0.015	27.387	−0.007	$2.54^{+0.15}_{-0.13}$	11.766684(6)	–	6.75(75)	AXP	427,428,429,430
3C 390.3	18 42 08.990	+79 46 17.13	0.017	111.438	27.074	1.3±0.2	–	–	[0.056159(464)]	Sey-1	56,62,134
IGR J18450−0435	18 45 01.9	−04 33 58	0.07	28.139	−0.659	2.3±0.7	–	–	3.6	HMXB (SG, SFXT)	431,432
Ginga 1843+009	18 45 37	+00 51 54	0.6	33.038	1.690	2.30±0.13	29.477(1)	–	12.5(2.5)	HMXB (Be, P, T)	1,433,434
PSR J1846−0258	18 46 24.5	−02 58 28	0.017	29.712	−0.238	3.96±0.08	0.3248636(1)	–	19	SNR (PWN)	435,436,437,438
IGR J18483−0311	18 48 15	−03 10 08	0.7	29.748	−0.736	–	–	18.55(3)	–	Unclassified (T)	103,126
3A 1845−024	18 48 17.7	−02 25 13	0.017	30.420	−0.405	25±10	94.8	242.18(1)	10.0	HMXB (Be, P, T)	24,30,103,439
IGR J18485−0047	18 48 28	−00 46 44	3.4	31.900	0.306	–	–	–	–	Unclassified	1
IGR J18490−0000	18 49 04	−00 01 30	1.4	32.639	0.516	–	–	–	–	Unclassified	126
3A 1850−087	18 53 04.86	−08 42 20.4	0.01	25.355	−4.320	0.42±0.04	–	0.01417	8.2(6)	LMXB (B)	321,404
IGR J18539+0727	18 53 54	+07 27 29	0.9	39.854	2.849	1.5±0.4	–	–	–	BHC (T)	126,440
V1223 Sgr	18 55 02.24	−31 09 48.5	0.017	4.958	−14.355	3.7±0.1	745.506	0.140244	$0.527^{+0.054}_{-0.043}$	CV (DQ Her)	6,311,312,441

Table 1. continued.

Name	R.A.	Dec. (J2000)	Error	l (deg)	b	N_H (10^{22} cm^{-2})	Spin (s)	Orbit (d)	Distance (kpc or [z])	Type	Ref.
XTE J1855−026	18 55 31.3	−02 36 24	0.017	31.076	−2.096	14.7±0.6	360.741(2)	6.0752(8)	10	HMXB (SG, P, T)	19,30,442,443
IGR J18559+1535	18 56 00.0	+15 38 13	0.017	47.411	6.076	~0.1	−	−	[0.0838(2)]	Sey-1	22,444,445
XTE J1858+034	18 58 43	+03 26 20	0.3	36.822	−0.049	~6	221.0(5)	−	−	HMXB (Be, P, QPO, T)	1,446,447
HETE J1900.1−2455	19 00 09.77	−24 54 04.3	0.002	11.325	−12.869	0.16±0.04	0.0027(1)	0.0578155(1)	5	LMXB (P, B, T)	448,449,450,451
XTE J1901+014	19 01 41.0	+01 26 18	0.017	35.381	−1.623	−	−	−	−	Unclassified (T, BHC?)	217
4U 1901+03	19 03 37.1	+03 11 31	0.017	37.162	−1.250	−	2.7626530(1)	22.5827(2)	−	HMXB (Be, P, T)	452,453
IGR J19048−1240	19 04 49	−12 39 40	4.2	23.082	−8.662	−	−	−	−	Unclassified (T)	1
SGR 1900+14	19 07 14.33	+09 19 20.1	0.002	43.021	0.766	$2.6^{+0.9}_{-0.7}$	5.18019(2)	−	13.5(1.5)	SGR (P)	454,455,456
XTE J1908+094	19 08 53.08	+09 23 04.9	0.004	43.263	0.434	2.50±0.16	−	−	2(1)	LMXB (BHC, QPO, T)	457,458,459
H 1907+097	19 09 37.9	+09 49 49	0.017	43.744	0.476	2.81±0.04	441.0932(3)	8.3753(1)	5	HMXB (SG, P, T)	24,460,461,462,463
AX J1910.7+0917	19 10 47	+09 17.1	0.96	43.391	−0.028	$2.63^{+1.37}_{-1.03}$	−	−	−	Unclassified	278
4U 1909+07	19 10 48	+07 35 46	0.4	41.895	−0.812	24.3±0.2	604.684(1)	4.4005(4)	7(3)	HMXB (SG, P)	1,19,464,465
Aql X−1	19 11 16.0	+00 35 06	0.017	35.718	−4.143	0.36±0.02	−	0.7904(8)	$5.2^{+0.7}_{-0.8}$	LMXB (B, T, A)	117,125,466,467
SS 433	19 11 49.56	+04 58 57.6	0.002	39.694	−2.245	0.907±0.002	−	13.075(17)	5.5(2)	HMXB (SG, BHC, muQSO)	103,403,468,469
IGR J19140+0951	19 14 04.23	+09 52 58.3	0.01	44.296	−0.469	10±3	−	13.558(4)	−	HMXB (SG)	470,471
GRS 1915+105	19 15 11.6	+10 56 44	0.017	45.366	−0.219	1.98±0.02	−	33.5(1.5)	11^{+1}_{-4}	LMXB (BHC, QPO, T)	125,291,472,473
4U 1916−053	19 18 47.78	−05 14 11.2	0.017	31.359	−8.463	0.69±0.02	−	0.0347297(1)	8.8(1.3)	LMXB (B, D)	19,93,125,474
SWIFT J1922.7−1716	19 22 37.0	−17 17 03	0.053	20.683	−14.521	0.15±0.02	−	−	8(3)	Unclassified (T, NS LMXB?, BHC?)	139,475
1RXS J192450.8−291437	19 24 51.056	−29 14 30.12	0.002	9.344	−19.607	0.088±0.006	−	−	[0.352000(33)]	BL Lac	56,62,476
IGR J19267+1325	19 26 41	+13 25 30	3.7	48.874	−1.532	−	−	−	−	Unclassified	1
IGR J19284+0107	19 28 24	+01 07 08	1.3	38.177	−7.700	−	−	−	−	Unclassified (T)	126
IGR J19308+0530	19 30 46	+05 30 07	1.4	42.359	−6.175	−	−	−	−	Unclassified (T)	126
1H 1934−063	19 37 33.1	−06 13 05	0.017	32.591	−13.074	~0.1	−	−	0.01059	Sey-1	22,477,478
IGR J19378−0617	19 37 39	−06 13 05	4.4	32.602	−13.096	−	−	−	−	Sey-1	1
RX J1940.2−1025	19 40 11.47	−10 25 25.1	0.002	28.984	−15.503	8±2	12146.5(3)	0.140235(5)	0.230	CV (AM Her)	6,9,479,480
IGR J19405−3016	19 40 29	−30 15 58	5.4	9.549	−23.146	−	−	−	−	AGN	1
NGC 6814	19 42 40.4	−10 19 24	0.017	29.351	−16.011	~0.05	−	−	0.00520	Sey-1.5	16,56,166
IGR J19443+2117	19 44 17	+21 17 13	4.9	57.787	−1.374	−	−	−	−	Unclassified	1
IGR J19473+4452	19 47 19.37	+44 49 42.4	0.01	78.642	9.734	11±1	−	−	[0.0532(2)]	Sey-2	85,445
IGR J19487+5120	19 48 44	+51 20 10	4.4	84.593	12.620	−	−	−	−	Unclassified (T)	1
KS 1947+300	19 49 35.6	+30 12 31	0.017	66.099	2.083	0.43±0.03	18.70969(5)	40.415(10)	9.5(1.1)	HMXB (Be, P, T)	24,481,482,483
3C 403	19 52 14.80	+02 30 28.0	0.017	42.262	−12.310	45^{+7}_{-6}	−	−	0.059	Sey-2	403,484,485
3A 1954+319	19 55 42.272	+32 05 48.82	0.011	68.392	1.927	28±2	18300(200)	−	1.7	LMXB (P, Symb, T)	486,487
Cyg X−1	19 58 21.68	+35 12 05.8	0.017	71.335	3.067	0.621±0.022	−	5.6008(7)	2.10(25)	HMXB (SG, BHC, muQSO)	17,19,488,489
QSO B1957+405	19 59 28.36	+40 44 01.9	0.002	76.190	5.755	38±8	−	−	[0.05615(16)]	Sey-2	16,56,66
IGR J20006+3210	20 00 21.9	+32 11 23	0.017	68.986	1.134	−	−	−	−	HMXB (T)	73
SWIFT J2000.6+3210	20 00 21.9	+32 11 22	0.06	68.986	1.134	$1^{+2.2}_{-0.7}$	−	−	−	HMXB (Be)	139
ESO 399−20	20 06 57.2	−34 32 54	0.017	6.749	−29.721	$0.048^{+0.044}_{-0.036}$	−	−	0.024951	Sey-1 (NL)	84,490,491
IGR J20187+4041	20 18 38.55	+40 41 00.4	0.07	78.114	2.671	$6.1^{+3.2}_{-2.2}$	−	−	−	AGN (Blazar?)	492

Table 1. continued.

Name	R.A. (J2000)	Dec.	Error	l (deg)	b	N_H (10^{22} cm^{-2})	Spin (s)	Orbit (d)	Distance (kpc or [z])	Type	Ref.
IGR J20188+3647	20 18.8	+36 48	3.4	74.920	0.460	–	–	–	–	Unclassified (T, SFXT?)	392
IGR J20286+2544	20 28 35.1	+25 44 01	0.017	67.005	−7.572	$42.3^{+19.5}_{-28.5}$	–	–	0.013	Sey-2	3,56,127
EXO 2030+375	20 32 15.2	+37 38 15	0.034	77.152	−1.242	2.6±0.3	41.691798(16)	46.0214(5)	7.1(2)	HMXB (Be, P, T)	221,493,494,495
Cyg X−3	20 32 25.78	+40 57 27.9	0.017	79.845	0.700	8.5±0.1	–	0.1996907(7)	9.0	HMXB (SG, BHC, muQSO)	19,30,496,497
4C 74.26	20 42 37.180	+75 08 02.52	0.002	108.998	19.527	0.189±0.005	–	–	[0.103999(23)]	QSO	56,498,499
SAX J2103.5+4545	21 03 35.71	+45 45 05.5	0.002	87.130	−0.685	3.8±0.1	355(3)	12.673(4)	3.2(8)	HMXB (Be, P, T)	19,500,501,502
IGR J21117+3427	21 11.8	+34 28	3.5	79.788	−9.425	–	–	–	–	Unclassified (T, SFXT?)	392
S5 2116+81	21 14 00.50	+82 04 47.1	0.058	115.978	22.344	0.098±0.021	–	–	0.084	Sey-1	271,503
IGR J21178+5139	21 17.8	+51 39	3	93.039	1.629	–	–	–	–	AGN	16
V2069 Cyg	21 23 44.83	+42 18 02.2	0.017	87.122	−5.686	–	–	0.311683(2)	1.65	CV (IP)	6,9,504
IGR J21247+5058	21 24 41	+50 58 19	1	93.321	0.389	~0.1	–	–	0.020	Sey-1	1,16,22
IGR J21272+4241	21 27 10	+42 41 31	5.5	87.850	−5.848	–	–	–	–	Unclassified	1
IGR J21277+5656	21 27 44.95	+56 56 39.7	0.017	97.803	4.368	~0.1	–	–	[0.0144(2)]	Sey-1	22,93,445
SWIFT J2127.4+5654	21 27 45.4	+56 56 35	0.056	97.802	4.367	$1^{+2.2}_{-0.7}$	–	–	0.0147	Sey-1 (NL)	139,505
IGR J21335+5105	21 33 30	+51 05 31	1.2	94.410	−0.476	–	570.823(13)	0.2997(7)	1.4	CV (IP)	9,126,506
IGR J21347+4737	21 34 42	+47 37 12	4.5	92.207	−3.169	–	–	–	–	Unclassified	1
RX J2135.9+4728	21 35 54.38	+47 28 28.3	0.313	92.260	−3.413	–	–	–	–	Sey-1	507
SS Cyg	21 42 42.80	+43 35 09.9	0.002	90.559	−7.111	~0.050	–	0.2751	$0.166^{+0.014}_{-0.012}$	CV (DN)	9,147,508,509
Cyg X−2	21 44 41.2	+38 19 18	0.017	87.328	−11.316	0.19±0.05	–	9.8444(3)	$13.4^{+1.9}_{-2.0}$	LMXB (B, Z)	117,125,510,511
NGC 7172	22 02 01.70	−31 52 18.0	0.017	15.126	−53.065	$10.18^{+0.80}_{-0.78}$	–	–	[0.008616(47)]	Sey-2	56,512,513
BL Lac	22 02 43.29	+42 16 40.0	0.017	92.590	−10.441	0.30±0.03	–	–	0.0688	BL Lac	62,485,514
3A 2206+543	22 07 56.24	+54 31 06.4	0.002	100.603	−1.106	$0.88^{+0.21}_{-0.19}$	–	9.5591(7)	2.6	HMXB (Be)	515,516,517,518
FO Aqr	22 17 55.43	−08 21 04.6	0.017	53.000	−49.158	32±4	1254.451(1)	0.2020596(1)	0.575(36)	CV (IP)	6,311,312,519,520
IGR J22234−4116	22 23 24	−41 15 43	5.3	358.238	−56.610	–	–	–	–	Unclassified	1
IGR J22292+6647	22 29 11	+66 47 17	4.8	109.558	7.685	–	–	–	–	Radio Galaxy	1
NGC 7314	22 35 46.06	−26 03 01.7	0.017	27.135	−59.742	$0.122^{+0.009}_{-0.014}$	–	–	[0.004790(117)]	Sey-1.9	40,56,149
Mrk 915	22 36 46.50	−12 32 42.6	0.017	51.058	−55.294	–	–	–	[0.024043(130)]	Sey-1	56,173
3C 454.3	22 53 57.75	+16 08 53.6	0.017	86.111	−38.184	$0.5^{+0.5}_{-0.4}$	–	–	[0.85900(17)]	Blazar	56,62,134
1H 2251−179	22 54 05.88	−17 34 55.3	0.002	46.197	−61.326	$0.237^{+0.028}_{-0.015}$	–	–	0.06398	Sey-1	122,166,521
NGC 7469	23 03 15.75	+08 52 25.9	0.017	83.099	−45.467	0.061±0.002	–	–	0.01639	Sey-1.2	54,55,522
MCG−02−58−022	23 04 43.48	−08 41 08.6	0.017	64.092	−58.758	$0.034^{+0.012}_{-0.001}$	–	–	[0.047156(300)]	Sey-1.5	56,122,523
IGR J23130+8608	23 13 03	+86 07 59	4.8	121.177	23.601	–	–	–	–	Unclassified	1
NGC 7603	23 18 56.61	+00 14 36.5	0.017	80.067	−54.740	0.045±0.006	–	–	[0.029297(237)]	Sey-1.5	54,55,56
Cas A	23 23 27.94	+58 48 42.4	0.01	111.742	−2.135	1.25±0.03	–	–	$3.4^{+0.3}_{-0.1}$	SNR	524,525
IGR J23308+7120	23 30 47	+71 20 10	4.5	116.511	9.477	–	–	–	–	Unclassified (AGN?)	1
IGR J23524+5842	23 52 27	+58 42 00	4	115.320	−3.297	–	–	–	–	Unclassified	1

Name: One commonly used name for the source
R.A.: Right Ascension (J2000) in *hh mm ss.ss*
Dec.: Declination in *dd mm ss.ss*
Error: Error radius in minutes
l: Galactic longitude in degrees
b: Galactic latitude in degrees
$N_{\rm H}$: Column density in 10^{22} cm^{-2}
Spin: Spin period in seconds
Orbit: Orbital period in days
Distance: Distance in kpc for galactic sources (including LMC/SMC), or redshift (in brackets) for extragalactic sources
Type: A (atoll), AGN (active galactic nucleus), AXP (anomalous X-ray pulsar), B (burster), Be (Be star), BHC (black hole candidate), CV (cataclysmic variable), E (eclipsing), D (dipping), DN (dwarf nova), F (flaring), GRS (gamma-ray source), HMXB (high-mass X-ray binary), IP (intermediate polar), LMXB (low-mass X-ray binary), Mol. Cloud (molecular cloud), muQSO (micro-quasar), N (nova), P (pulsar), PWN (pulsar wind nebula), QPO (quasi-periodic oscillations), QSO (quasar), RP (radio pulsar), Sey (Seyfert galaxy), SFXT (supergiant fast X-ray transient), SG (OB supergiant), SGR (soft gamma repeater), SNR (supernova remnant), Symb (symbiotic star), T (transient), Z (Z-track)
References: References for the listed parameters

[1] Bird A.J., Malizia A., Bazzano A., et al., 2007, ApJ, in press, astro-ph/0611493
[2] Bikmaev I.F., Revnivtsev M.G., Burenin R.A., & Sunyaev R.A., 2006, AstL, 32, 588
[3] Masetti N., Bassani L., Bazzano A., et al., 2006, A&A, 455, 11
[4] Ruiz-Lapuente P., 2004, ApJ, 612, 357
[5] Kuiper L., Hartog P.R.D., & Hermsen W., 2006, ATel, 939, 1
[6] Downes R., Webbink R.F., & Shara M.M., 1997, PASP, 109, 345
[7] de Martino D., Matt G., Mukai K., et al., 2001, A&A, 377, 499
[8] Bonnet-Bidaud J.M., Mouchet M., de Martino D., et al., 2001, A&A, 374, 1003
[9] Barlow E.J., Knigge C., Bird A.J., et al., 2006, MNRAS, 372, 224
[10] Nowak M.A., Paizis A., Wilms J., et al., 2004, ATel, 369, 1
[11] Paizis A., Nowak M.A., Wilms J., et al., 2005, A&A, 444, 357
[12] Burderi L., di Salvo T., Riggio A., et al., 2006, ChJAS, 6, 192
[13] Galloway D.K., Markwardt C.B., Morgan E.H., et al., 2005, ApJ, 622, L45
[14] Falanga M., Kuiper L., Poutanen J., et al., 2005, A&A, 444, 15
[15] Laurent-Muehleisen S.A., Kollgaard R.I., Ryan P.J., et al., 1997, A&AS, 122, 235
[16] Bassani L., Molina M., Malizia A., et al., 2006, ApJ, 636, L65
[17] Perryman M.A.C., Lindegren L., Kovalevsky J., et al., 1997, A&A, 323, L49
[18] den Hartog P.R., Hermsen W., Kuiper L., et al., 2006, A&A, 451, 587
[19] Wen L., Levine A.M., Corbet R.H.D., & Bradt H.V., 2006, ApJS, 163, 372
[20] Negueruela I. & Reig P., 2004, ATel, 285, 1
[21] Snellen I.A.G., McMahon R.G., Hook I.M., & Browne I.W.A., 2002, MNRAS, 329, 700
[22] Sazonov S., Revnivtsev M., Krivonos R., et al., 2007, A&A, 462, 57
[23] Yu P.-C. & Hwang C.-Y., 2005, ApJ, 631, 720
[24] Liu Q.Z., van Paradijs J., & van den Heuvel E.P.J., 2000, A&AS, 147, 25
[25] Buckley D.A.H., Coe M.J., Stevens J.B., et al., 2001, MNRAS, 320, 281
[26] Corbet R., Marshall F.E., Lochner J.C., et al., 1998, IAU Circ., 6803, 1
[27] Galache J.L., Corbet R.H.D., Coe M.J., et al., 2005, ATel, 674, 1
[28] Smith M.A., Cohen D.H., Gu M.F., et al., 2004, ApJ, 600, 972
[29] Harmanec P., Habuda P., Štefl S., et al., 2000, A&A, 364, L85
[30] Grimm H.-J., Gilfanov M., & Sunyaev R., 2002, A&A, 391, 923
[31] Massey P., 2002, ApJS, 141, 81
[32] Naik S. & Paul B., 2004, A&A, 418, 655
[33] Corbet R.H.D., Finley J.P., & Peele A.G., 1999, ApJ, 511, 876
[34] Crampton D., Hutchings J.B., & Cowley A.P., 1985, ApJ, 299, 839
[35] Reig P., Chakrabarty D., Coe M.J., et al., 1996, A&A, 311, 879
[36] Campana S., Gastaldello F., Stella L., et al., 2001, ApJ, 561, 924
[37] Tamura K., Tsunemi H., Kitamoto S., et al., 1992, ApJ, 389, 676
[38] Negueruela I. & Okazaki A.T., 2001, A&A, 369, 108
[39] da Costa L.N., Willmer C.N.A., Pellegrini P.S., et al., 1998, AJ, 116, 1
[40] Risaliti G., 2002, A&A, 386, 379
[41] Polletta M., Bassani L., Malaguti G., et al., 1996, ApJS, 106, 399
[42] Reig P., Negueruela I., Papamastorakis G., et al., 2005, A&A, 440, 637
[43] Loveday J., 1996, MNRAS, 278, 1025
[44] Hewitt A. & Burbidge G., 1991, ApJS, 75, 297
[45] Hulleman F., van Kerkwijk M.H., & Kulkarni S.R., 2004, A&A, 416, 1037
[46] Göhler E., Wilms J., & Staubert R., 2005, A&A, 433, 1079
[47] Pigulski A., Kopacki G., & Kołaczkowski Z., 2001, A&A, 376, 144
[48] Mereghetti S., Tiengo A., Israel G.L., & Stella L., 2000, A&A, 354, 567
[49] Burenin R., Mescheryakov A., Sazonov S., et al., 2006, ATel, 883, 1
[50] Den Hartog P.R., Kuiper L., Hermsen W., et al., 2005, ATel, 394, 1
[51] Kennea J.A., Racusin J.L., Burrows D.N., et al., 2005, ATel, 673, 1
[52] Argyle R.W. & Eldridge P., 1990, MNRAS, 243, 504
[53] Kuiper L., Hermsen W., in 't Zand J., & den Hartog P.R., 2005, ATel, 665, 1
[54] Cotton W.D., Condon J.J., & Arbizzani E., 1999, ApJS, 125, 409
[55] Pfefferkorn F., Boller T., & Rafanelli P., 2001, A&A, 368, 797
[56] Paturel G. & Petit C., 2002, LEDA (2002), 0
[57] Clements E.D., 1981, MNRAS, 197, 829
[58] Krongold Y., Nicastro F., Elvis M., et al., 2005, ApJ, 620, 165
[59] Arribas S., Mediavilla E., del Burgo C., & García-Lorenzo B., 1999, ApJ, 511, 680
[60] Leahy D.A., Harrison F.A., & Yoshida A., 1997, ApJ, 475, 823
[61] Taylor A.R. & Gregory P.C., 1982, ApJ, 255, 210
[62] Ma C., Arias E.F., Eubanks T.M., et al., 1998, AJ, 116, 516
[63] Weaver K.A., Wilson A.S., Henkel C., & Braatz J.A., 1999, ApJ, 520, 130
[64] Fischer J.-U., Hasinger G., Schwope A.D., et al., 1998, AN, 319, 347

[65] Cappi M., Panessa F., Bassani L., et al., 2006, A&A, 446, 459

[66] Titov O.A., 2004, ARep, 48, 941

[67] Karachentsev I.D., Karachentseva V.E., Kudrya Y.N., et al., 1999, Bull. Special Astrophys.Obs., 47, 5

[68] Keel W.C., 1996, ApJS, 106, 27

[69] Ishwara-Chandra C.H. & Saikia D.J., 1999, MNRAS, 309, 100

[70] Beasley A.J., Gordon D., Peck A.B., et al., 2002, ApJS, 141, 13

[71] Enya K., Yoshii Y., Kobayashi Y., et al., 2002, ApJS, 141, 23

[72] Vrielmann S., Ness J.-U., & Schmitt J.H.M.M., 2005, A&A, 439, 287

[73] Burenin R., Mescheryakov A., Revnivtsev M., et al., 2006, ATel, 880, 1

[74] Lawrence A., Rowan-Robinson M., Ellis R.S., et al., 1999, MNRAS, 308, 897

[75] Unger S.J., Norton A.J., Coe M.J., & Lehto H.J., 1992, MNRAS, 256, 725

[76] Kreykenbohm I., Mowlavi N., Produit N., et al., 2005, A&A, 433, L45

[77] Stella L., White N.E., Davelaar J., et al., 1985, ApJ, 288, L45

[78] Negueruela I., Roche P., Fabregat J., & Coe M.J., 1999, MNRAS, 307, 695

[79] di Salvo T., Burderi L., Robba N.R., & Guainazzi M., 1998, ApJ, 509, 897

[80] Delgado-Martí, H., Levine A.M., Pfahl E., & Rappaport S.A., 2001, ApJ, 546, 455

[81] Lyubimkov L.S., Rostopchin S.I., Roche P., & Tarasov A.E., 1997, MNRAS, 286, 549

[82] Fomalont E.B., Frey S., Paragi Z., et al., 2000, ApJS, 131, 95

[83] Motch C., Guillout P., Haberl F., et al., 1998, A&AS, 132, 341

[84] Lauberts A., 1982, ESO/Uppsala survey of the ESO(B) atlas (Garching: European Southern Observatory (ESO), 1982)

[85] Sazonov S., Churazov E., Revnivtsev M., Vikhlinin A., & Sunyaev R., 2005, A&A, 444, L37

[86] Masetti N., Morelli L., Palazzi E., et al., 2006, A&A, 459, 21

[87] Remillard R.A., Bradt H.V.D., Brissenden R.J.V., et al., 1993, AJ, 105, 2079

[88] Takata T., Yamada T., Saito M., Chamaraux P., & Kazes I., 1994, A&AS, 104, 529

[89] Kulkarni S.R., Kaplan D.L., Marshall H.L., et al., 2003, ApJ, 585, 948

[90] Haberl F., Dennerl K., & Pietsch W., 2003, A&A, 406, 471

[91] Dennerl K., Haberl F., & Pietsch W., 1995, IAU Circ., 6184, 2

[92] Götz D., Mereghetti S., Merlini D., et al., 2006, A&A, 448, 873

[93] Fuhrmeister B. & Schmitt J.H.M.M., 2003, A&A, 403, 247

[94] Naik S. & Paul B., 2002, JApA, 23, 27

[95] Levine A.M., Rappaport S.A., & Zojcheski G., 2000, ApJ, 541, 194

[96] Han J.L. & Tian W.W., 1999, A&AS, 136, 571

[97] Kirsch M.G.F., Schönherr G., Kendziorra E., et al., 2006, A&A, 453, 173

[98] Lyne A.G., Pritchard R.S., & Graham-Smith F., 1993, MNRAS, 265, 1003

[99] Trimble V., 1973, PASP, 85, 579

[100] Mukherjee U. & Paul B., 2005, A&A, 431, 667

[101] Steele I.A., Negueruela I., Coe M.J., & Roche P., 1998, MNRAS, 297, L5

[102] Cui W., Feng Y.X., Zhang S.N., et al., 2002, ApJ, 576, 357

[103] Levine A.M. & Corbet R., 2006, ATel, 940, 1

[104] Haardt F., Galli M.R., Treves A., et al., 2001, ApJS, 133, 187

[105] Hirayama M., Nagase F., Endo T., et al., 2002, MNRAS, 333, 603

[106] Livingstone M.A., Kaspi V.M., & Gavriil F.P., 2005, ApJ, 633, 1095

[107] Ramsay G. & Cropper M., 2002, MNRAS, 334, 805

[108] Pavlenko E.P., 2006, Astrophysics, 49, 105

[109] Matt G., Bianchi S., de Rosa A., et al., 2006, A&A, 445, 451

[110] Helou G. & Walker D.W., eds. 1988, IRAS catalogs and atlases. Volume 7: The small scale structure catalog

[111] Kennea J.A., Markwardt C.B., Tueller J., et al., 2005, ATel, 677, 1

[112] Morelli L., Masetti N., Bassani L., et al., 2006, ATel, 785, 1

[113] Chenevez J., Budtz-Jorgensen C., Lund N., et al., 2004, ATel, 223, 1

[114] Mauch T., Murphy T., Buttery H.J., et al., 2003, MNRAS, 342, 1117

[115] Brinkmann W. & Siebert J., 1994, A&A, 285, 812

[116] Cappi M., Bassani L., Comastri A., et al., 1999, A&A, 344, 857

[117] Liu Q.Z., van Paradijs J., & van den Heuvel E.P.J., 2001, A&A, 368, 1021

[118] Piraino S., Santangelo A., Ford E.C., & Kaaret P., 1999, A&A, 349, L77

[119] Ford E., Kaaret P., Tavani M., et al., 1997, ApJ, 475, L123

[120] Paerels F., Brinkman A.C., van der Meer R.L.J., et al., 2001, ApJ, 546, 338

[121] Araujo-Betancor S., Gänsicke B.T., Hagen H.-J., et al., 2003, A&A, 406, 213

[122] Barkhouse W.A. & Hall P.B., 2001, AJ, 121, 2843

[123] Malizia A., Bassani L., Capalbi M., et al., 2003, A&A, 406, 105

[124] Sidoli L., Parmar A.N., & Oosterbroek T., 2005, A&A, 429, 291

[125] Jonker P.G. & Nelemans G., 2004, MNRAS, 354, 355

[126] Bird A.J., Barlow E.J., Bassani L., et al., 2006, ApJ, 636, 765

[127] Landi R., Malizia A., Bassani L., et al., 2006, astro-ph/0610358

[128] Revnivtsev M.G., Sazonov S.Y., Molkov S.V., et al., 2006, AstL, 32, 145

[129] Porquet D., Reeves J.N., O'Brien P., & Brinkmann W., 2004, A&A, 422, 85

[130] Pavlov G.G., Zavlin V.E., Sanwal D., et al., 2001, ApJ, 552, L129

[131] Caraveo P.A., De Luca A., Mignani R.P., & Bignami G.F., 2001, ApJ, 561, 930

[132] Belloni T., Hasinger G., Pietsch W., et al., 1993, A&A, 271, 487

[133] Kennea J.A. & Campana S., 2006, ATel, 818, 1

[134] Grandi P., Malaguti G., & Fiocchi M., 2006, ApJ, 642, 113

[135] Orlandini M., dal Fiume D., Frontera F., et al., 1998, A&A, 332, 121

[136] Kreykenbohm I., Coburn W., Wilms J., et al., 2002, A&A, 395, 129

[137] Sadakane K., Hirata R., Jugaku J., et al., 1985, ApJ, 288, 284

[138] Kirhakos S., Strauss M.A., Yahil A., et al., 1991, AJ, 102, 1933

[139] Tueller J., Barthelmy S., Burrows D., et al., 2005, ATel, 669, 1

[140] Juett A.M. & Chakrabarty D., 2003, ApJ, 599, 498

[141] Voges W., Aschenbach B., Boller T., et al., 1999, A&A, 349, 389

[142] Pineda F. & Schnopper H.W., 1978, IAU Circ., 3190, 3

[143] Balestra I., Bianchi S., & Matt G., 2004, A&A, 415, 437

[144] Paizis A., Gotz D., Sidoli L., et al., 2006, ATel, 865, 1

[145] Shrader C.R., Sutaria F.K., Singh K.P., & Macomb D.J., 1999, ApJ, 512, 920

[146] Ajello M., Greiner J., Küpcü Yoldas A., et al., 2006, ATel, 864, 1

[147] Zacharias N. Urban S.E. Zacharias M.I. et al., 2003, VizieR Online Data Catalog, 1289

[148] Ho L.C., Filippenko A.V., & Sargent W.L., 1995, ApJS, 98, 477

[149] Veron-Cetty M.-P. & Veron P., 1996, A Catalogue of quasars and active nuclei (ESO Scientific Report, Garching: European Southern Observatory (ESO), 1996, 7th ed.)

[150] Vignali C. & Comastri A., 2002, A&A, 381, 834

[151] Reig P. & Roche P., 1999, MNRAS, 306, 100

[152] Masetti N., Pretorius M.L., Palazzi E., et al., 2006, A&A, 449, 1139

[153] Burderi L., Di Salvo T., Robba N.R., et al., 2000, ApJ, 530, 429

[154] Nagase F., Corbet R.H.D., Day C.S.R., et al., 1992, ApJ, 396, 147

[155] Hutchings J.B., Cowley A.P., Crampton D., et al., 1979, ApJ, 229, 1079

[156] Steeghs D., Torres M.A.P., & Jonker P.G., 2006, ATel, 768, 1

[157] Smith D.M., Bezayiff N., & Negueruela I., 2006, ATel, 773, 1

[158] Sidoli L., Paizis A., & Mereghetti S., 2006, A&A, 450, L9

[159] Krivonos R., Molkov S., Revnivtsev M., et al., 2005, ATel, 545, 1

[160] De Rosa A., Piro L., Fiore F., et al., 2002, A&A, 387, 838

[161] in 't Zand J. & Heise J., 2004, ATel, 362, 1

[162] Corbet R.H.D. & Remillard R., 2005, ATel, 377, 1

[163] Ray P.S. & Chakrabarty D., 2002, ApJ, 581, 1293

[164] Cook M.C. & Warwick R.S., 1987, MNRAS, 227, 661

[165] Stevens J.B., Reig P., Coe M.J., et al., 1997, MNRAS, 288, 988

[166] Beckmann V., Gehrels N., Shrader C.R., & Soldi S., 2006, ApJ, 638, 642

[167] Becker R.H., White R.L., & Helfand D.J., 1995, ApJ, 450, 559

[168] Risaliti G., Gilli R., Maiolino R., & Salvati M., 2000, A&A, 357, 13

[169] Li J. & Jin W., 1996, A&AS, 120, 201

[170] La Barbera A., Segreto A., Santangelo A., et al., 2005, A&A, 438, 617

[171] Leahy D.A., 2002, A&A, 391, 219

[172] Tueller J., Gehrels N., Mushotzky R.F., et al., 2005, ATel, 591, 1

[173] Clements E.D., 1983, MNRAS, 204, 811

[174] Guainazzi M., Perola G.C., Matt G., et al., 1999, A&A, 346, 407

[175] Fairall A.P., Woudt P.A., & Kraan-Korteweg R.C., 1998, A&AS, 127, 463

[176] Torrejón J.M. & Orr A., 2001, A&A, 377, 148

[177] Perryman M.A.C. & ESA., 1997, The HIPPARCOS and TYCHO catalogues. Astrometric and photometric star catalogues derived from the ESA HIPPARCOS Space Astrometry Mission (Publisher: Noordwijk, Netherlands: ESA Publications Division, 1997, Series: ESA SP Series vol no: 1200, ISBN: 9290923997 (set))

[178] Jackson C.A., Wall J.V., Shaver P.A., et al., 2002, A&A, 386, 97

[179] Bassa C.G., Jonker P.G., in 't Zand J.J.M., & Verbunt F., 2006, A&A, 446, L17

[180] Boller T., Haberl F., Voges W., Piro L., & Heise J., 1997, IAU Circ., 6546, 1

[181] Jerjen H. & Dressler A., 1997, A&AS, 124, 1

[182] Boirin L. & Parmar A.N., 2003, A&A, 407, 1079

[183] in 't Zand J.J.M., Kuulkers E., Verbunt F., et al., 2003, A&A, 411, L487

[184] Mahdavi A. & Geller M.J., 2001, ApJ, 554, L129

[185] Arnaud M., Aghanim N., Gastaud R., et al., 2001, A&A, 365, L67

[186] Chernyakova M., Lutovinov A., Rodriguez J., & Revnivtsev M., 2005, MNRAS, 364, 455

[187] Bicay M.D., Stepanian J.A., Chavushyan V.H., et al., 2000, A&AS, 147, 169

[188] Done C., Madejski G.M., Życki P.T., & Greenhill L.J., 2003, ApJ, 588, 763

[189] Odewahn S.C. & Aldering G., 1996, Private Communication, 1

[190] Palumbo G.G.C., et al., 1988, in Accurate positions of Zwicky galaxies (1988), 0–+
[191] Nilson P., 1973, Nova Acta Regiae Soc.Sci.Upsaliensis Ser.V, 0
[192] Evans D.A., Kraft R.P., Worrall D.M., et al., 2004, ApJ, 612, 786
[193] Church M.J., Reed D., Dotani T., Bałucińska-Church M., & Smale A.P., 2005, MNRAS, 359, 1336
[194] Parmar A.N., Gottwald M., van der Klis M., & van Paradijs J., 1989, ApJ, 338, 1024
[195] Kaldare R., Colless M., Raychaudhury S., & Peterson B.A., 2003, MNRAS, 339, 652
[196] Demircan O., Eker Z., Karataş Y., & Bilir S., 2006, MNRAS, 366, 1511
[197] Willmer C.N.A., Maia M.A.G., Mendes S.O., et al., 1999, AJ, 118, 1131
[198] Papadakis I.E., Kazanas D., & Akylas A., 2005, ApJ, 631, 727
[199] Piconcelli E., Sánchez-Portal M., Guainazzi M., et al., 2006, A&A, 453, 839
[200] Imamura J.N., Steiman-Cameron T.Y., & Wolff M.T., 2000, PASP, 112, 18
[201] Wright A.E., Griffith M.R., Hunt A.J., et al., 1996, ApJS, 103, 145
[202] Matt G., Guainazzi M., Maiolino R., et al., 1999, A&A, 341, L39
[203] Bianchi S., Balestra I., Matt G., et al., 2003, A&A, 402, 141
[204] Nicastro F., Piro L., De Rosa A., et al., 2000, ApJ, 536, 718
[205] Crenshaw D.M. & Kraemer S.B., 1999, ApJ, 521, 572
[206] West R.M., Surdej J., Schuster H.-E., et al., 1981, A&AS, 46, 57
[207] DeLaney T., Gaensler B.M., Arons J., & Pivovaroff M.J., 2006, ApJ, 640, 929
[208] Livingstone M.A., Kaspi V.M., Gavriil F.P., & Manchester R.N., 2005, ApJ, 619, 1046
[209] Gaensler B.M., Brazier K.T.S., Manchester R.N., et al., 1999, MNRAS, 305, 724
[210] Iaria R., Di Salvo T., Burderi L., & Robba N.R., 2001, ApJ, 561, 321
[211] Robba N.R., Burderi L., Di Salvo T., et al., 2001, ApJ, 562, 950
[212] Baykal A., Inam S.Ç., & Beklen E., 2006, A&A, 453, 1037
[213] Reynolds A.P., Bell S.A., & Hilditch R.W., 1992, MNRAS, 256, 631
[214] in 't Zand J.J.M., Corbet R.H.D., & Marshall F.E., 2001, ApJ, 553, L165
[215] Farinelli R., Frontera F., Masetti N., et al., 2003, A&A, 402, 1021
[216] Wang Z. & Chakrabarty D., 2004, ApJ, 616, L139
[217] Stephen J.B., Bassani L., Molina M., et al., 2005, A&A, 432, L49
[218] Haberl F., Motch C., & Zickgraf F.-J., 2002, A&A, 387, 201
[219] de Martino D., Bonnet-Bidaud J.-M., Mouchet M., et al., 2006, A&A, 449, 1151
[220] Klemola A.R., Jones B.F., & Hanson R.B., 1987, AJ, 94, 501
[221] Kazarovets E.V., Samus N.N., & Durlevich O.V., 2001, IBVS, 5135, 1
[222] Corbel S., Tomsick J.A., & Kaaret P., 2006, ApJ, 636, 971
[223] Orosz J.A., Groot P.J., van der Klis M., et al., 2002, ApJ, 568, 845
[224] Smale A.P., 1991, PASP, 103, 636
[225] Woudt P.A. & Kraan-Korteweg R.C., 2001, A&A, 380, 441
[226] Greco M.V., Miller J.M., & Steeghs D., 2006, ATel, 858, 1
[227] Wachter S., Hoard D.W., Bailyn C.D., et al., 2002, ApJ, 568, 901
[228] Tomsick J.A., Chaty S., Rodriguez J., et al., 2006, ApJ, 647, 1309
[229] Kaspi V.M., Crawford F., Manchester R.N., et al., 1998, ApJ, 503, L161
[230] Gotthelf E.V., Petre R., & Hwang U., 1997, ApJ, 487, L175
[231] Torii K., Gotthelf E.V., Vasisht G., et al., 2000, ApJ, 534, L71
[232] Caswell J.L., Murray J.D., Roger R.S., et al., 1975, A&A, 45, 239
[233] Garmire G.P., Pavlov G.G., Garmire A.B., & Zavlin V.E., 2000, IAU Circ., 7350, 2
[234] Reynoso E.M., Green A.J., Johnston S., et al., 2004, PASA, 21, 82
[235] McNamara B.J., Harrison T.E., Zavala R.T., et al., 2003, AJ, 125, 1437
[236] Bradshaw C.F., Geldzahler B.J., & Fomalont E.B., 2003, ApJ, 592, 486
[237] Vanderlinde K.W., Levine A.M., & Rappaport S.A., 2003, PASP, 115, 739
[238] Campana S., Belloni T., Homan J., et al., 2006, ATel, 688, 1
[239] Markwardt C.B. & Swank J.H., 2005, ATel, 679, 1
[240] Wachter S., Wellhouse J.W., Patel S.K., et al., 2005, ApJ, 621, 393
[241] Parmar A.N., Oosterbroek T., Boirin L., & Lumb D., 2002, A&A, 386, 910
[242] Christian D.J. & Swank J.H., 1997, ApJS, 109, 177
[243] Kennea J.A., Burrows D.N., Nousek J.A., et al., 2005, ATel, 459, 1
[244] Beckmann V., Kennea J.A., Markwardt C., et al., 2005, ApJ, 631, 506
[245] Rodriguez J. & Goldwurm A., 2003, ATel, 201, 1
[246] Schartel N., Ehle M., Breitfellner M., et al., 2003, IAU Circ., 8072, 3
[247] Walter R., Zurita Heras J.A., Bassani L., et al., 2006, A&A, 453, 133
[248] Filliatre P. & Chaty S., 2004, ApJ, 616, 469
[249] Rodriguez J., Bodaghee A., Kaaret P., et al., 2006, MNRAS, 366, 274
[250] Corbet R., Barbier L., Barthelmy S., et al., 2005, ATel, 649, 1
[251] Orlandini M., Fiume D.D., Frontera F., et al., 1998, ApJ, 500, L163
[252] Owens A., Oosterbroek T., & Parmar A.N., 1997, A&A, 324, L9
[253] Middleditch J., Mason K.O., Nelson J.E., & White N.E., 1981, ApJ, 244, 1001

[254] Tomsick J.A., Corbel S., Goldwurm A., & Kaaret P., 2005, ApJ, 630, 413
[255] Kouveliotou C., Patel S., Tennant A., et al., 2003, IAU Circ., 8109, 2
[256] Patel S.K., Zurita Heras J.A., Del Santo M., et al., 2006, ApJ, in press, astro-ph/0610768
[257] Ebeling H., Mullis C.R., & Tully R.B., 2002, ApJ, 580, 774
[258] McHardy I.M., Lawrence A., Pye J.P., & Pounds K.A., 1981, MNRAS, 197, 893
[259] Bodaghee A., Walter R., Zurita Heras J.A., et al., 2006, A&A, 447, 1027
[260] Thompson T.W.J., Tomsick J.A., Rothschild R.E., et al., 2006, ApJ, 649, 373
[261] Vrtilek S.D., McClintock J.E., Seward F.D., et al., 1991, ApJS, 76, 1127
[262] Strohmayer T.E. & Markwardt C.B., 2002, ApJ, 577, 337
[263] Galloway D.K., Psaltis D., Muno M.P., & Chakrabarty D., 2006, ApJ, 639, 1033
[264] Corbet R., Barbier L., Barthelmy S., et al., 2006, ATel, 779, 1
[265] Smith D.M., 2004, ATel, 338, 1
[266] Kuiper L., Jonker P., Hermsen W., & O'Brien K., 2005, ATel, 654, 1
[267] Markwardt C.B., Swank J.H., & Smith E., 2005, ATel, 465, 1
[268] Ebisawa K., Bourban G., Bodaghee A., et al., 2003, A&A, 411, L59
[269] Manchester R.N., Lyne A.G., Camilo F., et al., 2001, MNRAS, 328, 17
[270] Netzer H., Lemze D., Kaspi S., et al., 2005, ApJ, 629, 739
[271] Donato D., Sambruna R.M., & Gliozzi M., 2005, A&A, 433, 1163
[272] Brocksopp C., McGowan K.E., Krimm H., et al., 2006, MNRAS, 365, 1203
[273] Tueller J., Markwardt C., Ajello M., et al., 2006, ATel, 835, 1
[274] Kinnunen T. & Skiff B.A., 2000, IBVS, 4863, 1
[275] Oosterbroek T., Parmar A.N., Dal Fiume D., et al., 2000, A&A, 353, 575
[276] Kuster M., Wilms J., Staubert R., et al., 2005, A&A, 443, 753
[277] Reynolds A.P., Quaintrell H., Still M.D., et al., 1997, MNRAS, 288, 43
[278] Sugizaki M., Mitsuda K., Kaneda H., et al., 2001, ApJS, 134, 77
[279] Chakrabarty D., Wang Z., Juett A.M., et al., 2002, ApJ, 573, 789
[280] Orlandini M., dal Fiume D., del Sordo S., et al., 1999, A&A, 349, L9
[281] Baykal A., 2000, MNRAS, 313, 637
[282] Chakrabarty D., Grunsfeld J.M., Prince T.A., et al., 1993, ApJ, 403, L33
[283] Audley M.D., Nagase F., Mitsuda K., et al., 2006, MNRAS, 367, 1147
[284] Krauss M.I., Juett A.M., Chakrabarty D., et al., 2006, ATel, 777, 1
[285] Kennea J.A., Marshall F.E., Steeghs D., et al., 2006, ATel, 704, 1
[286] Miller J.M., Raymond J., Fabian A.C., et al., 2004, ApJ, 601, 450
[287] Hynes R.I., Steeghs D., Casares J., et al., 2004, ApJ, 609, 317
[288] Boroson B., Vrtilek S.D., Kallman T., & Corcoran M., 2003, ApJ, 592, 516
[289] Hong J. & Hailey C.J., 2004, ApJ, 600, 743
[290] Ankay A., Kaper L., de Bruijne J.H.J., et al., 2001, A&A, 370, 170
[291] Kazarovets E.V., Samus N.N., & Durlevich O.V., 2000, IBVS, 4870, 1
[292] Iaria R., Di Salvo T., Robba N.R., et al., 2004, ApJ, 600, 358
[293] Wachter S. & Margon B., 1996, AJ, 112, 2684
[294] Oosterbroek T., Penninx W., van der Klis M., et al., 1991, A&A, 250, 389
[295] Asai K., Dotani T., Hoshi R., et al., 1998, PASJ, 50, 611
[296] Remillard R.A., Orosz J.A., McClintock J.E., & Bailyn C.D., 1996, ApJ, 459, 226
[297] Rea N., Oosterbroek T., Zane S., et al., 2005, MNRAS, 361, 710
[298] in 't Zand J.J.M., Cornelisse R., & Méndez M., 2005, A&A, 440, 287
[299] Di Salvo T., Iaria R., Méndez M., et al., 2005, ApJ, 623, L121
[300] in 't Zand J.J.M., Heise J., Lowes P., & Ubertini P., 2003, ATel, 160, 1
[301] Negueruela I. & Schurch M., 2007, A&A, 461, 631
[302] Jonker P.G., Méndez M., Nelemans G., et al., 2003, MNRAS, 341, 823
[303] Kennea J.A., Burrows D.N., Nousek J.A., et al., 2005, ATel, 476, 1
[304] Ritter H. & Kolb U., 2003, A&A, 404, 301
[305] Wilson C.A., Patel S.K., Kouveliotou C., et al., 2003, ApJ, 596, 1220
[306] Edge A.C. & Stewart G.C., 1991, MNRAS, 252, 414
[307] Nevalainen J., Oosterbroek T., Bonamente M., & Colafrancesco S., 2004, ApJ, 608, 166
[308] Cocchi M., Bazzano A., Natalucci L., et al., 2001, Mem. Soc. Astron. Italiana, 72, 757
[309] Downes R.A., Webbink R.F., Shara M.M., et al., 2001, PASP, 113, 764
[310] de Martino D., Matt G., Belloni T., et al., 2004, A&A, 415, 1009
[311] Norton A.J., Wynn G.A., & Somerscales R.V., 2004, ApJ, 614, 349
[312] Suleimanov V., Revnivtsev M., & Ritter H., 2005, A&A, 435, 191
[313] Cornelisse R., Charles P.A., & Robertson C., 2006, MNRAS, 366, 918
[314] Cadolle Bel M., Rodriguez J., Sizun P., et al., 2004, A&A, 426, 659
[315] Nagata T., Kato D., Baba D., et al., 2003, PASJ, 55, L73
[316] Bykov A.M., Krassilchtchikov A.M., Uvarov Y.A., et al., 2006, A&A, 449, 917
[317] Zurita Heras J.A., de Cesare G., Walter R., et al., 2006, A&A, 448, 261

[318] Corbet R.H.D., Markwardt C.B., & Swank J.H., 2005, ApJ, 633, 377
[319] Steeghs D., Torres M.A.P., Koviak K., et al., 2005, ATel, 629, 1
[320] Kennea J.A., Burrows D.N., Chester M., et al., 2005, ATel, 632, 1
[321] Kuulkers E., den Hartog P.R., in 't Zand J.J.M., et al., 2003, A&A, 399, 663
[322] Gänsicke B.T., Marsh T.R., Edge A., et al., 2005, MNRAS, 361, 141
[323] Church M.J. & Balucińska-Church M., 2001, A&A, 369, 915
[324] D'Aí, A., di Salvo T., Iaria R., et al., 2006, A&A, 448, 817
[325] Strohmayer T.E., Zhang W., Swank J.H., et al., 1996, ApJ, 469, L9
[326] Hernanz M. & Sala G., 2002, Science, 298, 393
[327] Munari U. & Zwitter T., 2002, A&A, 383, 188
[328] Paul B., Dotani T., Nagase F., et al., 2005, ApJ, 627, 915
[329] Hinkle K.H., Fekel F.C., Joyce R.R., et al., 2006, ApJ, 641, 479
[330] Chelovekov I.V., Grebenev S.A., & Sunyaev R.A., 2006, AstL, 32, 456
[331] Marti J., Mirabel I.F., Chaty S., & Rodriguez L.F., 1998, A&A, 330, 72
[332] Molina M., Malizia A., Bassani L., et al., 2006, MNRAS, 371, 821
[333] Corbet R.H.D., Thorstensen J.R., Charles P.A., et al., 1986, MNRAS, 222, 15P
[334] Smith D.M., Heindl W.A., Markwardt C.B., et al., 2006, ApJ, 638, 974
[335] Sakano M., Koyama K., Murakami H., et al., 2002, ApJS, 138, 19
[336] Negueruela I., Smith D.M., Harrison T.E., & Torrejón J.M., 2006, ApJ, 638, 982
[337] Torres M.A.P., Steeghs D., Garcia M.R., et al., 2006, ATel, 784, 1
[338] in 't Zand J.J.M., Verbunt F., Kuulkers E., et al., 2002, A&A, 389, L43
[339] Sidoli L., Belloni T., & Mereghetti S., 2001, A&A, 368, 835
[340] Torres M.A.P., Garcia M.R., McClintock J.E., et al., 2004, ATel, 264, 1
[341] Kong A.K.H., 2006, ATel, 745, 1
[342] Kennea J.A., Burrows D.N., Nousek J., & Gehrels N., 2005, ATel, 617, 1
[343] Rupen M.P., Dhawan V., & Mioduszewski A.J., 2004, ATel, 335, 1
[344] Martí, J., Mirabel I.F., Chaty S., & Rodríguez L.F., 2000, A&A, 363, 184
[345] Gallo E. & Fender R.P., 2002, MNRAS, 337, 869
[346] Smith D.M., Heindl W.A., & Swank J.H., 2002, ApJ, 578, L129
[347] White N.E. & van Paradijs J., 1996, ApJ, 473, L25
[348] Reid M.J. & Brunthaler A., 2004, ApJ, 616, 872
[349] Bélanger G., Goldwurm A., Renaud M., et al., 2006, ApJ, 636, 275
[350] Miller J.M., Raymond J., Homan J., et al., 2006, ApJ, 646, 394
[351] Corbel S., Kaaret P., Fender R.P., et al., 2005, ApJ, 632, 504
[352] Porquet D., Rodriguez J., Corbel S., et al., 2003, A&A, 406, 299
[353] Revnivtsev M.G., Sunyaev R.A., Varshalovich D.A., et al., 2004, AstL, 30, 382
[354] Wijnands R., Miller J.M., & Wang Q.D., 2002, ApJ, 579, 422
[355] Kong A.K.H., Wijnands R., & Homan J., 2005, ATel, 641, 1
[356] Werner N., in 't Zand J.J.M., Natalucci L., et al., 2004, A&A, 416, 311
[357] Revnivtsev M.G., Churazov E.M., Sazonov S.Y., et al., 2004, A&A, 425, L49
[358] Juett A.M., Kaplan D.L., Chakrabarty D., et al., 2005, ATel, 521, 1
[359] Kennea J.A., Burrows D.N., Markwardt C., & Gehrels N., 2005, ATel, 500, 1
[360] Oosterbroek T., Barret D., Guainazzi M., & Ford E.C., 2001, A&A, 366, 138
[361] McClintock J., Murray S., Garcia M., & Jonker P., 2003, ATel, 205, 1
[362] Bhattacharyya S., Strohmayer T.E., Markwardt C.B., & Swank J.H., 2006, ApJ, 639, L31
[363] Torii K., Kinugasa K., Katayama K., et al., 1998, ApJ, 508, 854
[364] Paizis A., Nowak M.A., Rodriguez J., et al., 2006, ATel, 907, 1
[365] Sidoli L., Parmar A.N., Oosterbroek T., et al., 2001, A&A, 368, 451
[366] in 't Zand J.J.M., Hulleman F., Markwardt C.B., et al., 2003, A&A, 406, 233
[367] Still M., 2005, ATel, 555, 1
[368] Morris D.C., Burrows D.N., Racusin J., et al., 2005, ATel, 552, 1
[369] Türler M., Shaw S.E., Kuulkers E., et al., 2006, ATel, 790, 1
[370] in 't Zand J.J.M., 2005, A&A, 441, L1
[371] Pellizza L.J., Chaty S., & Negueruela I., 2006, A&A, 455, 653
[372] Lutovinov A., Revnivtsev M., Molkov S., & Sunyaev R., 2005, A&A, 430, 997
[373] Sidoli L. & Mereghetti S., 2002, A&A, 388, 293
[374] Iaria R., di Salvo T., Robba N.R., et al., 2005, A&A, 439, 575
[375] Hill A.B., Walter R., Knigge C., et al., 2005, A&A, 439, 255
[376] Combi J.A., Ribó M., Martí J., & Chaty S., 2006, A&A, 458, 761
[377] Markwardt C.B., Juda M., & Swank J.H., 2003, IAU Circ., 8095, 2
[378] Falanga M., Bonnet-Bidaud J.M., Poutanen J., et al., 2005, A&A, 436, 647
[379] Kaplan D.L., Fox D.W., Kulkarni S.R., et al., 2002, ApJ, 564, 935
[380] Molkov S., Hurley K., Sunyaev R., et al., 2005, A&A, 433, L13
[381] Tiengo A., Esposito P., Mereghetti S., et al., 2005, A&A, 440, L63

[382] Corbel S. & Eikenberry S.S., 2004, A&A, 419, 191
[383] Kaspi V.M., Roberts M.E., Vasisht G., et al., 2001, ApJ, 560, 371
[384] Roberts M.S.E., Tam C.R., Kaspi V.M., et al., 2003, ApJ, 588, 992
[385] Torii K., Tsunemi H., Dotani T., et al., 1999, ApJ, 523, L69
[386] Gotthelf E.V., 2003, ApJ, 591, 361
[387] Ubertini P., Bassani L., Malizia A., et al., 2005, ApJ, 629, L109
[388] Brogan C.L., Gaensler B.M., Gelfand J.D., et al., 2005, ApJ, 629, L105
[389] Ueda Y., Murakami H., Yamaoka K., et al., 2004, ApJ, 609, 325
[390] Corbet R.H.D., 2003, ApJ, 595, 1086
[391] Bandyopadhyay R.M., Shahbaz T., Charles P.A., & Naylor T., 1999, MNRAS, 306, 417
[392] Sguera V., Bird A.J., Dean A.J., et al., 2006, ATel, 873, 1
[393] Farinelli R., Frontera F., Zdziarski A.A., et al., 2005, A&A, 434, 25
[394] Dhawan M.P.R.V. & Mioduszewski A.J., 2006, ATel, 721, 1
[395] Miller J.M., Homan J., Steeghs D., & Wijnands R., 2006, ATel, 746, 1
[396] Sala G. & Greiner J., 2006, ATel, 791, 1
[397] Gehrels M.S.N., Steeghs D., Torres M.A.P., et al., 2005, ATel, 588, 1
[398] in 't Zand J., Jonker P., Mendez M., & Markwardt C., 2006, ATel, 915, 1
[399] Kinugasa K., Torii K., Hashimoto Y., et al., 1998, ApJ, 495, 435
[400] Voges W., Aschenbach B., Boller T., et al., 2000, IAU Circ., 7432, 1
[401] Migliari S., Fender R.P., Rupen M., et al., 2004, MNRAS, 351, 186
[402] Revnivtsev M., Sazonov S., Churazov E., & Trudolyubov S., 2006, A&A, 448, L49
[403] Douglas J.N., Bash F.N., Bozyan F.A., et al., 1996, AJ, 111, 1945
[404] Juett A.M. & Chakrabarty D., 2005, ApJ, 627, 926
[405] Iaria R., Di Salvo T., Burderi L., & Robba N.R., 2001, ApJ, 557, 24
[406] Jonker P.G. & van der Klis M., 2001, ApJ, 553, L43
[407] Hellier C. & Mason K.O., 1989, MNRAS, 239, 715
[408] Mason K.O. & Cordova F.A., 1982, ApJ, 262, 253
[409] Monet D. & et al. 1998, in The PMM USNO-A2.0 Catalog. (1998), 0–+
[410] Martocchia A., Motch C., & Negueruela I., 2005, A&A, 430, 245
[411] Casares J., Ribó M., Ribas I., et al., 2005, MNRAS, 364, 899
[412] Thompson T.W.J., Rothschild R.E., Tomsick J.A., & Marshall H.L., 2005, ApJ, 634, 1261
[413] Homer L., Charles P.A., & O'Donoghue D., 1998, MNRAS, 298, 497
[414] Kong A.K.H., Homer L., Kuulkers E., et al., 2000, MNRAS, 311, 405
[415] Safi-Harb S., Harrus I.M., Petre R., et al., 2001, ApJ, 561, 308
[416] Camilo F., Ransom S.M., Gaensler B.M., et al., 2006, ApJ, 637, 456
[417] Schmitz M., 1991, NED Team Report, 1, 1 (1991), 1, 1
[418] de Rosa A., Piro L., Tramacere A., et al., 2005, A&A, 438, 121
[419] Grandi P., Urry C.M., & Maraschi L., 2002, New A Rev., 46, 221
[420] Parmar A.N., Oosterbroek T., Sidoli L., Stella L., & Frontera F., 2001, A&A, 380, 490
[421] Deutsch E.W., Margon B., & Anderson S.F., 2000, ApJ, 530, L21
[422] Malizia A., Bassani L., Stephen J.B., et al., 2005, ApJ, 630, L157
[423] Foster R.S., Cadwell B.J., Wolszczan A., & Anderson S.B., 1995, ApJ, 454, 826
[424] Molkov S.V., Cherepashchuk A.M., Lutovinov A.A., et al., 2004, AstL, 30, 534
[425] Halpern J.P., Gotthelf E.V., Helfand D.J., et al., 2004, ATel, 289, 1
[426] Bamba A., Yokogawa J., Ueno M., et al., 2001, PASJ, 53, 1179
[427] Wachter S., Patel S.K., Kouveliotou C., et al., 2004, ApJ, 615, 887
[428] Morii M., Sato R., Kataoka J., & Kawai N., 2003, PASJ, 55, L45
[429] Vasisht G. & Gotthelf E.V., 1997, ApJ, 486, L129
[430] Sanbonmatsu K.Y. & Helfand D.J., 1992, AJ, 104, 2189
[431] Sguera V., Bird A.J., Dean A.J., et al., 2007, A&A, 462, 695
[432] Coe M.J., Fabregat J., Negueruela I., et al., 1996, MNRAS, 281, 333
[433] Piraino S., Santangelo A., Segreto A., et al., 2000, A&A, 357, 501
[434] Israel G.L., Negueruela I., Campana S., et al., 2001, A&A, 371, 1018
[435] Gotthelf E.V., Vasisht G., Boylan-Kolchin M., & Torii K., 2000, ApJ, 542, L37
[436] Helfand D.J., Collins B.F., & Gotthelf E.V., 2003, ApJ, 582, 783
[437] Livingstone M.A., Kaspi V.M., Gotthelf E.V., & Kuiper L., 2006, ApJ, 647, 1286
[438] Becker R.H. & Helfand D.J., 1984, ApJ, 283, 154
[439] Soffitta P., Tomsick J.A., Harmon B.A., et al., 1998, ApJ, 494, L203
[440] Lutovinov A.A. & Revnivtsev M.G., 2003, AstL, 29, 719
[441] Beuermann K., Harrison T.E., McArthur B.E., et al., 2004, A&A, 419, 291
[442] Corbet R.H.D. & Mukai K., 2002, ApJ, 577, 923
[443] Corbet R.H.D., Marshall F.E., Peele A.G., & Takeshima T., 1999, ApJ, 517, 956
[444] Harris D.E., Forman W., Gioa I.M., et al., 1996, VizieR Online Data Catalog, 9013, 0
[445] Bikmaev I.F., Sunyaev R.A., Revnivtsev M.G., & Burenin R.A., 2005, AstL, in press, astro-ph/0511405

[446] Paul B. & Rao A.R., 1998, A&A, 337, 815
[447] Takeshima T., Corbet R.H.D., Marshall F.E., et al., 1998, IAU Circ., 6826, 1
[448] Rupen M.P., Mioduszewski A.J., & Dhawan V., 2005, ATel, 530, 1
[449] Campana S., 2005, ATel, 535, 1
[450] Kaaret P., Morgan E.H., Vanderspek R., & Tomsick J.A., 2006, ApJ, 638, 963
[451] Kawai N. & Suzuki M., 2005, ATel, 534, 1
[452] Galloway D.K., Remillard R., & Morgan E., 2003, IAU Circ., 8081, 2
[453] Galloway D.K., Wang Z., & Morgan E.H., 2005, ApJ, 635, 1217
[454] Frail D.A., Kulkarni S.R., & Bloom J.S., 1999, Nature, 398, 127
[455] Esposito P., Mereghetti S., Tiengo A., et al., 2007, A&A, 461, 605
[456] Vrba F.J., Henden A.A., Luginbuhl C.B., et al., 2000, ApJ, 533, L17
[457] Rupen M.P., Dhawan V., & Mioduszewski A.J., 2002, IAU Circ., 7874, 1
[458] in 't Zand J.J.M., Miller J.M., Oosterbroek T., & Parmar A.N., 2002, A&A, 394, 553
[459] Chaty S., Mignani R.P., & Israel G.L., 2006, MNRAS, 365, 1387
[460] Cusumano G., di Salvo T., Burderi L., et al., 1998, A&A, 338, L79
[461] Baykal A., İnam S.C., & Beklen E., 2006, MNRAS, 369, 1760
[462] in 't Zand J.J.M., Baykal A., & Strohmayer T.E., 1998, ApJ, 496, 386
[463] Cox N.L.J., Kaper L., & Mokiem M.R., 2005, A&A, 436, 661
[464] Levine A.M., Rappaport S., Remillard R., & Savcheva A., 2004, ApJ, 617, 1284
[465] Morel T. & Grosdidier Y., 2005, MNRAS, 356, 665
[466] Wijnands R., Maitra D., Bailyn C., & Linares M., 2006, ATel, 871, 1
[467] Chevalier C. & Ilovaisky S.A., 1991, A&A, 251, L11
[468] Brinkmann W., Kotani T., & Kawai N., 2005, A&A, 431, 575
[469] Blundell K.M. & Bowler M.G., 2004, ApJ, 616, L159
[470] in 't Zand J.J.M., Jonker P.G., Nelemans G., et al., 2006, A&A, 448, 1101
[471] Corbet R.H.D., Hannikainen D.C., & Remillard R., 2004, ATel, 269, 1
[472] Martocchia A., Matt G., Belloni T., et al., 2006, A&A, 448, 677
[473] Harlaftis E.T. & Greiner J., 2004, A&A, 414, L13
[474] Juett A.M. & Chakrabarty D., 2006, ApJ, 646, 493
[475] Falanga M., Belloni T., & Campana S., 2006, A&A, 456, L5
[476] Sambruna R.M., 1997, ApJ, 487, 536
[477] Véron-Cetty M.-P. & Véron P., 2003, A&A, 412, 399
[478] Wang J., Wei J.Y., & He X.T., 2006, ApJ, 638, 106
[479] Andronov I.L., Baklanov A.V., & Burwitz V., 2006, A&A, 452, 941
[480] Rana V.R., Singh K.P., Barrett P.E., & Buckley D.A.H., 2005, ApJ, 625, 351
[481] Naik S., Callanan P.J., Paul B., & Dotani T., 2006, ApJ, 647, 1293
[482] Galloway D.K., Morgan E.H., & Levine A.M., 2004, ApJ, 613, 1164
[483] Tsygankov S.S. & Lutovinov A.A., 2005, AstL, 31, 88
[484] Evans D.A., Worrall D.M., Hardcastle M.J., et al., 2006, ApJ, 642, 96
[485] Liu F.K. & Zhang Y.H., 2002, A&A, 381, 757
[486] Masetti N., Orlandini M., Palazzi E., et al., 2006, A&A, 453, 295
[487] Mattana F., Götz D., Falanga M., et al., 2006, A&A, 460, L1
[488] Schulz N.S., Cui W., Canizares C.R., et al., 2002, ApJ, 565, 1141
[489] Ziółkowski J., 2005, MNRAS, 358, 851
[490] Zhou H.-Y. & Wang T.-G., 2002, Chinese J. Astron. Astrophys., 2, 501
[491] NED Team, 1992, NED Team Report, 1, 1 (1992), 1, 1
[492] Bykov A.M., Krassilchtchikov A.M., Uvarov Y.A., et al., 2006, ApJ, 649, L21
[493] Reig P. & Coe M.J., 1999, MNRAS, 302, 700
[494] Camero Arranz A., Wilson C.A., Connell P., et al., 2005, A&A, 441, 261
[495] Wilson C.A., Finger M.H., Coe M.J., et al., 2002, ApJ, 570, 287
[496] Weekes T.C. & Geary J.C., 1982, PASP, 94, 708
[497] Stark M.J. & Saia M., 2003, ApJ, 587, L101
[498] Lara L., Cotton W.D., Feretti L., et al., 2001, A&A, 370, 409
[499] Ballantyne D.R., 2005, MNRAS, 362, 1183
[500] Cutri R.M., Skrutskie M.F., van Dyk S., et al., 2003, The IRSA 2MASS All-Sky Point Source Catalog, NASA/IPAC Infrared Science Archive. (http://irsa.ipac.caltech.edu/applications/Gator/)
[501] Baykal A., Stark M.J., & Swank J.H., 2002, ApJ, 569, 903
[502] Sidoli L., Mereghetti S., Larsson S., et al., 2005, A&A, 440, 1033
[503] Falcone A., Tueller J., Markwardt C., et al., 2006, ATel, 846, 1
[504] Thorstensen J.R. & Taylor C.J., 2001, MNRAS, 326, 1235
[505] Halpern J.P., 2006, ATel, 847, 1
[506] Bonnet-Bidaud J.M., Mouchet M., de Martino D., et al., 2006, A&A, 445, 1037
[507] Motch C., Guillout P., Haberl F., et al., 1997, A&AS, 122, 201
[508] Mauche C.W., 2004, ApJ, 610, 422

[509] Harrison T.E., McNamara B.J., Szkody P., & Gilliland R.L., 2000, AJ, 120, 2649
[510] Costantini E., Freyberg M.J., & Predehl P., 2005, A&A, 444, 187
[511] Casares J., Charles P.A., & Kuulkers E., 1998, ApJ, 493, L39
[512] Stickel M., Lemke D., Klaas U., et al., 2004, A&A, 422, 39
[513] Dadina M., Bassani L., Cappi M., et al., 2001, A&A, 370, 70
[514] Ravasio M., Tagliaferri G., Ghisellini G., et al., 2003, A&A, 408, 479
[515] Hog E., Kuzmin A., Bastian U., et al., 1998, A&A, 335, L65
[516] Masetti N., Dal Fiume D., Amati L., et al., 2004, A&A, 423, 311
[517] Ribó M., Negueruela I., Blay P., et al., 2006, A&A, 449, 687
[518] Blay P., Negueruela I., Reig P., et al., 2006, A&A, 446, 1095
[519] Patterson J., Kemp J., Richman H.R., et al., 1998, PASP, 110, 415
[520] Barrett P., 1996, PASP, 108, 412
[521] Gibson R.R., Marshall H.L., Canizares C.R., & Lee J.C., 2005, ApJ, 627, 83
[522] Scott J.E., Kriss G.A., Lee J.C., et al., 2005, ApJ, 634, 193
[523] George I.M., Turner T.J., Netzer H., et al., 1998, ApJS, 114, 73
[524] Hwang U., Laming J.M., Badenes C., et al., 2004, ApJ, 615, L117
[525] Reed J.E., Hester J.J., Fabian A.C., & Winkler P.F., 1995, ApJ, 440, 706